

POLITECNICO DI TORINO

I Facoltà di Ingegneria

Corso di Laurea in Ingegneria Aerospaziale



Tesi di Laurea Magistrale

Design and simulation analysis of Attitude and Determination Control System for the CubeSat 12U ATISE

Design process, dynamic analysis, control law development and implementation of simulation models for the ADCS on the project CubeSat 12U ATISE, for different modes and configurations during the whole space mission.

Relatore:

Corpino Sabrina

Candidato:

Catanzaro Alessandro Rocco

Acknowledgments

First, I would like to express my gratitude to my project manager, Mr. Fabien Apper, whose dedication and interest towards ATISE project has influenced me a lot during these six months, and of study cycle internship. It was a true pleasure working under his guidance at CSUT. In addition, I want to thank all the equip of CSUT, which has been a guide for me in this my work experience, in all aspects, for all their cooperation, precious time and kind help throughout my internship.

I would like to thank the Politecnico di Torino, which has been part of my life for 5 years, for better or for worse, no matter; it raised me and allowed me to achieve wonderful goals, as engineer as person.

I would like to mention what amazing opportunity I had given by the university, participating at this Erasmus Program in Toulouse; It has been the perfect final step of my student career. I experienced new point of views, met people from all around the world, studied new aspects of aerospace domain, participated on a real space project, approached to the work environment, and so on... Thanks to everyone, my gratitude for that is enormous.

Thanks to all professors, assistants and people that gave me day by day something to add at myself, coming back home, in some way, different.

Thanks to all colleagues with which I had the possibility to confront, to help, and also challenge each other.

Thanks to all the obstacles which I over took with all my will, and thanks to all the errors that I did, without whom I would not know what I is the road that I want to follow, and goals that I can reach.

A giant thanks to all my friends, I would like to thank you each one, you have been, are, and will be like a family, with which I can be myself, no matter where we will be, which situation we will face, or how much time will pass.

And last but not least, an infinite thank you to my parents, my sister, and my entire family, who for insufficient it is, to compensate for all their support, encouragement, strength, and confidence that they have given me in the last few years; despite sometimes their silly questions and their incomprehension about my work, nevertheless provided me with an important stimulus. Very special thanks go to my parents and my sister. I would like to express my gratitude by dedicating this thesis to them.

Abstract

The ability of satellites to actively control their attitude has changed the way we live. Navigation systems, satellite television, and weather forecasting, for example, all rely on satellites which are able to determine and control their attitude accurately. After a short introduction to the argument, in order to accompany you through the various phases of this project, you need to understand the Model Theory, explained in the second chapter, with the analysis about different control system, focusing on the space control. Then, the third chapter will show what is the Attitude Determination Control System, how acts in a satellite mission, which architecture can assume, with different solutions and with all the steps needed for design and validation.

The fourth chapter open with the real project that was aimed at designing and analysing an attitude determination and control system (ADCS) for a 20 kg observation satellite, the CubeSat 12U ATISE, with the Centre Spatial Universitaire de Toulouse (CSUT), which has been the base over developed this thesis, going through all different step of the design process; starting with the requirements analysis, to the equipment architecture and modes chosen, and then the mathematical approach with the computation of control laws. At the end there is a precise analysis on the models developed able to simulate different modes during its life; they are Safe Mode and Mission Mode. A realistic simulation toolset, which includes the space environment, sensor, and actuator models, was created using MATLAB and Simulink.

Table of Contents

1. INTRODUCTION	14
1.1. INTERNSHIP OBJECTIVE	14
1.2. WORK ENVIRONMENT PRESENTATION	15
1.2.1. <i>Partners & Clients</i>	15
1.2.2. <i>General Planning</i>	16
1.2.3. <i>Team & Projects</i>	16
1.2.4. <i>Events & Meetings</i>	17
2. MODEL OF A SYSTEM	18
2.1. MODELS THEORY	19
2.2. MATHEMATIC MODEL OF A SYSTEM	22
2.3. CONTROL SYSTEM FUNDAMENTALS	24
2.3.1. <i>Closed Loop Control System</i>	25
2.3.1.1. Closed Loop Summing Points	27
2.3.1.2. Closed Loop System Transfer Function	27
2.4. SPACECRAFT CONTROL	28
3. ATTITUDE DETERMINATION CONTROL SYSTEM (ADCS)	30
3.1. DESIGN PROCESS	32
3.2. ATTITUDE CONTROL MODES	33
3.3. DISTURBANCE TORQUES	33
3.4. ADCS ARCHITECTURE	36
3.4.1. <i>Passive Methods</i>	37
3.4.2. <i>Active Methods</i>	40
3.4.3. <i>Attitude Determination</i>	46
4. CUBESAT ATISE	51
4.1. ACDS OBJECTIVES	53
4.1.1. <i>Attitude Profiles</i>	53
4.1.2. <i>Attitude Control</i>	54
4.2. ADCS ARCHITECTURE	54
4.2.1. <i>COMAT Reaction Wheels</i>	55
4.2.2. <i>New Space System Magnetorquers NTCR-M012</i>	56
4.2.3. <i>GOM Space NanoSense FSS-4</i>	57
4.2.4. <i>ZARM AMR Magnetometer</i>	58
4.2.5. <i>Auriga Star Tracker</i>	59
4.3. ACDS MODES	59
4.3.1. <i>Launch Mode and End of Life Mode (LM/EOL)</i>	60
4.3.2. <i>Safe Mode</i>	60
4.3.3. <i>Mission Mode</i>	61
4.4. ADCS CONTROL LAWS	62
4.4.1. <i>Euler parameter</i>	63
4.4.2. <i>Unit Quaternions</i>	64
4.4.2.1. Euler to Quaternion Conversion	65
4.4.2.2. Quaternion To Rotation Vector Conversion	66

4.4.2.3.	Rotation between Frames	66
4.4.3.	<i>Reference Frame</i>	66
4.4.3.1.	Inertial Frame J_{2000} (IR)	66
4.4.3.2.	Satellite Frame (SR)	68
4.4.3.3.	Orbital Frame (OR)	69
4.4.4.	<i>Safe mode Dynamic</i>	69
4.4.4.1.	Dynamic during the detumbling	74
4.4.4.2.	Dynamic during the sun pointing	75
4.4.4.3.	Regulation Reaction Wheel Kinetic Momentum	76
4.4.4.4.	Final Result	79
4.4.5.	<i>Mission Mode Dynamic</i>	79
4.4.5.1.	Star Tracker Computation	81
4.4.5.2.	Speed Estimator Filter	81
4.4.5.3.	Reaction Wheels Control PID	82
4.4.5.4.	Magnetorquers Control Law	84
4.5.	ADCS SIMULATION	86
4.5.1.	<i>Orbit and Environment</i>	87
4.5.2.	<i>Space Perturbations</i>	88
4.5.3.	<i>Safe Mode Simulator</i>	89
4.5.3.1.	Sensors	91
4.5.3.1.1.	Magnetometer	91
4.5.3.1.2.	Sun Sensor	93
4.5.3.1.3.	Single Sun Sensor	93
Eclipse Model	94	
Field Of View Control	96	
Sensor FOW	97	
Panel Shadow	98	
4.5.3.1.4.	Multiple Sun Sensors	100
4.5.3.2.	Safe Mode Controller	102
4.5.3.2.1.	Precaution Controllers	102
4.5.3.2.2.	Angular Speed Reduction	106
4.5.3.2.3.	Inertia Wheel Spinning	107
4.5.3.2.4.	Sun Pointing	107
4.5.3.3.	Actuators	108
4.5.3.3.1.	Reaction Wheels	109
4.5.3.3.2.	Single Reaction Wheel	110
Results	111	
4.5.3.3.3.	Magnetorquers	111
Results	113	
4.5.3.4.	Satellite Dynamics	114
4.5.4.	<i>Phases and Graph Analysis</i>	116
4.5.5.	<i>Mission Mode Simulator</i>	119
4.5.5.1.	Star Tracker	121
4.5.5.2.	Estimator	122
4.5.5.3.	Guidance	123
4.5.5.4.	Mission Mode Controller	125
4.5.5.4.1.	Sun Pointing Controller	126
4.5.5.4.2.	Target Controller	128
4.5.5.5.	Results	129
5.	CONCLUSION	135

5.1.	TECHNICAL SYNTHESIS	135
5.2.	RECOMMENDATIONS	135
6.	GLOSSARY	138
7.	BIBLIOGRAPHY	139

Table of Figures & Tables

FIGURE 1 - MODELS CLASSIFICATION.....	19
FIGURE 2 - V MODEL.....	22
FIGURE 3 - BLOCK EXAMPLES	22
FIGURE 4 - DEVELOPMENT MODEL PROCESS.....	23
FIGURE 5 - ANALYSIS PHASE.....	23
FIGURE 6 - IDENTIFICATION PHASE.....	23
FIGURE 7 - OPEN LOOP CONTROL SYSTEM.....	24
FIGURE 8 - CLOSED LOOP CONTROL SYSTEM	25
FIGURE 9 - CLOSED LOOP SATELLITE CONTROL SYSTEM.....	25
FIGURE 10 - ANGULAR MOMENT THEORY.....	38
FIGURE 11 - SATELLITE USING THE EARTH'S MAGNETIC FIELD	39
FIGURE 12 - ACTUATORS CLASSIFICATION AVAILABLE.....	40
FIGURE 13 - EXPLODED VISUALISATION OF A REACTION WHEEL	41
FIGURE 14 - REACTION WHEEL MOMENTUM	42
FIGURE 15 - TETRAHEDRON CONFIGURATION.....	42
FIGURE 16 - MOMENTUM WHEEL DYNAMICS.....	44
FIGURE 17 - CMG DYNAMIC	44
FIGURE 18 - MAGNETORQUERS DYNAMIC	45
FIGURE 19 - GEMINI THRUSTER	45
FIGURE 20 - SENSORS CLASSIFICATION	47
FIGURE 21 - SUN SENSOR MECHANISM	48
FIGURE 22 : PRINCIPLE OF A FIZEAU INTERFEROMETER	51
FIGURE 23: PAYLOAD OVERVIEW.....	52
FIGURE 24 : MONA OVERVIEW.....	52
FIGURE 25 : MONA'S AVIONICS RACK.....	53
FIGURE 26 - EQUIPMENT TRADE OFF	55
FIGURE 27 - COMAT REACTION WHEEL UNIT.....	55
FIGURE 28 - NSS MAGNETORQUER.....	56
FIGURE 29 - THE DIPOLE MOMENT VARIATION VERSUS CURRENT.....	57
FIGURE 30 - GOM SPACE NANOSENSE FSS-4.....	57
FIGURE 31 - ZARM AMR MAGNETOMETER	58
FIGURE 32 - AURIGA STAR TRACKER	59
FIGURE 33 - MISSION PHASES PROFILE.....	61
FIGURE 34 - SIMPLIFIED DYNAMIC FEEDBACK LOOP FOR SPACECRAFT ATTITUDE CONTROL	62
FIGURE 35 - CONCEPT OF EULER'S ROTATIONAL THEOREM OF A QUATERNION.....	65
FIGURE 36 - ILLUSTRATION OF ORBITAL PARAMETERS	67
FIGURE 37 - INERTIAL REFERENCE.....	69
FIGURE 38 - ORBITAL REFERENCE.....	69
FIGURE 39 - MISSION MODE LOOP SCHEME.....	79
FIGURE 40 - OSCILLATION FREQUENCY AT THE STABILITY LIMIT	83
FIGURE 41- OSCILLATION STABILITY LIMIT IN OUR CONTROLLER	84
FIGURE 42 - MODELS DEVELOPMENT PLAN	87
FIGURE 43 - DATA AND ORBIT BLOCK.....	88
FIGURE 44 - ENVIRONMENT BLOCK	88
FIGURE 45 - PERTURBATIONS BLOCK.....	89

FIGURE 46 - EXTERNAL TORQUES CALCULATION	89
FIGURE 47-SAFE MODE SIMULINK MODEL.....	90
FIGURE 48 - SENSORS MODEL	91
FIGURE 49-MAGNETOMETER	91
FIGURE 50-MAGNETOMETER INSIDE THE SIMULINK MODEL	92
FIGURE 51 - SATELLITE MAGNETIC FIELD.....	92
FIGURE 52 - SINGLE SUN SENSOR BLOCK	93
FIGURE 53 - MULTIPLE SUN SENSOR BLOCK	93
FIGURE 54 -INSIDE THE SINGLE SUN SENSOR MODEL.....	94
FIGURE 55 - ECLIPSE BLOCK	94
FIGURE 56 - ECLIPSE MODEL.....	95
FIGURE 57 - DURING THE ECLIPSE.....	95
FIGURE 58 - OUT THE ECLIPSE	96
FIGURE 59 - FIELD OF VIEW BLOCK.....	96
FIGURE 60 - INSIDE THE FOW MODEL	97
FIGURE 61 - SENSOR FIELD MODEL	97
FIGURE 62 - TEST SUN DIRECTION OUT FOW	98
FIGURE 63 - TEST SUN DIRECTION IN FOW	98
FIGURE 64 - PANEL SHADOW MODEL	99
FIGURE 65 - SIMULATION OF SHADOW PROBLEM.....	100
FIGURE 66 - VIEW OF THE SENSOR -Y DIRECTION	100
FIGURE 67 - MULTIPLE SUN SENSOR MODEL	101
FIGURE 68 - VALIDATION SUN SENSOR MODEL	101
FIGURE 69 - CONTROLLER BLOCK	102
FIGURE 70 - CONTROLLER MODEL.....	103
FIGURE 71 - ECLIPSE CHECK MODEL	103
FIGURE 72 - SUN DIRECTION AVERAGE MODEL	104
FIGURE 73 - SAFE MODE CONTROLLER MODEL	105
FIGURE 74 - SPEED CHECK MODEL	105
FIGURE 75 - REDUCTION ANGULAR MOMENT MODEL	106
FIGURE 76 - INERTIA WHEEL SPINNING MODEL.....	107
FIGURE 77- SUN POINTING MODEL	108
FIGURE 78 – ACTUATORS	109
FIGURE 79 - REACTION WHEEL TORQUE COMMAND VECTOR SPLITTING	110
FIGURE 80 - SINGLE REACTION WHEEL BLOCK.....	110
FIGURE 81 - COMMAND LINE REACTION WHEEL MODEL.....	111
FIGURE 82 - RESULT IN SPEED AND TORQUE FOR RWS	111
FIGURE 83 - EARTH MAGNETIC FIELD.....	112
FIGURE 84 - MAGNETORQUERS MODEL	113
FIGURE 85 - SATURATION OF MAGNETORQUERS.....	113
FIGURE 86 - MAGNETIC TORQUES REQUESTED	114
FIGURE 87 - SATELLITE DYNAMICS BLOCK	115
FIGURE 88 - COMPUTING SATELLITE SPEED MODEL.....	116
FIGURE 89 - SATELLITE DYNAMICS MODEL WITH A ZOOM ON THE SATELLITE POSITION COMPUTATION	116
FIGURE 90 - PHASES ANALYSIS	117
FIGURE 91 – DE-TUMBLING.....	117
FIGURE 92 - ZOOM ON THE ANGULAR SPEED IN X AXIS.....	118

FIGURE 93 - SUN MISALIGNMENT	119
FIGURE 94 - MISSION MODE MODEL.....	120
FIGURE 95 - BIAS TO THE QUATERNION.....	121
FIGURE 96 - STAR TRACKER MODEL.....	121
FIGURE 97 - ESTIMATOR IN MISSION MODE	122
FIGURE 98 - ROTATION SPEEDS AVERAGE	122
FIGURE 99 - COMPUTATION OF MAGNETIC FIELD ROTATION.....	123
FIGURE 100 - COMPUTATION OF QUATERNION SPEED ROTATION	123
FIGURE 101 - DISCRETE STATE-SPACE FILTER.....	123
FIGURE 102 - GUIDANCE MODEL.....	124
FIGURE 103 - SWITCH COMMAND MODEL.....	124
FIGURE 104 - COMMAND QUATERNION COMPUTATION MODEL.....	124
FIGURE 105 - MISSION MODE CONTROLLER MODEL WITH ECLIPSE CHECK AND EXCLUSION CHECK	125
FIGURE 106 - VECTOR TRANSFORMATION INTO QUATERNION AND COMMAND VALUE	126
FIGURE 107 - SUN POINTING CONTROLLER MODEL.....	126
FIGURE 108 - REACTION WHEELS PID CONTROLLER.....	127
FIGURE 109 - MAGNETORQUERS CONTROL LAW	127
FIGURE 110 - TARGET CONTROLLER MODEL.....	128
FIGURE 111 - ZOOM ON THE SUN DIRECTION NORMALIZED VECTOR SENT TO THE CONTROLLER.....	129
FIGURE 112 - ERROR BETWEEN PANEL DIRECTION AND SUN DIRECTION FOR MISSION MODE	129
FIGURE 113 - TARGET ERROR IN DEGREE.....	130
FIGURE 114 - SATELLITE ANGULAR SPEED FOR MISSION MODE.....	131
FIGURE 115 - DIFFERENCE BETWEEN REAL AND ESTIMATED SPEED.....	132
FIGURE 116 - PHASE ANALYSIS BETWEEN DESATURATION AND BPOINT LAW.....	132
FIGURE 117 - MAGNETIC TORQUE ANALYSIS	133
FIGURE 118 - ANGULAR MOMENTUM ANALYSIS IN MISSION MODE.....	134
TABLE 1 - DESIGN PROCESS.....	33
TABLE 2 - ATTITUDE PROFILES REQUIREMENTS	53
TABLE 3 - ATTITUDE CONTROL REQUIREMENTS	54
TABLE 4 - COMAT REACTION WHEEL PERFORMANCES [1].....	56
TABLE 5 - NSS MAGNTORQUER PERFORMANCES [2]	57
TABLE 6 - NANOSENSE PERFORMANCES [3]	58
TABLE 7 - AMR MAGNETOMETER PERFORMANCES [4]	59
TABLE 8 - AURIGA STAR TRACKER PERFORMANCES [5]	59
TABLE 9 - SYSTEMS USED FOR EACH MODE	60
TABLE 10 - ORBIT CONFIGURATION.....	68
TABLE 11 - FINAL GAINS FOR SAFE MODE CONTROL LAW	79
TABLE 12 - ZIEGLER-NICHOLS PID TUNING TABLE	84

1. Introduction

Through this thesis my purpose will be to show you what is the role of ADCS in a space mission, to explain how it should work, and it could be built and run; all this it has been possible thanks to my experience and work done during my internship at ISAE Supaero, working for the CSUT (Centre Spatial Universitaire de Toulouse) on the CubeSat project 12U ATISE, in collaboration with the CSUG (Centre Spatial Universitaire de Grenoble), which has the mission to observe the polar auroras.

We will see a general and theoretical view of ADCS, to introduce why this system exists, that means why it's called Attitude Determination Control System, in which part of the satellite is positioned and how that particular system allows to command and control a complex system, as a satellite, during all the mission's phases.

The first step will be to analyse the whole mission, modes and configurations, and in a specific view, what ATISE needs from ADCS, and what it should take in account as environment, perturbations, orbit etc.; then, as second phase, it will be to understand what it is ADCS's equipment, for example which actuators and sensors there are, and how they work; and the third step it will be to develop a mathematical model and implement it as a block in Matlab/Simulink; the last step it should be a test process, with all the necessary simulations and verifications able to give the real satellite's behaviour.

1.1. Internship Objective

I started my internship at the beginning of the project's Phase B, that means the preliminary definition, about selection of technical solutions for system concept selected in phase A. It needs to acquire a precise and coherent definition at every level of the project. My first task was to have a look at the previous work done by other interns on the ADCS, that was a draft of the Safe Mode, not completed and to be improved, adding models and modifying the control laws; and then there has been the design of Mission Mode.

First of all, I studied different paper works about ATISE and ADCS of other projects, in order to have all the necessary information useful for the design. I had the access to a cloud of ATISE project, in which I found every document related to it, and as well, tasks and requirements that I should have faced for my work.

I faced with all the system models, using the software MATLAB-Simulink and a library already created for CubeSat projects; then I started to try some modification and design test, it means build and verify for each system component close to the real behaviour. In particular with a satellite, I had to develop models able to simulate different modes during its life.

The second objective, behind the first and most important, it should improve this library called PILIA, where we can find all system models; so, one part of the work is to get better it in order to give to all the next projects the possibility to use it, without wasting time, and setting just them CubeSat's data. It means, that all models had to be modular, easy to use, and with comments and guide to show how it works

1.2. Work Environment Presentation

I worked for the CSUT, Centre Spatial Universitaire de Toulouse, in the DCAS department at ISAE-Supaero. The scientific interest group "Centre Spatial Universitaire de Toulouse" is a multidisciplinary thematic network aiming to federate public actors in higher education and research who develop an activity in the field of space nanosystems: nano satellites, ground segment, associated launch systems, balloons... and to promote associated projects. It aims to develop relationships with private and institutional partners.

The convention of the GIS Centre Spatial Universitaire de Toulouse was signed on 28 June 2016 at the Toulouse Space Show.

The motivation of the CSUT is multiple:

- To promote mutual knowledge of training and research activities carried out within the various partners, in particular through the organisation of workshops and seminars,
- Coordinate means and/or methods for the realization of space nanosystems projects, publications and common responses to calls for projects and realization of projects,
- Ensure national and international visibility for projects carried out within the framework of the CSUT through, in particular, the organization of conferences and summer schools,
- Promote the development and use of space nanosystems.

1.2.1. Partners & Clients

It is supported by ISAE-SUPAERO and brings together eight academic and research partners:

- **ENAC**, National School of Civil Aviation;
- **INP** Toulouse, bringing together the engineering schools: ENSAT, ENSEEIHT, ENSIACET, ENIT, ENM and PURPAN;
- **INSA** Toulouse, Institut National des Sciences Appliquées ;
- **ISAE-SUPAERO**, Higher Institute of Aeronautics and Space, holder of the CSUT;
- **UT3**, University of Toulouse 3-Paul Sabatier;

- **IRAP**, Research Institute of Astrophysics and Planetology (Observatoire Midi Pyrénées);
- **LAAS**, Laboratory of Automation and Systems Architecture;
- **ONERA**, Office National d'Etudes et de Recherches Aérospatiales ;
- **CNES**, Centre National d'Etudes Spatiales, is an associate member of the CSUT and supports the CSUT through the PERSEUS (launchers) and JANUS (student Nano satellites) projects.

1.2.2. General Planning

The CSUT organizes the development and implementation of collaborative and innovative space nanosystems projects using mainly Nano-satellites (CubeSats) or stratospheric balloon flights to carry out scientific or technological missions. It thus participates in the training of future space actors and supports the research activities of its members or partners in the field of miniaturized space systems.

The CSUT also ensures national and international visibility of the projects in which it participates through the organization of workshops and seminars, conferences and summer schools and the publication of the results obtained.

1.2.3. Team & Projects

The CSUT is based on a team of 8 engineers and permanent teachers/researchers, and 7 fixed-term contract engineers. Ongoing projects aim to develop a CubeSat 3U die (a U corresponding to a 10 cm cube on each side) and a CubeSat 12U die. The CSUT is thus involved in the implementation of three 3U projects:

- **ENTRYSAT**: first 3U CubeSat developed by ISAE-SUPAERO, for the study of atmospheric re-entry. To be launched at the end of 2018.
- **EYE-SAT**: high-performance 3U CubeSat developed by CNES in a student context for a scientific astronomy mission. To be launched in early 2019.
- **NIMP**H: 3U CubeSat, an in-orbit test of opto-electronic components for future space communications, based on the capitalization and experience of the two previous CubeSats. Should be launched in 2020.

The CSUT also participates in the implementation of 2 12U projects:

- **ATISE**: 12 U CubeSat developed in cooperation with the CSUG (Centre Spatial Universitaire de Grenoble), for the study of the polar aurora.
- **HESTIA**: 12U CubeSat developed for the study of urban heat islands with a miniaturized instrument in thermal Infrared.

Thanks to this internship, I had the opportunity to join this amazing team. I have been in the same office of my direct project manager, Fabien Apper, and other colleges responsible for several projects and different space systems. I had my personal desk,

but the open space concept of the office allowed to communicate and have a confront with my manager and colleagues.

1.2.4. Events & Meetings

Since when I start my internship, I had the opportunity to participate a several events connected to the space domain; the main project review of Phase B of the NIMPH project, and I work personally on the review Phase B.1 of the ATISE project. Indeed, I had to write a technical report about my ADCS progress, presenting results and proofs of my work in front of a public with experts and colleagues.

I also participate at the Toulouse Space Show as a member of the CSUT, working for our stand, and looking for partners and producers interesting to CubeSat projects.

I have been involved also in a Space Summer School project in the ISAE- Supaero, which is consisted into presenting our work to some american students and trying to teach something useful to them.

Last but not least, in the first period, in order to give an idea of the progress reached during the week before, weekly I had to make a short presentation in front almost all my colleagues, useful as experience as constructive discussion. As well, we had the possibility to participate at reunions in order to discuss the next step of project, interesting meetings with experts.

2. Model of a System

With the purpose to study the real behaviour of systems recurs at a simplified representation: a System Model.

We can recognise two types of models:

- **Physics:** realization, usually in scale, of the system built it to highlight and analyse experimentally the system itself characteristics.
- **Mathematics:** equations set, which represents the behaviour of the system, and which depend on physic properties, satisfying determinate initial conditions, which are the environment conditions in which the system works.

Below that, we can distinguish also different systems typology:

- **Deterministic System:** a precise input provides a, as well, precise output, it means that it exists a mathematic law which bonds the output to the input.
- **Probabilistic System:** provided an input, it is not possible to certainly know the output.
- **Linear and Not Linear System:** a system is defined linear, if for itself is worth the superposition principle; otherwise it is not linear, and they are a lot hard to resolve, especially for the variables stability in output.
- **Time Independent System:** a system is called time-invariant, if the parameters, which characterize it, remain unchanged over time.
- **Time Dependent System:** a system is called time-variant, if the parameters which characterize it, depend on the time.
- **Continuous System:** a continuous system is a system which their values of output variables take on, with continuity, all range values of real numbers set.
- **Discrete System:** a discrete system is a system which their values of the at least one variable of output can be matched with those belonging to a subset Z of real numbers, so the signal assumes only integer values.

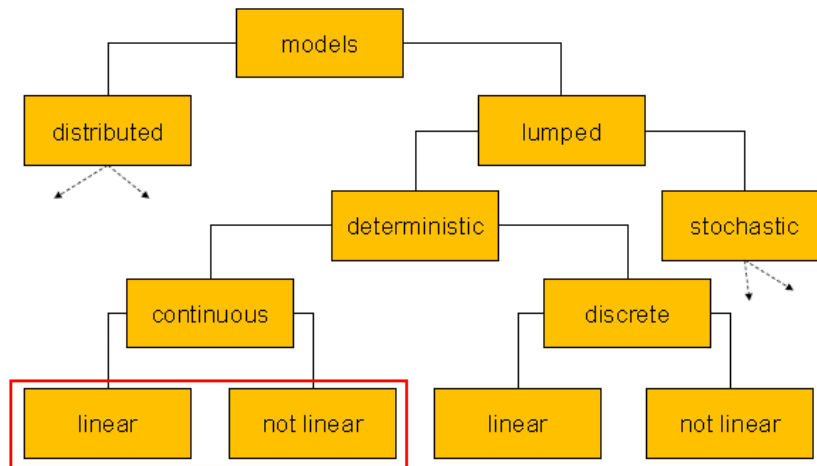


Figure 1 - Models Classification

Whatever model represents necessarily a simplification and schematization of real phenomena. At this point, the main problem raised is the model choice: if it is too complex, and it contains parameters hard to be evaluate, it can conduct to result which hide the main phenomena, while a model too simple cannot be sufficient to represent details behaviours.

2.1. Models Theory

Branch of knowledge which takes care of the laws study with whom export test results on a model to the real case.

The engineering, for the complexity of phenomena, which characterize it, take advantages often on researches which use models. That happens especially not only because the nature phenomena and laws, which rule it, cannot be compute by theoretic way (complexity of mathematic problem), but also because, in general, the real test can be practical impossible, or characterized by huge cost. For these reasons, it is common to used “experimental” test on models. The Models Theory handles how it is possible to find out the maximum number of information’s from the minimum number of test, and to expand and to generalize the results achieved on models to the prototype through laws of generic interpretation.

The Models Theory is based on two cornerstones:

- Dimensional Analysis
- Theory of Similitude

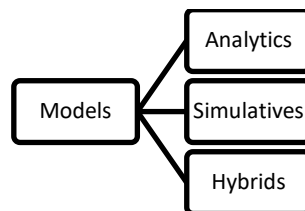
The use of models for the evaluation and the behaviour study of systems becomes essential in the phase of systems project not existent (which the technics of direct measurement or artificial are not applicable) and mainly for the first stages of project,

in that it is important to discern between different alternatives without going into high level of detail.

A model is a representation abstract of the system which includes only relevant aspects with the purpose to study the system. A model is defined at a determinate level of abstraction, that is the system described with an exact detail level, including in the representation only those components and interactions between components, which are deemed necessary for the intended purpose. At the model definition follows its parametrization, to consider the alternatives of study, and the evaluation or solution to obtain the relative information's for the system study.

The methodology to evaluate the systems performances can be distinguished in two main categories: measurement technics and modelers technics. The system performance of elaboration can be quantified by merit figures or performance index which describe efficiency of its functions development.

In the first case, the performance indexes of system are measured, while in the second case are calculated, applying and elaborating analytic models, or estimated, using and running simulation models. There are:



- In an analytic model the components and the system load are represented by variables and parameters, and interactions between components by relations between these quantities. The system evaluation effectuated using the analytic model need the computation of its solution through analytic method and numeric solutions.
- A simulation model reproduces the dynamic behaviour of the system over time, representing the components and interaction in term of functional interactions. The evaluation of the system by simulation model need the execution (run) of a simulation program, or a simulator which represents the “temporal” evolution of the system, and on which measurements are made to estimate the quantities of interest.

Summing up, the definition and utilization of a model for the study of a system shows several advantages, among them:

a) Knowledge increased

The definition of a model helps to organize the knowledge theoretical and the empiric observations on the system, bringing at a higher level of understanding of the system itself; indeed, during the abstraction process it is necessary to identify which are the components and relevant interaction for the study purpose.

b) System analysis

Used of a model facilitates the system analysis.

c) Modifiability

The model is mainly modifiable and manipulable respect to the system itself, allowing the evaluation of different alternatives, compatibly with the definition and level of abstraction adopted.

d) Different objectives of study

The use of different models of the same system allows an evaluation of different objectives.

Otherwise there are some disadvantages using models, limits and problems of modeler technics we notice:

a) Model choice

The choice of an accurate abstraction level can be a not simple task; the use of a model not accurate can clearly lead to valuation errors.

b) Wrong use of model

There is the rick to use a model beyond its field of validity, which is also when the assumptions and hypothesis, which contribute to define it, are not verified; in other words, it need to pay attention at a wrong use of the model due to an extraction of data beyond its applicability field.

Finally, it is important to remember, that the process, which lead us to a model, is iterative.

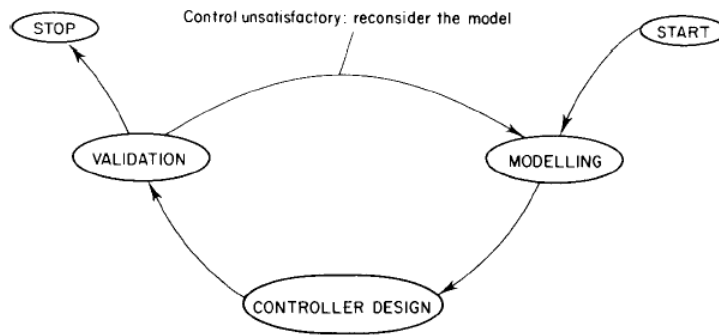


Figure 2 - V Model

2.2. Mathematic Model of a System

To build a mathematic model of a system is useful to divide the same into simpler parts: **Subsystems**. Then, the subsystems further are split into **components**, and each of them needs inputs and outputs.

- The definition of a system **input variable** is: sizes which act on the system, and whose origin is external to it; their variations over the time are dependent by what happens inside the system.
- The definition of system **output variable** is: quantities which, every moment, define the system physic condition.

So, for the development of a mathematic model is extremely useful a system block diagram to which the model refers. This diagram is a graphic representation of the cause-effect relations existents between the several quantities of the system, and what allows to have a general view of present connections between the different parts constituting it. Each block of the diagram represents a subsystem or a component, and it is built with a rectangle containing an existent functional relation between output and input variables.

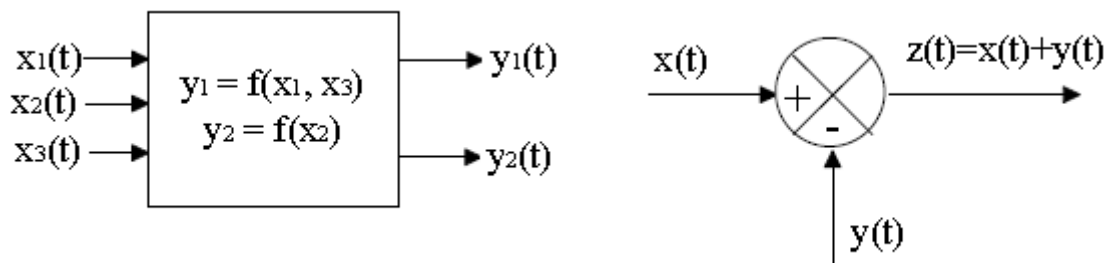


Figure 3 - Block Examples

Four different orders are distinguished as study subject during the development of a mathematic system model:



Figure 4 - Development Model Process

1) Analysis

The dynamic system analysis establishes a basilar problem. Operatively it happens, modifying the inputs as a function of time and with preestablished modes, and determining as consequence relative's trends of outputs. Thus, assigned or known the parameters S_i and known the functions X_i as function of time, compute the functions Y_i over time.

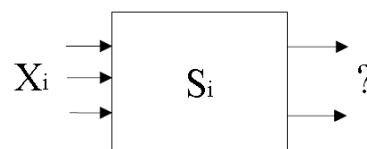


Figure 5 - Analysis Phase

2) Identification

Known the trends of X_i and Y_i , relatives at a real system, (generally obtained by an experimental process) determine a correct mathematic model (with relative parameters S_i) in order to should be satisfied the relations between X_i and Y_i .

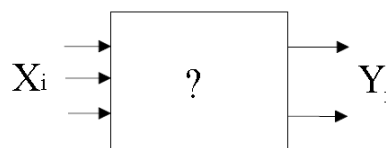


Figure 6 - Identification Phase

3) Synthesis

Known the trends of X_i and assigned the trends of Y_i , determine the mathematic model of the system or, if it is already known, the values to give at its parameters S_i in order to should be satisfied the Y_i trends.

4) Optimization

Defined a standard with which compare quantitatively the correct working of the system under investigation, choose between various mathematic models of the system (or between different assumed values by some parameters of a specific mathematic model) which provides the "best" performance. It is the overrun of synthesis problems.

2.3. Control System Fundamentals

A control system is a complex of equipment through it obtains some quantities, defined outputs of system and characterizing the physic system status or its working condition, which follows a preestablished trend (or of reference), determined by other quantities as inputs. Especially it monitors and changes the status of a system in order to achieve some desired requirements. A control system can be classified as:

- An **open loop** control system
- A **closed loop** control system (also feedback control system)

It is usual to represent a system by means of a blocks diagram, in which each block represents a single element of the system.

It can be synthetized in four basic tasks, and what it could be done by means of the following elements:

- **Plant:** understand the system's behaviour;
- **Sensor:** observe the system's current behaviour;
- **Controller:** decide what to do;
- **Actuators:** do it;

Based on this simple concept, it is possible to build thousands of different control systems. An open loop makes decision without observe and collect data from system's behaviour;

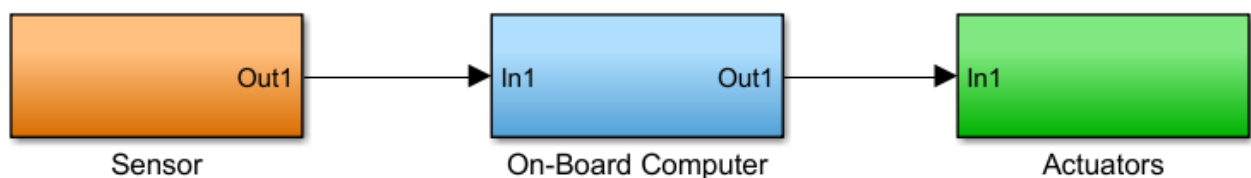


Figure 7 - Open loop control system

On the other side a closed loop bases on the system's behaviour, collecting data from sensors, the command law and the whole ADCS. The attitude sensors send their measurements to the proper on-board computer which determines the attitude and actives the actuators for its control.

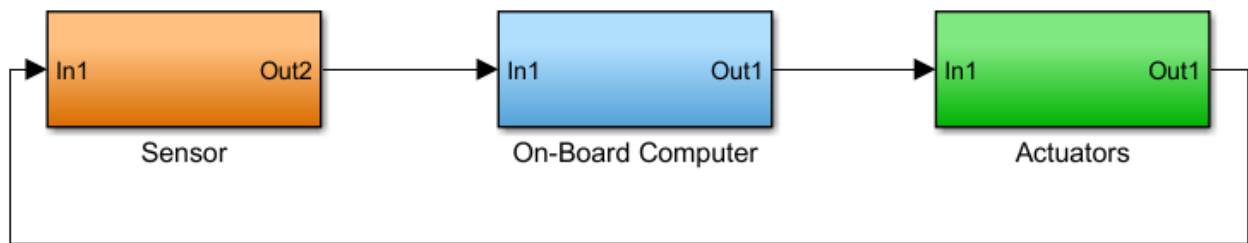


Figure 8 - Closed loop control system

2.3.1. Closed Loop Control System

Unlike an open-loop control scheme in which control variables are generated without taking into account the actual assumptions of the controlled variables, a closed-loop control scheme measures, directly or indirectly, the controlled variables and uses the results of these measures to generate the control variables. In other words, in these systems the output is measured continuously (or periodically) and the result of the measurement is compared with the desired value that the measured quantity should take; the difference between the actual measured value and the desired one, that is the system error, is used to correct the value of an input in the direction necessary to reduce the error. In this way the measured quantity - or some other output from this employee - is forced to follow a predetermined cycle of values.

The fundamental concept of a closed loop control system in a space environment relies in the measurement by means of sensors, of the spacecraft actual attitude and its comparison with the desired attitude. The discrepancy between the two values of attitude (actual and requirement) is an error signal; taking into account the error value, control torques are generated by difficult, if not impossible, to achieve the desired attitude with only one control command. The correction process is therefore continuous. In the figure, the block diagram representing a closed loop control system is shown; it refers to a simple active control system called Single-Input Single-Output system (SISO):

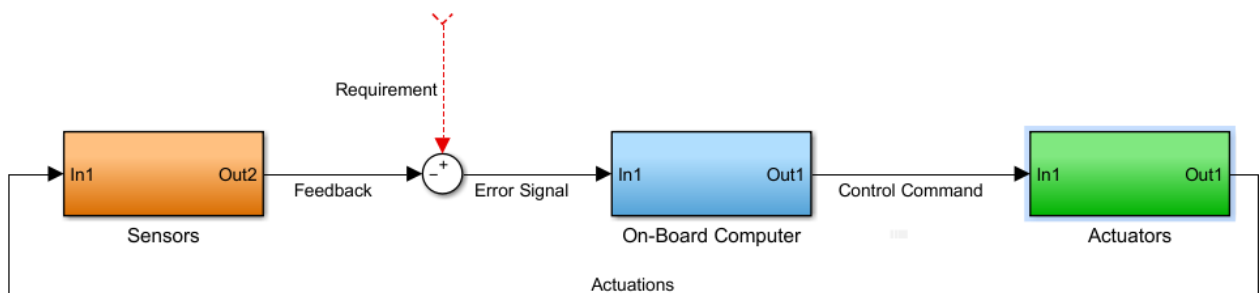


Figure 9 - Closed loop satellite control system

The term Closed-loop control always implies the use of a feedback control action in order to reduce any errors within the system, and its “feedback” which distinguishes

the main differences between an open-loop and a closed-loop system. The accuracy of the output thus depends on the feedback path, which in general can be made very accurate and within electronic control systems and circuits, feedback control is more commonly used than open-loop or feed forward control. In several applications, the corrective element is a standard control, placed in cascade with the system to be controlled. The most common between these controllers is indicated as **P.I.D.**, and can be diagrammed with three blocks in parallel, whose outputs are respectively proportional to the input signal (**Proportional Control**), its integral (**Integral Control**), and derivate (**Derivate Control**). The high spread of standard control is due mainly to have a control computing, with opportune procedures, just three constant K_p, K_i, K_d , even without to know the transfer function of the system to be controlled. In any case, the proportional control carries out its function as soon as there is an error, the integrative is useful in long term deleting the permanent error, and the derivative is adapted for phenomena in short term.

Closed-loop systems have many advantages over open-loop systems. The primary advantage of a closed-loop feedback control system is its ability to reduce a system's sensitivity to external disturbances, for example opening of the dryer door, giving the system a more robust control as any changes in the feedback signal will result in compensation by the controller.

Then we can define the main characteristics of Closed-loop Control as being:

- To reduce errors by automatically adjusting the systems input.
- To improve stability of an unstable system.
- To increase or reduce the systems sensitivity.
- To enhance robustness against external disturbances to the process.
- To produce a reliable and repeatable performance.

Whilst a good closed-loop system can have many advantages over an open-loop control system, its main disadvantage is that in order to provide the required amount of control, a closed-loop system must be more complex by having one or more feedback paths. Also, if the gain of the controller is too sensitive to changes in its input commands or signals it can become unstable and start to oscillate as the controller tries to over-correct itself, and eventually something would break. So, we need to "tell" the system how we want it to behave within some pre-defined limits.

In order to define how define our control system, there are two main milestones to consider: Summing Point and Transfer Function.

2.3.1.1. Closed Loop Summing Points

For a closed-loop feedback system to regulate any control signal, it must first determine the error between the actual output and the desired output. This is achieved using a summing point, also referred to as a comparison element, between the feedback loop and the systems input. These summing points compare systems set point to the actual value and produce a positive or negative error signal which the controller responds too. where:

$$Error = Set\ point - Actual$$

The symbol used to represent a summing point in closed-loop systems block-diagram is that of a circle with two crossed lines as shown. The summing point can either add signals together in which a Plus (+) symbol is used showing the device to be a “summer” (used for positive feedback), or it can subtract signals from each other in which case a Minus (-) symbol is used showing that the device is a “comparator” (used for negative feedback) as shown.

AS well, the summing points can have more than one signal as inputs either adding or subtracting but only one output which is the algebraic sum of the inputs. Also, the arrows indicate the direction of the signals. Summing points can be cascaded together to allow for more input variables to be summed at a given point.

2.3.1.2. Closed Loop System Transfer Function

The Transfer Function of any electrical or electronic control system is the mathematical relationship between the systems input and its output, and hence describes the behaviour of the system. Note also that the ratio of the output of a particular device to its input represents its gain. Then we can correctly say that the output is always the transfer function of the system times the input.

$$G(s) = \frac{\bar{x}(s)}{\bar{F}(s)}$$

That is a preferential way, because the system analysis wants to individuate a mathematic model that expressing a functional relation between input and output variables. This relation is often made of differential equations associated to determinate initial conditions. The differential equations, at partial or total derivate, linear or not linear, with constant or not coefficients, can be resolved using different methods. In the case of differential equations at total derivate, linear of n order or not linear of 1° order, usually it is easy to find an analytic solution. In all the other cases, it should use methods with approximate solutions, and in that case, it used the technic of Numeric Solution.

A popular method for solving mathematical models linear to constant coefficients is to use the **transformed of Laplace**. Given a function $f(t)$ defined for $t > 0$, if any a positive real number b for which the following limit has a finished value:

$$\lim_{t \rightarrow \infty} e^{-b*t} f(t)$$

then its Laplace $F(s)$ transform exists for the $f(t)$ defined by:

$$F(s) = L[f(t)] = \int_0^{\infty} f(t) * e^{-s*t} dt$$

Where s represents a complex number. Transformation is an operation that allows you to pass from a function of the real variable (time) to a function of the complex auxiliary variable s . The use of Laplace transforms for the study of system models is due to the extremely simple form that can take on the function of transform and the interesting mathematical properties that Laplace transforms enjoy. Therefore, the fundamental characteristic of the Laplace transformations is that of transforming a linear differential equation into an algebraic equation (even if of complex variable), thus facilitating the obtaining of the general solution.

If the block is characterized by temporal elements, represented by differential equations, the output signal depends not only on the input value, but also on the variation in time of the latter. In this case the relationship between input and output signal cannot be expressed as a simple algebraic expression. However, by using T.d.L., passing from temporal signals to functions of complex variable, it has been seen how it is possible to express the transfer function as algebraic expression of the complex variable (this also applies to blocks containing not temporal elements).

If you are dealing with blocks whose transfer function is an algebraic form, it makes sense to speak of algebra in the block diagrams. It has already been pointed out that it is convenient to break down the regulation system into blocks that are as elementary as possible in order to facilitate analysis. It is also possible to replace two or more elementary blocks with a single block whose transfer function corresponds to the combination of the transfer functions of the individual constituent blocks. With this process the whole system can be represented as a single block with an appropriate transfer function.

2.4. Spacecraft Control

We focus on two important applications of the process for spacecraft, controlling:

- **Orbit**, the spacecraft's path in space, translating the satellite in space.

- **Attitude**, the spacecraft's orientation in space, rotating the satellite about its centre of mass.

And the motion of a spacecraft is specified by four quantities:

- **Position and Speed**, these two quantities describe the translational motion of the centre of mass of the spacecraft and are the subject of what is variously called orbit analysis, celestial mechanics, or space navigation.
- **Attitude and Attitude Rate**, these two quantities describe the rotational motion of the body of the spacecraft about the centre of mass and are the subject of attitude analysis or spacecraft dynamics.

Orbit and Attitude related on-board systems are the hardware, software and processes used to analyse, design measure and control these elements. We are interested in all aspects of spacecraft orbit and attitude, that means how they are determined, controlled and how the future motion is predicted and adjusted; we also deal with measurement systems which are an integral part of the orbit and attitude process, because they are interdependent. For example, in low Earth orbit the attitude affects atmospheric drag which in turn affects the orbit. The orbit determines the spacecraft position, which determines both the atmospheric density and the magnetic field which, in turn, affects the attitude. Traditionally this coupling has been largely ignored and analysis, design and engineering has been separated into the discrete topics of orbit or attitude. Saying that they are interdependent means that orbit and attitude:

- Are both elements of spacecraft dynamics responding to internal and external forces and torques
- Operate under similar control laws
- Are frequently implemented with the same hardware

In spite of a strong interrelationship, orbit and attitude problems gave different background, both in terms of historical development and how they have been traditionally implemented in space systems; for example, the orbit has traditionally been analysed, determined, measured, and controlled by the ground, and on the other side, with remarkably few exceptions, attitude is controlled on board the spacecraft with autonomous system.

3. Attitude Determination Control System (ADCS)

The Attitude Determination and Control System stabilizes the vehicle and orients it in desired directions during the mission despite the external disturbance torques acting on it. This requires that the vehicle determines its attitude using sensors, and controls it using actuators.

- **Attitude Determination** refers to the process of measuring spacecraft orientation. Determining the attitude of a spacecraft means to measure, and thus to know, the attitude of spacecraft (of its coordinate frame) with respect to a coordinate frame chosen as reference, for example the orbital reference frame.
- **Attitude Control** implies a process, usually occurring more or less continuously, of returning the spacecraft to a desired orientation, given that the measurement reveals discrepancy. In the end, it is the process by means of which the spacecraft can achieve, change, or maintain the desired attitude (orientation) in space. To control means to measure the actual attitude of the spacecraft, to compare it with the desired attitude, and to impose a rotating motion to the spacecraft in order to reach the desired attitude.

Some major issue and concepts are related to and affect the attitude determination and control system, especially mass properties, disturbance torques, angular momentum and reference vectors.

A body in space is subject to small, but persistent **disturbance torques** from a variety of sources, among which are atmospheric grad, gravity gradient, solar radiation pressure, and planet's magnetic field.

Mass properties (i.e. location of centre of mass or gravity C_G , elements of inertia matrix as moments and products of inertia, direction of principal axes) of a spacecraft are key in determining the size of control and disturbance torques. We need to know how these properties change with time, as fuel or other consumables are used, or as appendages are moved or deployed.

Angular momentum plays an important role in space, where torques typically are small and spacecraft are unconstrained. For a body initially at rest, an external torque will cause the body angularly to accelerate proportionally to the torque, resulting in an increasing angular velocity. Conversely, if the body is initially spinning about an axis perpendicular to the applied torque, then the body spin axis will precess, moving with a constant angular velocity proportional to the torque. Thus, spinning bodies act like gyroscopes, inherently resisting disturbance torques in 2 axes by responding with constant, rather than increasing, angular velocity. This property of spinning bodies, called gyroscopic stiffness, can be used to reduce the effect of small, cyclic disturbance torques. This is true whether the entire body spins or just a portion of it, such as a

momentum wheel or spinning rotor. Conservation of vehicle angular momentum requires that only external torques change the system net angular momentum. Thus, external disturbances must be resisted by external control torques (i.e. thrusters or magnetorquers) or the resulting momentum build up must be stored internally (i.e. reaction wheels) without reorienting the vehicle beyond its allowable limits. The momentum builds up due to secular disturbance ultimately must be reduced by applying compensating external control torques.

To orient the vehicle correctly, **external references** must be used to determine the vehicle's absolute attitude. These references include the Sun, the Earth's horizon, the local magnetic field direction, and the stars. In addition, the inertial sensors (gyroscopes) also can be carried to provide a short-term attitude reference between external updates. External references (i.e. Sun angles) are usually measured as body-centred angular distances to a vector. Each such vector measurement provides only two of the three independent parameters needed to specify the orientation of the spacecraft. For many spacecraft, the ADCS must control vehicle attitude during firing of large liquid or solid rocket motors, which may be used during orbit insertion or for orbit changes. Large motors create large disturbance torques, which can drive the design to larger actuators than are needed one on station. Once the spacecraft is on station, the payload pointing requirements usually dominate. These may require Earth relative or inertial attitudes, and fixed or spinning field of view. In addition, we must define the need for and frequency of attitude slew manoeuvres. Such manoeuvres may be necessary to:

- Re-point the payload's sensing system to targets of opportunity
- Manoeuvre the attitude control system's sensors to celestial targets for attitude determination
- Track stationary or moving targets
- Acquire the desired satellite attitude initially or after a failure

ADCS is often considered the most complex and least intuitive of the space vehicle design disciplines, but most significant features of ADCS design can be understood in terms of rigid body rotational mechanics modified by the effects of flexibility and internal energy dissipation. Attitude dynamic analysis is necessarily complex due to attitude information inherently vectorial, requiring three coordinates for its complete specification; with rotating, hence not inertial, frames and rotations are inherently order dependent in their description.

ADCS is typically a major vehicle subsystem, with requirements that quite often drive the overall spacecraft design. Its components tend to be relatively massive, power consuming, and demanding for specific orientation, alignment tolerance, field of view, structural frequency response, and structural damping.

3.1. Design Process

A complex system such this needs clearly to identify what is the design process of the system, which steps, inputs and outputs are required. Especially in the space field, it must follow exactly procedures in order to consider all possible issues and requirements. The following figure show a summary of the ADCS Design Process:

	Step	Inputs	Outputs	Example
1a	Define Control Modes	<ul style="list-style-type: none"> Mission requirements Mission profile Type of insertion for launch vehicle 	<ul style="list-style-type: none"> List of different control modes during mission 	<ul style="list-style-type: none"> Orbit Injection: none-provided by launch vehicle Nominal: nadir pointing, <0.2°; autonomous determination (Earth relative) Operation slew: one 30° manoeuvre per month to a target of opportunity
1b	Define or derive system level requirements	<ul style="list-style-type: none"> Mission requirements Mission profile Type of insertion for launch vehicle 	<ul style="list-style-type: none"> Requirements and constraints 	
2	Select type of spacecraft Control	<ul style="list-style-type: none"> Payload, thermal and power needs: Orbit, pointing direction Disturbance environment 	<ul style="list-style-type: none"> Method for stabilizing and control: 3-axes, spinning, or gravity gradient 	<ul style="list-style-type: none"> Momentum bias stabilization with a pitch wheel, electro-magnets for momentum dumping, and optionally, thrusters for slewing (shared with ΔV system in navigation)
3	Quantify disturbance environment	<ul style="list-style-type: none"> Spacecraft geometry and mass properties, Orbit Solar/magnetic models Mission profile 	<ul style="list-style-type: none"> Values for forces from gravity gradient, magnetic, aerodynamics, solar pressure, internal disturbance, and powered flight effects on control 	<ul style="list-style-type: none"> Gravity gradient: $1.8e^{-6}$ Nm normal pointing; $4.4e^{-5}$ Nm during target-of-opportunity mode Magnetic: $4.5e^{-5}$ Nm Solar: $6.6e^{-6}$ Nm Aerodynamic: $3.4e^{-6}$ Nm
4	Select and size ADCS Hardware	<ul style="list-style-type: none"> Spacecraft geometry, and mass properties, Pointing accuracy, Orbit condition, Mission requirements 	<ul style="list-style-type: none"> Sensor suite: Earth, Sun inertial, or other sensing devices Control actuators, reaction wheels, thrusters, or magnetic torquers Data processing requirements for other subsystems or ground computer 	<ul style="list-style-type: none"> Momentum Wheel, momentum 40 Nms Horizon sensors, scanning 0.1° accuracy Electromagnets, dipole moment 10 Am² Sun Sensors, 0,1° accuracy 3-axes magnetometer, 0.1°
5	Define determination	<ul style="list-style-type: none"> All of above 	<ul style="list-style-type: none"> Algorithms, Parameters Logic for each determination Control mode 	<ul style="list-style-type: none"> Determination: horizon data filtered for pitch and roll. Magnetometer and Sun Sensors used for yaw

	and control algorithms			<ul style="list-style-type: none"> Control: proportional-plus-derivative for pitch, coupled roll-yaw control with electromagnets
6	Iterate and document	<ul style="list-style-type: none"> All of above 	<ul style="list-style-type: none"> Refined requirements Design subsystem specification 	

Table 1 - Design Process

3.2. Attitude Control Modes

In general, the control modes are not a lot, and it is preferable to have few of them, because it will be easier to control them. We can define:

- Orbit insertion**
 Period during and after boost while spacecraft is brought to final orbit. Options include no spacecraft control, simple spin stabilization of solid rocket motor, and full spacecraft control using liquid propulsion system.
- Acquisition**
 Initial determination of attitude and stabilization of vehicle. Also, may be used to recover power upsets or emergencies.
- Nominal/On-Station**
 Used for the vast majority of the mission. Requirements for this mode should drive system design.
- Slew**
 Reorienting the vehicle when required.
- Contingency/Safe**
 Used in emergencies if regular mode fails or is disabled. May use less power or sacrifice nominal operation to meet power or thermal constraints.
- Special**
 Requirements may be different for special targets or time periods, such as eclipses.

3.3. Disturbance Torques

Even if the space looks like empty, there are a lot perturbation which can disturb and compromise the attitude control; they are torques, which push and move for several

reasons the satellite. A body in space is subject to small but persistent disturbance torques (e.g., 1054Nm) from a variety of sources. These torques are categorized as cyclic, varying in a sinusoidal manner during an orbit, or secular, accumulating with time, and not averaging out over an orbit. These torques would quickly reorient the vehicle unless resisted in some way. An ADCS system resists these torques either passively, by exploiting inherent inertia or magnetic properties to make the "disturbances" stabilizing and their effects tolerable, or actively, by sensing the resulting motion and applying corrective torques. We have:

- **Aerodynamic Torque** due to the tiny existent density of the atmosphere

The role of the upper atmosphere in producing satellite drag was already mentioned in connection with orbit decay. The same drag force will, in general, produce disturbance torque on the spacecraft due to any offset that exists between the aerodynamic centre of pressure and the centre of mass. Assuming r_{cp} to be the centre of pressure (CP) vector in body coordinates, the aerodynamic torque is:

$$\vec{T}_a = \vec{r}_{cp} \times \vec{F}_a \quad \text{with} \quad \vec{F}_a = \frac{1}{2} \rho V^2 S C_D \vec{V}$$

Drag coefficient uncertainties can easily be of order 50%, while upper atmosphere density variations approaching an order of magnitude relative to the standard model are not uncommon. Thus, if aerodynamic torques are large enough to be a design factor for the attitude control system, they need to be treated with appropriate conservatism.

- **Sun Torque** due to the solar pressure caused by the solar radiation.

Solar radiation torque is independent of spacecraft position or velocity, as long as the vehicle is in sunlight, and is always perpendicular to the sun line. It will, in many cases, thus have no easily visualized relationship with the previously considered aerodynamic and gravity gradient disturbance torques. As noted, however, the solar torque is independent of position, while the aerodynamic torque is proportional to atmospheric density. Above 1000km altitude, solar radiation pressure usually dominates the spacecraft disturbance torque environment.

$$\vec{T}_s = \vec{r}_{sp} \times \vec{F}_s$$

With

\vec{r}_{sp}
= vector from body centre of mass to satellite optical centre of pressure

$$F_s = (1 + K)p_s A_{\perp}$$

$K = \text{satellite surface reflectivity}, \quad 0 < K < 1$

$A_{\perp} = \text{satellite projected area normal to sun vector}$

$$p_s = \frac{I_s}{c} \quad \text{with } I_s = 1370 \frac{W}{m^2} \text{ to } 1 \text{ AU} \quad c = 2.9979 * 10^8 \frac{m}{s}$$

At geostationary orbit altitude, solar radiation pressure can be the primary source of disturbance torque, and designers must take care to balance the geometrical configuration to avoid centre of mass to centre of pressure offsets. The useful lifetime of a geostationary satellite is often controlled by the mass budget available for station keeping and attitude control fuel. Poor estimates of the long-term effect of disturbance torques and forces can and do result in premature loss of on orbit capability.

- **Gravity Gradient Torque** due to the earth mass, as consequence gravity attraction.

Planetary gravitational fields decrease with distance r from the centre of the planet according to the Newtonian $1/r^2$ law, provided higher order harmonics are neglected. Thus, an object in orbit will experience a stronger attraction on its "lower" side than on its "upper" side. This differential attraction, if applied to a body having unequal principal moments of inertia, results in a torque tending to rotate the object to align its "long axis" (minimum inertia axis) with the local vertical. Perturbations from this equilibrium produce a restoring torque toward the stable vertical position, causing a periodic oscillatory or "vibrational" motion. Energy dissipation in the spacecraft will ultimately damp this motion. The gravity gradient torque for a satellite in a near-circular orbit is:

$$\vec{T}_g = 2n^2 \hat{r} \times [I_{Sat}] \hat{r}$$

With

$$\hat{r} = \frac{\vec{r}}{r}$$

$$n^2 = \frac{\mu}{a^3} = \frac{\mu}{R^3} = \text{orbital rate}$$

$\mu = \text{gravitation constant}$

$I_{Sat} = \text{satellite inertia matrix}$

- **Magnetic Torque** due to the influence by earth magnetic field. The magnetic torque on the satellite is given by:

$$\vec{T}_m = \vec{M} \times \vec{B}$$

M is the spacecraft magnetic dipole moment due to current loops and residual magnetization in the spacecraft, measured in Am^2 per turns. B is the Earth magnetic field vector expressed in spacecraft coordinates, and measured in tesla, T; its magnitude is proportional to the magnetic moment of the Earth ($7.96 \times 10^{22} \text{ Tm}^3$) and to $1/r^3$, where r is the radius vector to the spacecraft.

Earth's magnetic field at an altitude of 200 km is approximately 0.3 G or 3×10^{-5} T. A typical small spacecraft might possess a residual magnetic moment on the order of 0.1 Am^2 . The magnetic torque on such a spacecraft in low orbit would then be approximately $3 \times 10^{-6} \text{ Nm}$.

Magnetic torque may well be a disturbance torque. However, it is common to reverse the viewpoint and take advantage of the planetary magnetic field as a control torque to counter the effects of other disturbances.

3.4. ADCS Architecture

Since disturbance torques cannot be completely eliminated, we can say that every spacecraft will need to be provided with an attitude control system. Tasks of this system is to generate control torques to contrast (at least) disturbance torques. The attitude determination and control system encompass both the hardware and the process by means of which the attitude is determined and controlled. In general, every ADCS is constituted by:

- **Attitude sensors**, whose task is to determine the position of a reference body (Sun, Earth, etc..) with respect to the spacecraft in order to define its attitude;
- Process or **Control Law**, whose task is to determine when the control must operate, which control torques must be generated and how they can be activated;
- Control Hardware or **Actuators**, which supply the control torques.

Attitude control systems can be classified as **Active systems** and **Passive systems**. Moreover, the active attitude control systems (more correctly called ADCS) can be classified as open loop control system or closed loop control system.

Passive stabilization techniques take advantage of basic physical principles and naturally occurring forces by designing the spacecraft to enhance the effect of one force while reducing others. In effect, we use the disturbance torques to control the spacecraft, choosing a design to emphasize one and mitigate the others. This kind of control method uses the interaction between the spacecraft and natural phenomena happening in the operational environment (depending on the particular mission), and/or uses the mass characteristics of the spacecraft itself.

The basic concept of active attitude control is that the spacecraft attitude is measured and compared with a desired value. The error signal so developed is then used to determine a corrective action (control torque) to generate a manoeuvre by means of the on-board actuators.

Advantages and disadvantages of active and passive control system:

- **Active Control Systems**

Advantages are the very high pointing accuracy and the very high attitude rate of change which can be obtained.

Disadvantages are the cost, the technical complexity and usually the limited life.

- **Passive Control Systems**

Major *advantage* of every passive control system is the ability to obtain a very long spacecraft lifetime, not limited by on-board consumables or, possibly, even by wear and tear on moving parts.

Disadvantages are the low pointing accuracy that can be attained and the impossibility to change in response of external events. Moreover, we should remember that natural phenomena can change with time, for example during an orbit time. This fact can cause a passively stabilized spacecraft to experience unexpected motions, such as oscillations. In most cases a passive control system includes also some processes and devices devoted to the damping of undesired effects.

3.4.1. Passive Methods

A basic passive technique is that of **Spin Stabilization**, where in the intrinsic gyroscopic stiffness of a spinning body is used to maintain its orientation in inertial space. If no external disturbance torques are experienced, the angular momentum vector remains fixed in space, constant in both direction and magnitude. If a nutation angle exists, either from initial conditions or as the result of a disturbance torque, a properly designed energy damper will quickly (within seconds or minutes) remove this angle, so that the spin axis and the angular momentum vector are coincident. An applied torque will, in general, have components both perpendicular and parallel to the momentum vector. The parallel component spins the spacecraft causing a displacement of H in the direction of T. This is illustrated in the figure below, where the external force F causing the torque T is perpendicular to the plane containing H. Note then that ΔH , while parallel to T, is perpendicular to the actual disturbance force F, since:

$$\vec{T} = \vec{r} \times \vec{F}$$

The magnitude of the angular momentum displacement is found from:

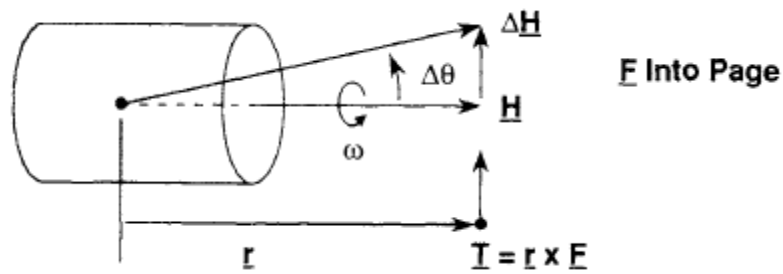


Figure 10 - Angular Momentum Theory

$$\frac{dH}{dt} = T = rF \cong \frac{\Delta H}{\Delta t}$$

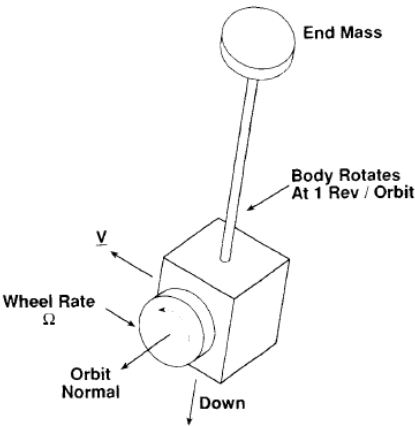
$$\Delta H = 2H \sin\left(\frac{\Delta\theta}{2}\right) \cong H\Delta\theta = I\omega\Delta\theta$$

$$\Delta\theta \cong \frac{rF\Delta t}{H} = \frac{rF\Delta t}{I\omega}$$

The higher the angular momentum value, the smaller the perturbation angle $\Delta\theta$ that a given disturbance torque will introduce.

A spacecraft in a reasonably low orbit will tend to stabilize with its minimum inertia axis in a vertical orientation, that is **Gravity Gradient Stabilisation**. This property can obviously be used to advantage by the designer when a nadir or zenith orientation is desired for particular instruments. The principal design feature of such a satellite again involves the inertia ratio; the vehicle must possess an axis such that $I_z \ll I_x, I_y$. Even when the spacecraft is designed in this fashion, the control torques are small, and additional damping is required to remove pendulum like oscillations due to disturbance. These oscillations, or vibrations, are typically controlled through the use of magnetic hysteresis rods or eddy current dampers. Active “damping” (really active control) is also possible and, as might be expected, typically offers better performance. The usual way of obtaining the required spacecraft inertia properties (i.e., long and thin) is to deploy a motor driven boom with a relatively heavy (several kilograms or more) and mass. The “boom” will often be little more than a reel of pre-stressed metallic tape, similar to the familiar carpenter’s measuring tape, which when unrolled springs into a more or less cylindrical form. Such an “open stem” boom will have substantial (for its mass) lateral stiffness, but little torsional rigidity. The possibility of coupling between easily excited, lightly damped torsional modes and the vibrational modes then arises, and often cannot be analytically dismissed. Again, careful selection of damping mechanism is required. Pure gravity gradient attitude control provides no inherent yaw stability; the spacecraft is completely free to rotate about its vertical axis.

When this is unacceptable, additional measures must be taken. One possibility is to add a momentum wheel with its axis perpendicular to the spacecraft vertical axis:



A stable condition then occurs with the wheel angular momentum aligned along the positive orbit normal. Such a configuration has been flown on numerous satellite, though not with uniform success. Large amplitude vibrations are sometimes observed, often during particular orbital “seasons” (i.e., sun angles). Oscillations of sufficient magnitude to invert the spacecraft gravity gradient boom that are excited by solar thermal input under the right conditions. Gravity gradient stabilization is useful when long life on orbit is needed and

attitude stabilisation requirements are relatively broad. Vibration amplitudes of 10-20° are not uncommon, although better performance can be obtained with careful design.

Passive magnetic methods are other means of stabilisation for simple spacecraft. Permanent magnets can be used to align one of the body axes with the lines of the Earth’s magnetic field. Same advantages and disadvantages as for the gravity gradient stabilisation method apply. This is most effective in near-equatorial orbits where the field orientation stays almost constant for an Earth pointing vehicle.

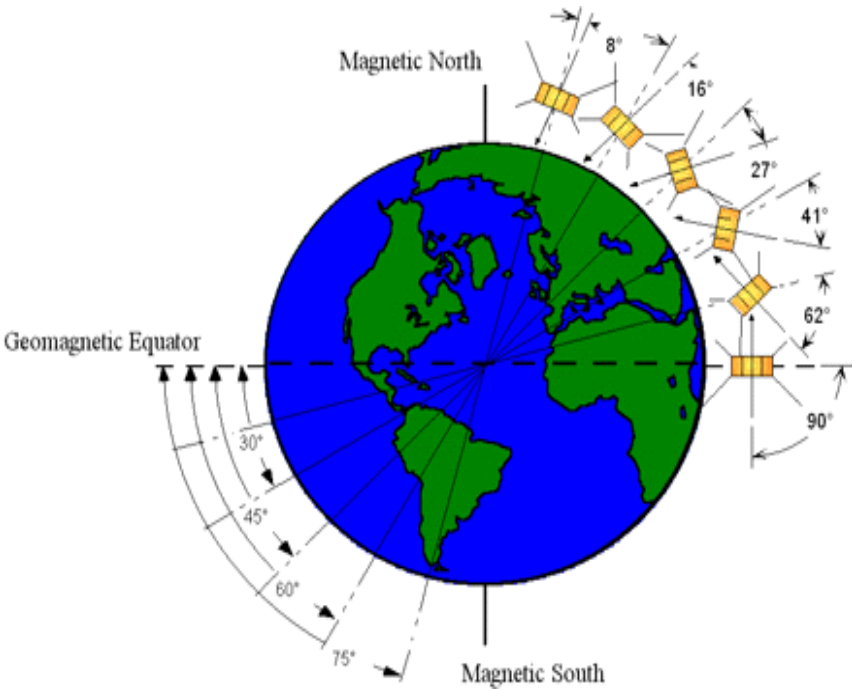


Figure 11 - Satellite using the Earth's magnetic field

The existence of aerodynamic and solar radiation pressure torques implies their use in spacecraft control. This has in fact been accomplished, although the flight history is considerably reduced compared to the gravity gradient and magnetic cases.

3.4.2. Active Methods

The basic concept of active attitude control is that the spacecraft attitude is measured and compared with a desired value. The error signal so developed is then used to determine a corrective action (control torque) to generate a manoeuvre by means of the on-board actuators.

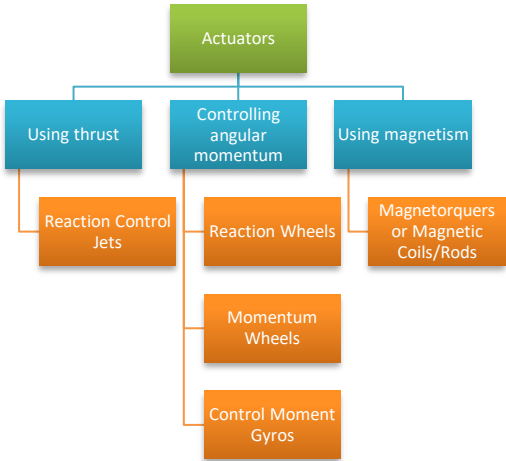


Figure 12 - Actuators Classification Available

The most common actuator for controlling attitude is actually a family of systems that all rely on **Angular Momentum**. The momentum control devices (reaction wheels, momentum wheels, control moment gyroscopes) actively vary the angular momentum of small masses within the spacecraft to change attitude.

Reaction Wheels are a common choice for active spacecraft attitude control, particularly with unmanned spacecraft. In this mode of control an electric motor attached to the spacecraft spins a small, freely rotating wheel, the rotational axis of which is aligned with a vehicle control axis. The spacecraft must carry one wheel per axis for full attitude control. Some redundancy is usually desired, requiring four or more wheels. The electric motor drives the wheel in response to a correction command computed as part of the spacecraft’s feedback control loop. Reaction wheels give very fast response relative to other systems. Reaction wheels are fairly heavy, cumbersome, expensive, and are potentially complex, with moving parts. They are capable of generating internal torques only; the wheel and spacecraft together produce no net system torque. With such a system, the wheel rotates one way and the spacecraft the opposite way in response to torques imposed externally on the spacecraft. From application of Euler’s momentum equation, the integral of the net torque applied over

a period of time will produce a particular value of total angular momentum stored on-board the spacecraft, resident in the rotating wheel or wheels, depending on how many axes are controlled. When it is spinning as fast as it compensates external torques. If further such torques are applied, the spacecraft will tumble. In practice it is desirable to avoid operation of a reaction wheel at speeds near saturation, not only because of the limited control authority but also because of the substantial jitter that is typically generated by an electric motor operating at maximum speed.

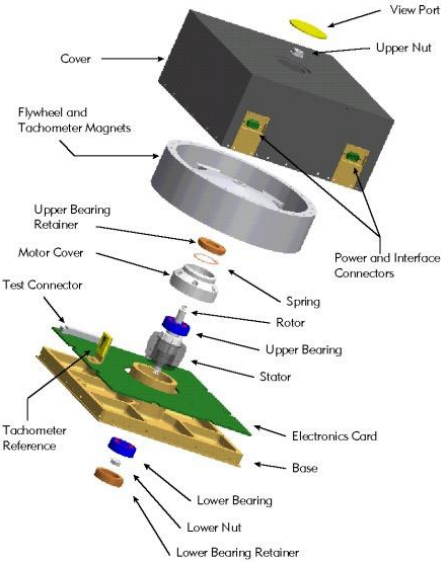


Figure 13 - Exploded Visualisation of a Reaction Wheel

A reaction wheel does not normally spin until the spacecraft needs to be reoriented or an outside torque is applied. When the spacecraft needs to slew to a new location or in response to outside torques. Without any outside torques the total angular momentum of the spacecraft (including the reaction wheels) is conserved. Thus, the angular momentum of the spacecraft plus the angular momentum of reaction wheels must add up to a constant vector quantity. Imagine one of the wheels being spun up using a motor. As the wheel’s rotation rate increases, its angular momentum also increases. But the total angular momentum of the wheel and the spacecraft must always sum to a constant value. We can express the total angular momentum of the spacecraft as:

$$\vec{H}_{tot} = \vec{H}_{Sat} + \vec{H}_{RWS}$$

If the reaction wheel is spun up, its angular momentum increases by an amount $\Delta\vec{H}_{RWS}$. Because the total angular momentum must stay constant, the spacecraft’s angular momentum must automatically decrease to compensate by a corresponding amount $\Delta\vec{H}_{Sat}$.

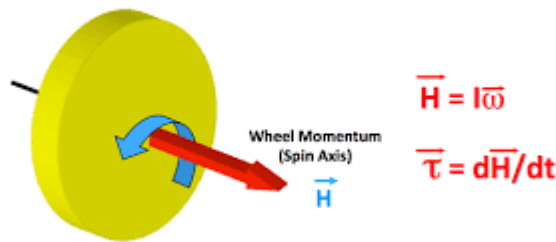


Figure 14 - Reaction Wheel momentum

To conserve momentum, the spacecraft must either slow its rotation or start rotating in the opposite direction. In either case, the spacecraft’s attitude has changed simply by spinning up a small mass inside.

Because reaction wheels can only store, and not remove, the sum of environmental torques imposed on the spacecraft, it is necessary periodically to impose upon the spacecraft a counteracting external torque to compensate for the accumulated on-board momentum. Known as “momentum dumping”, this can be done by magnetic torquers (useful in LEO) or control jets (in high orbit or about planets not having a magnetic field). Magnetic torqueing as a means of momentum dumping is greatly to be preferred, because when jets are used, the complexities of a second system and the problems of a limited consumable resource are introduced indeed, in many cases when jets must use, reaction wheels will lose much of their inherent utility, and the designer must weigh their drawbacks against their many positive features, among which are precision and reliability, particularly in the newer versions that make use of magnetic rather than mechanical bearings.

A reaction wheel operating about a given spacecraft axis has a straightforward control logic. If an undesirable motion about a particular axis is sensed, the spacecraft commands the reaction wheel to rotate in countervailing sense. The correction torque is computed as an appropriately weighted combination of position, the larger will be the computed correction torque.

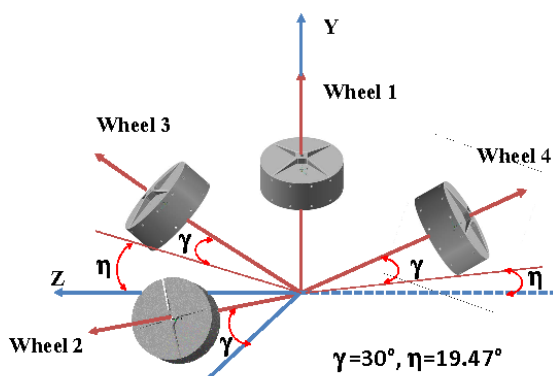


Figure 15 - Tetrahedron Configuration

As long as all of the axes having reaction wheels are mutually orthogonal, the control laws for each axis will be simple and straightforward. If full redundancy is desired, however, this approach has the disadvantage of requiring two wheels for each axis, bringing a penalty in power, weight, and expense to operate the system. A more common approach today is to mount four reaction wheels in the

form of a tetrahedron, coupling all wheels into all spacecraft axes. Any three wheels can then be used to control the spacecraft, the fourth wheel being redundant, allowing failure of any single wheel while substantially increasing momentum storage when all wheels are working. Thus, the system can operate for a longer period before needing to dump momentum.

Although reaction wheels operate by varying wheel speed in response to the imposition of external torques, that does not mean that the average speed of the wheels must necessarily be zero. The wheels can also be operated around a nominal low speed (possibly a few rpm) in what is called a momentum-bias system. The momentum-bias configuration has several advantages. It avoids the problem of having the wheel go through zero speed from, say, a minus direction to a plus direction in response to torques on the spacecraft. This in turn avoids the problem of sticking friction (stiction) on the wheel when it is temporarily stopped.

Because of the nonlinearity of the stiction term, the response of wheels to a control torque will be nonlinear in the region around zero speed, imposing a jerking or otherwise irregular motion on the spacecraft as it goes through this region. If this poses a problem in maintaining accurate, jitter-free control of the spacecraft then the system designer may favour a momentum-bias system, which avoids the region around zero. As a disadvantage, limit is reached, forcing momentum to be dumped from the spacecraft more frequently.

When a reaction wheel is intended to operate at relatively high speed (perhaps several tens of revolutions per minute), then a change of both terminology and control logic is employed. The spacecraft is said to possess a **Momentum Wheel**; a tachometer-based control loop maintains wheel speed at a nominally constant value with respect to the spacecraft body. This speed is adjusted slightly up or down in response to external torques. When the range of these adjustment exceeds what the control system designer has set as the limit, momentum dumping allows the wheel speed to be brought back into the desired range. When magnetic coils are used to unload the wheel, this is done more or less continuously, so that the tachometer circuit can operate around an essentially constant nominal value.

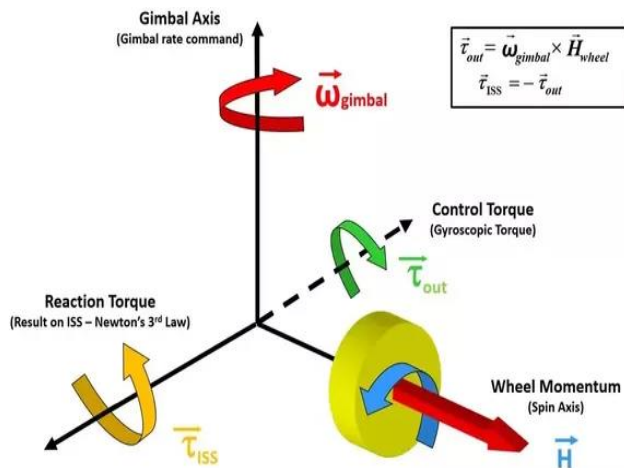


Figure 16 - Momentum Wheel Dynamics

Use of the momentum wheel on a spacecraft offers the advantage of substantial gyroscopic stability. That is, a given level of disturbance torque will produce a much smaller change in desired nominal position of the spacecraft, because of the relatively small percentage change it makes in the total spacecraft angular momentum vector. For this reason, momentum-wheel systems are generally confined to use on spacecraft requiring a relatively

consistent pointing direction.

An example might be a low orbit satellite where it is desired to have the vehicle angular momentum vector directed more or less continuously along the positive orbit normal, and to have the body of the spacecraft rotate slowly (i.e., 0.000175 Hz) to keep one side always facing the Earth. Use of a momentum wheel on the spacecraft aligned with its angular momentum vector along the orbit normal would be a common approach to such a requirement. The tachometer wheel control loop would function to keep the slowly rotating body facing correctly toward Earth. The momentum wheel system described represents an attitude control design referred to as dual-spin configuration.

Momentum wheel can be used in yet another configuration, as **Control Moment Gyros (CMG)**. The CMG is basically a gimbaled momentum wheel with the gimbal produces a change in the angular momentum perpendicular to the existing angular momentum vector \vec{H} , and thus a reaction torque on the body. Control moment gyros are relatively heavy, but can provide control authority higher by a factor of 100 or more than can reaction wheels. Because they offer much higher slew rates than reaction wheels, at comparable pointing accuracy, they are especially useful for tracking objects. Besides imposing a weight penalty, CMGs tend to be relatively noisy in an attitude control sense, with resonances at frequencies that are multiples of the spin rate. Because of their expense and complexity, CMGs are used only on systems that require extremely accurate pointing and tracking. In many

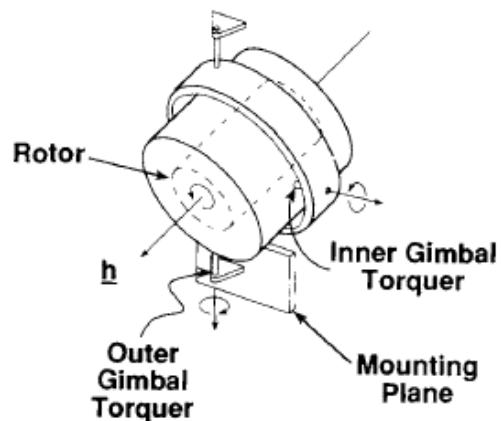


Figure 17 - CMG Dynamic

applications, however, CMGs offer an excellent high authority attitude control mechanism without the use of consumables such as reaction gas.

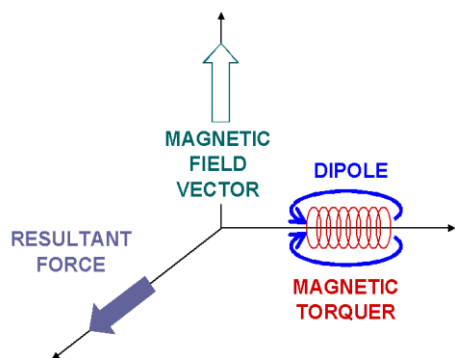


Figure 18 - Magnetorquers Dynamic

Running an electrical current around a piece of metal on-board creates an electromagnet. This electromagnet interferes with the external Earth's magnetic field trying to align itself to the magnetic field lines, dragging the rest of the spacecraft along with it.

They are the **Magnetorquers**, which offers a relatively cheap and simple way to control a spacecraft attitude. Furthermore, because they run on electrical power which is usually available, they are inexhaustible, unlike thrusters. However, they have two main limitation:

- Because their effectiveness depends directly on the strength of the external magnetic field, they become less and less useful in higher orbits;
- They are not very accurate ($\pm 30^\circ$ is the best they can do alone)

A spacecraft orbiting at relatively low altitude about a planet with an appreciable magnetic field can make effective use of magnetorquers, especially for initial attitude acquisition manoeuvres and for dumping excess angular momentum from reaction wheels. They prove particularly advantageous when the burden of carrying consumables, such as fuel for reaction jets, would be an impediment in spacecraft design or when exhaust gas flowing from such jets might contaminate or otherwise harm the spacecraft. A classic example in this regard, the HST, must have its primary mirror kept as clean as possible. As drawbacks, magnetorquers have relatively low control authority and can interfere with other components on the spacecraft.

Reaction Control Jets (Thrusters) are a common and effective means of providing spacecraft attitude control. They are standard equipment on manned spacecraft because they can quickly exert large control forces. They are also common on the

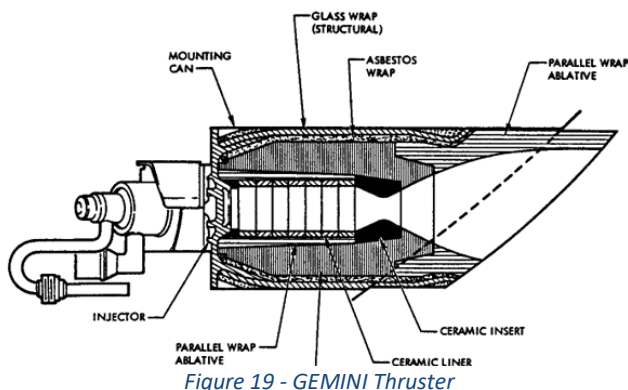


Figure 19 - GEMINI Thruster

satellites intended to operate in relatively high orbit, where a magnetic field will not be available for an angular momentum dumping. Offsetting these advantages, reaction control jets use consumables, such as a neutral gas (e.g., Freon or nitrogen) or hydrazine in either monopropellant or bipropellant

systems. Normally on/off operated, they do not readily lend themselves to proportional control, although that is possible by using pulse lengths of varying duration or mic of control jets, not all of which need to be used in every situation. It is usually not acceptable to have only one jet functioning for a given control axis, because its failure will leave the spacecraft disabled in that axis. Thus, jet control systems usually require redundant thrusters, which leads to complex plumbing and control. It is a very expensive system, both for the hardware and for the operations. Also, when attitude jets are used, there will likely be some coupling between the attitude and translation control systems. Unless a pure couple is introduced by opposing jets about the spacecraft's centre of mass, the intended attitude control manoeuvre will also produce a small component through the spacecraft's centre of mass. This will result in an orbital perturbation. We consider them to be:

- A *Hot Gas System*, either bipropellant or monopropellant, when a chemical reaction produces the energy
- A *Cold Gas System*, when energy comes from the work of compression without a phase change. Cold gas system usually applies to small spacecraft and low impulse requirements.

3.4.3. Attitude Determination

Attitude Determination is the process of deriving estimates of actual spacecraft attitude from measurements. Note that we use term "estimates". Complete determination is not possible; there will always be some error. ADCS engineers treat two broad categories of attitude measurements. The first single axis attitude determination, seeks the orientation of a single spacecraft axis in space (often, but not always, the spin axis of either a simple spinner or a dual spin spacecraft). The other, three axis attitude determination, seeks the complete orientation of the body in inertial space. This may be thought of as single axis attitude determination plus rotational, or clock, angle about that axis. **Single Axis Attitude** determination results when sensors yield an arc length measurement between the sensor boresight and the know reference point. The reference point may be the sun, the Earth nadir position, the moon, or a star. The crucial point is that only an arc length magnitude is known, rather than theoretically requires three independent measurements to obtain a sufficient number of parameters for the measurement. In practice, the engineer often selects two independent solutions caused by the under specification of parameters. The most common scheme entails using an a priori estimate of the true attitude and choosing the measurement that comes closest to the assumed value. To use the **Three Axis Attitude** determination requires two vectors that can be measured in the spacecraft body frame and have known vectors include, again, the sum the stars, and the Earth nadir. The key lies in the type of sensor used to compute the measurement rather than in the nature of the reference point. The sensor must measure not merely a simple boresight error,

as in single axis attitude determination, but two angular components of the error vector. The third vector component is known since only unit vectors need be considered in spacecraft attitude control.

Sensor	Typical Performance Range	Weight Range (kg)	Power Range (W)
Inertial measurement unit (Gyros and Accelerometers)	Gyro drift rate = 0.002 to 1 deg/hr	1 to 15	10 to 200
Sun sensors	Accuracy = 0.005 to 3 deg	0.1 to 2	0 to 3
Star sensors (Scanners and Mappers)	Attitude accuracy = 1 arc sec to 1 arc min (0.0003 to 0.01 deg)	2 to 5	5 to 20
Horizon Sensors <ul style="list-style-type: none"> • Scanner/pipper • Fixed head 	Attitude accuracy: <ul style="list-style-type: none"> • 0.1 to 1 deg (LEO) • < 0.1 to 0.25 deg 	<ul style="list-style-type: none"> • 1 to 4 • 0.5 to 3.5 	<ul style="list-style-type: none"> • 5 to 10 • 0.3 to 5
Magnetometer	Attitude accuracy = 0.5 to 3 deg	0.3 to 1.2	< 1

Figure 20 - Sensors Classification

Sun Sensors are visible-light detectors which measure one or two between their mounting base and incident sunlight. They popular, accurate and reliable, but require clear field of view. They can be used as part of the normal attitude determination system, part of the initial acquisition or failure recovery system, or part of an independent solar array orientation system. Since most low Earth orbits include eclipse periods, Sun Sensor based attitude determination systems must provide some way of tolerating the regular loss of this data without violating pointing constraints. Sun sensors can be near the ends of the vehicle to obtain an unobstructed field of view. Sun sensor accuracy can be limited by structural bending on large spacecraft. Spinning satellites use specially designed Sun sensors that measure the angle of the sun with respect to the spin axis of the vehicle. The data may be sent to the ground for processing or used in a closed loop control system on board the vehicle.

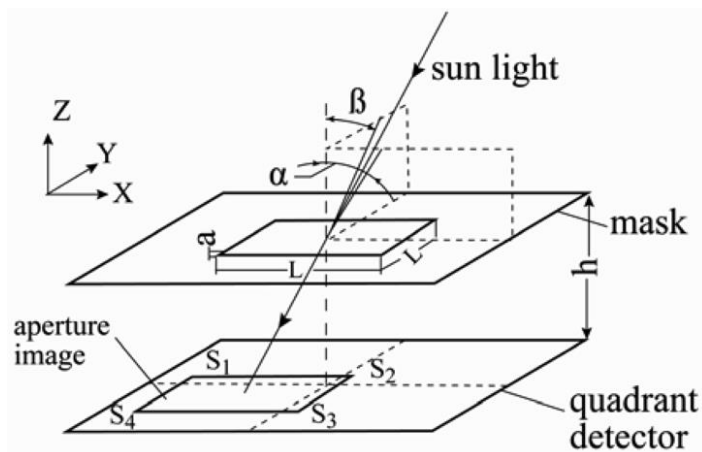


Figure 21 - Sun sensor Mechanism

There are various types of sun sensors, which differ in their technology and performance characteristics. Sun presence sensors provide a binary output, indicating when the sun is within the sensor's field of view. Analog and digital sun sensors, in contrast, indicate the angle of the sun by continuous and discrete signal outputs, respectively. In typical sun sensors, a thin slit at the top of a rectangular chamber

allows a line of light to fall on an array of photodetector cells at the bottom of the chamber. A voltage is induced in these cells, which is registered electronically, and computing an output in quaternion terms. By orienting two sensors perpendicular to each other, the direction of the sun can be fully determined. Often, multiple sensors will share processing electronics.

Star Sensors have evolved rapidly in the past few years, and represent the most common sensor for high accuracy missions. Star sensors can be scanners or trackers:

- *Scanners* are used on spinning spacecraft. Star pass through multiple slits in a scanner's field of view. After several star crossings, we can derive the vehicle's attitude.
- We use *Trackers* on 3 axis attitude stabilized spacecraft to track one or more stars to derive 2 or 3 axis attitude information. The most sophisticated units not only track the stars as bright spots, but identify which star pattern they are viewing and output the sensor's orientation compared to an inertial reference. Putting this software inside the sensor simplifies processing requirements of the remaining attitude control software.

While star sensors excel in accuracy, care is required in their specification and use. For example, the vehicle must be stabilized to some extent before the trackers can determine where they point. This stabilization may require alternate sensors. Which can increase total system cost. Also, star sensors are susceptible to being blinded by the Sun, Moon, or even planets, which must be accommodated in their application. Where the mission requires the highest accuracy and justifies a high cost, we use a combination of star trackers gyros. These two sensors complement each other nicely: the gyros can be used for initial stabilization, and during periods of sun or moon interference in the trackers, while the trackers can be used to provide a high accuracy,

low frequency, external reference unavailable to the gyros. Work continues to improve the sample rate of star trackers and to reduce their radiation sensitivity.

Horizon sensors are infrared devices that detect the contrast between the cold of deep space and the heat of the Earth's atmosphere (about 40 km above the surface in the sensed band). Simple narrow field of view fixed-head types (called pippers or *horizon crossing indicators*) are used on spinning spacecraft to measure Earth phase and chord angles which, together with orbit and mounting geometry, define two angles to the Earth (nadir) vector. *Scanning horizon sensors* use a rotating mirror or lens to replace (or augment) the spinning spacecraft body. They are often used in pairs for improved performance and redundancy. Some nadir-pointing spacecraft use *staring sensors* which view the entire Earth disk (from GEO) or a portion of the limb (from LEO). The sensor field of view stay fixed with respect to the spacecraft. This type works best for circular orbits. Horizon sensors provide Earth relative information directly for Earth-pointing spacecraft, which may simplify onboard processing. The scanning type require clear fields of view for their scan cones (typically 45, 60, 90 deg, half angle). Typical accuracies for systems using horizon sensors are 0.1 to 0.25 deg, with some applications approaching 0.03 deg. For the highest accuracy in low-Earth orbit, it is necessary to correct the data for Earth oblateness and seasonal horizon variations.

Magnetometers are simple, reliable, lightweight sensors that measure both the direction and size of the Earth's magnetic field. When compared to the Earth's know field, their output helps us establish the spacecraft's attitude. But their accuracy is not as good as that of star or horizon references. The Earth's field can shift with time and is not known precisely in the first place. To improve accuracy, we often combine their data from Sun or horizon sensors. When a vehicle using magnetic torquers passes through magnetic field reversals during each orbit, we use a magnetometer to control the polarity of the torquer output. The torquers usually must be turned off while the magnetometer is sampled to avoid corrupting the measurement.

GPS receivers are commonly known as high-accuracy navigation devices. Recently, GPS receivers has been used for attitude determination by employing the differential signals from separate antennas on a spacecraft. Such sensors offer the promise of low cost and weight for LEO missions, and are being used in low accuracy applications or as back-up sensors. Development continues to improve their accuracy, which is limited by the separation of the antennas, the ability to resolve small phase differences, the relatively long wavelength, and multipath effects due to reflections off spacecraft components.

Gyroscopes are inertial sensors which measure the speed or angle rotation from an initial reference, but without any knowledge of an external, absolute reference. We use them in spacecraft for precision attitude sensing when combined with external

references such as star or sun sensors, or, for brief periods, for nutation damping or attitude control during thruster firing. Manufacturers use a variety of physical phenomena, from simple spinning wheels (*iron gyros* using ball or gas bearings) to *ring lasers*, *hemispherical resonating surfaces*, and *laser fibre optic bundles*. The gyro manufacturers, driven by aircraft markets, steadily improve accuracy while reducing size and mass. Error models for gyroscopes vary with the technology, but characterize the deterioration of attitude knowledge with time (degrees per hour or per square-root of time). When used with an accurate external reference, such as star trackers, gyros can provide smoothing (filling in the measurement gaps between star tracker samples) and higher frequency information (tens to hundreds of hertz), while the star trackers provide the low frequency, absolute orientation information that the gyros lack. Individual gyros provide one or two axes of information, and are often grouped together as an *Inertial Reference Unit*, IRU, for three full axes. IRUs with accelerometers added for position/velocity sensing are called *Inertial Measurement Units*, IMUs.

4. CubeSat ATISE

ATISE is CubeSat 12U developed by CSUT and CSUG, with the mission to study the polar auroras and night airglows. Monitoring particle precipitation in the upper atmosphere is an important aspect of space weather studies since these particles can perturb technological systems and infrastructures on Earth and in space (satellites). These particles and especially electrons up to 10 keV, deposit their energy mainly in the 100 to 300 km range where auroras occur. These altitudes are too high for balloons which can reach altitudes up to 50 km and too low for satellites, which cannot survive for a long period at altitudes lower than 300km. This means that no long-term in-situ measurements can be made on regarding these particle precipitations. The currently available in-situ measurements have been obtained using rockets. Practically all other available data was collected by remote sensing of the ionosphere at these altitudes. Experimental techniques that target optical emissions are particularly powerful since these emissions are directly related to the excitation processes associated with the suprathermal particles.

ATISE is being conjointly developed by CSUG and CSUT. CSUG is in charge of the mission, the payload and the mission center whereas CSUT takes care of the system, the satellite's bus, the control center and the ground stations.

As a demonstration objective, ATISE's payload includes a spectrum-imager SPOC (Spectrometer on Chip), conceived by IPAG and ONERA. SPOC is based on a Fizeau interferometer and produces, from an interferogram, a spectrogram thanks to a Fourier transform.

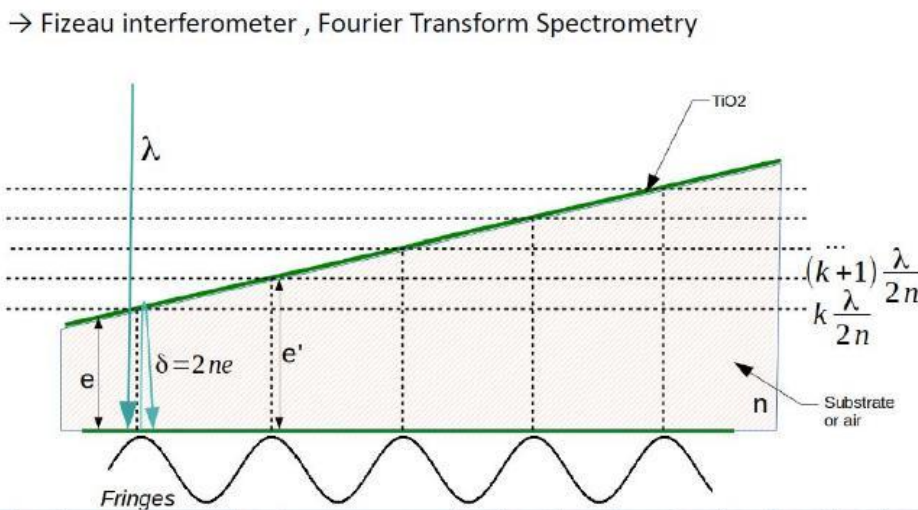


Figure 22 : Principle of a Fizeau interferometer

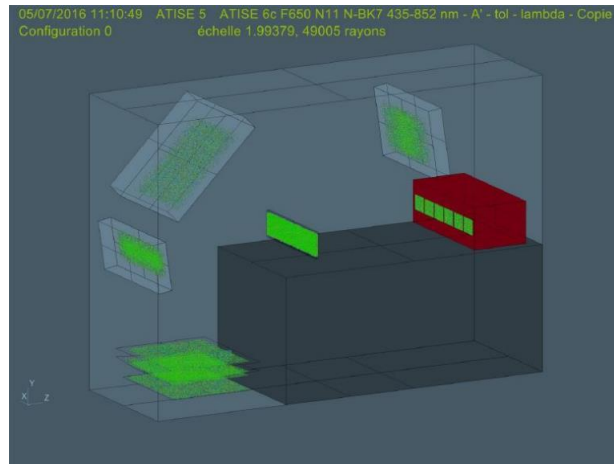


Figure 23: Payload overview

ATISE is dedicated to space meteorology (space weather) and has, as primary objective, the determination of the spectra of high-energy particles precipitating in Earth's upper atmosphere. ATISE will measure the upper atmosphere's emission spectra, and more specifically the Auroral ovals (polar light) as well as day- and nightglow. The observed spectrum will range between 380 and 900 nm. The observation region will be at altitudes between 100 and 350 km.

This leads to three major measurements:

- Long-term measurements of vertical profiles of the Auroral emission spectra
- Long-term measurements of vertical profiles of Dayglow emission spectra (lit side of the earth)
- Long-term measurements of vertical profiles of Nightglow emission spectra (dark side of the earth)

The satellite's bus is based on a 12U multi-missions CubeSat designed by CSUT, called MONA (Modular Nanosatellite).

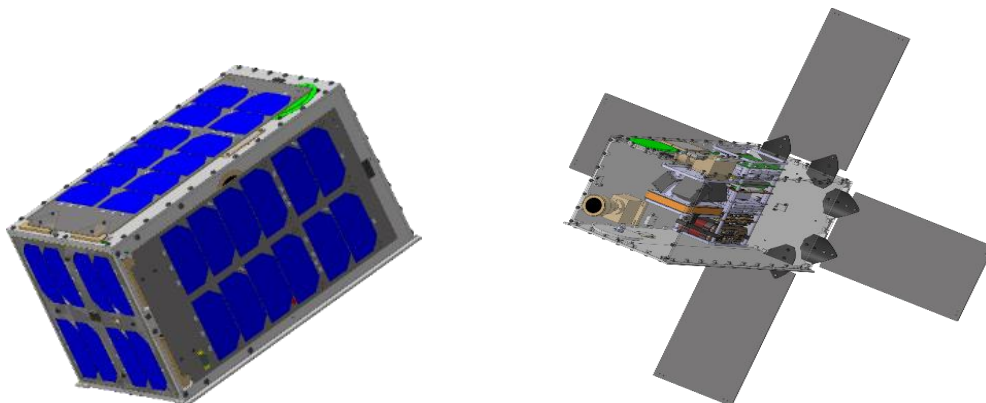


Figure 24 : MONA overview

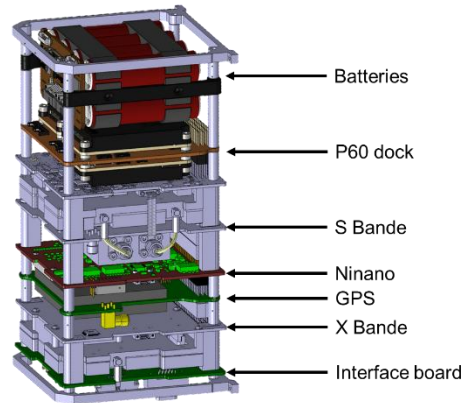


Figure 25 : MONA's avionics rack

4.1. ACDS Objectives

We have the following requirements to respect:

4.1.1. Attitude Profiles

All the requirement link to the profile which the satellite has to assume during the mission, depending on the mode used.

FUNCTION	CRITERIA	LEVEL
The bus shall prevent the payload instrument from being dazzled by the Sunlight	Minimum angle between instrument's line of sight and the direction Sun-Satellite during observations phases	60°
The bus shall prevent the payload instrument from being dazzled by the Sunlight	Minimum angle between instrument's line of sight and the direction Sun-Satellite during transmission phases	30°
The bus shall prevent the start tracker from being dazzled by the Sunlight, the Earth or the Moon	Angle between star tracker's line of sight and the direction Sun-Satellite during transmission phases	1°

Table 2 - Attitude Profiles requirements

4.1.2. Attitude Control

All the requirements link to the control and stability of the satellite, during an acquiring phase or the agility and accuracy for the pointing towards the sun or the mission objective:

FUNCTION	CRITERIA	LEVEL
The attitude of the bus is stable while acquiring	Max absolute pointing shift	0.02 °/s
The attitude of the bus is stable while acquiring	Maximum pointing knowledge	0.05°
The attitude of the bus is stable while acquiring	Pointing accuracy	0,1° Vertical ; 0,25° Horizontal
The bus can perform transitions between modes quickly	Agility	hoped 1°/s

Table 3 - Attitude Control requirements

4.2. ADCS Architecture

In this section it will be shown which actuators and sensors respect our requirements, and which are already available on market. Then, according to the ATISE mission, it will be explained for each mode, which one will be activated. At this point in the initial ADCS analysis the hardware should be chosen. Except for the high accuracy sensor that is required during imaging, a sun sensor (or sun sensors) is required if sun tracking is to be performed. Determining the sun position using the solar panels is not always feasible, since solar panels will not necessarily be on all the facets of the satellite. Both a coarse sun sensor (CSS) and a fine sun sensor (FSS) were chosen for the 20 kg satellite to enable coarse sun tracking during de-tumbling and fine sun tracking during normal operation. A 3-axis magnetometer was also added to enable magnetic control, which is to be used during de-tumbling and for managing the reaction wheel angular momentum. Although star trackers are traditionally only used on larger satellites. These advances bring forth the ability to achieve precision pointing on smaller satellites and a star tracker was thus chosen to provide accurate measurements during imaging. As mentioned before, 3-axis magnetic control will be used to manage the wheel angular momentum. The magnetorquers must thus be able to generate enough torque to overcome the disturbance torques that will cause an angular momentum build-up in the wheels.

At this point, knowing the requirements and modes, I perform a trade-off for the equipment not yet defined, contacting different producers, and asking about data sheets and properties; then I did a confront between them, and at the end I found that one matching with our requirements, and able to be fit inside our platform.

That it was performed using an excel sheet, with all the equipment available on the market, and relative properties.

Trade-off équipements SCAO									
	A	B	C	D	E	F	G	H	I
3	Magnétomètre	Fabriquant	Prix	Déjà volé ?	Fabriquant connu	Plage de mesure	Résolution	lien	commentaire
4	HMC2003 magnetic hybrid	honeywell				+/- 2G	40µG	Magnétomètre	Capteur de la HMR2300
5	HMR2300 smart digital magnetometer	honeywell				+/- 2G	<70µG	Magnétomètre	traitement de la HMC2003
6	NanoSense M315	Gomspace		non		+/- 800µT		https://gomspa	Pas de datasheet
7	New Space DS Magnetometer	New Space Systems		oui		+/- 80µT	10nT	Magnétomètre	New Space Systems\NewSpace-DS-Magnetom
9	Magnéto-coupleur	Fabriquant	Prix	Déjà volé ?		Moment dipolaire Max	Moment dipolaire Nominal	lien	commentaire
10	MTQ400.50	Hyperion technologies		non		2Am²	0,5Am²	http://hyperion	pas de datasheet
11	MTQ400.40	Hyperion technologies				1,5Am²	0,4Am²	http://hyperion	pas de datasheet
12	MAGNETORQUER ROD	New Space Systems		oui		1Am² à 100Am²		Magnéto-coupleur	sur mesure
14	Roues	Fabriquant	Prix	Déjà volé ?		Moment cinétique max	Couple max	lien	commentaire
15	NanoTorque GSW-600	Gomspace		non		60mNms	2mNm	Roues\Gomspa	sortent en avril
16	RW400 series	Hyperion technologies				15-30-60mNms	2mNm (option à 5mNm)	Roues\Hyperion\HT-RW400-V1.01	Flyer.pdf
17	SmallSat Reaction Wheel 01-00754	Clyde space	34,300 \$				40mNm	https://www.clyde.space/products/11-smallsat-reaction-wheel	
18	RWP050	Blue Canyon Tech				0,05Nms	7mNm	Roues\Blue Canyon Tech\DataSheet_RW_06 (1).pdf	
19	RWP100	Blue Canyon Tech				0,1Nms	7mNm	Roues\Blue Canyon Tech\DataSheet_RW_06 (1).pdf	
20	RW-0.03	Sinclair Interplanetary	25,000\$ each	oui		0,03Nms (pic : 0,04Nms)	+/- 2mNm à 0,02 Nms	Roues\Sinclair Interplanetary\30 mNm-sec wheel 2016a.pdf	
21	RW3-0,060	Sinclair Interplanetary	35,000\$ each	oui		0,06Nms (pic : 0,18Nms)	+/- 20mNm à 0,12Nms	Roues\Sinclair Interplanetary\60 mNm-sec wheel 2016a.pdf	
22	SatBus 4RW	Nano Avionics	4000€ per unit 15000€ system (4 wheel)			2mNms	3,2mNm	http://n-avionics.com/cubesat-components/attitude-control	
23	RW 35	Astrofein		flight proven		0,1 Nms	0,005Nm	Roues\Astrofein\Datenblatt_RW35.pdf	
24	RSI 01-5/15	Rockwell Collins		oui		0,04Nms	5mNm	https://www.rockwellcollins.com/Products_and_Services/Def	

Figure 26 - Equipment Trade Off

Obviously other requirements as power, size and avionic connection..., there were defined by other colleges working on the same project, on which I was not responsible.

4.2.1. COMAT Reaction Wheels

The configuration with three reaction wheels from Comat allows a satellite of 20 kg to turn 10° in 10s.

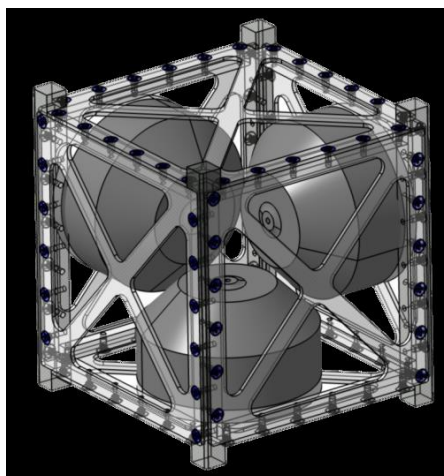


Figure 27 - Comat Reaction Wheel Unit

Performances:

Torque	Kinetic Moment	Mass	Volume	Life Expectancy	Consumption max	Precision	Data Interface	Power Interface
4 mNm	30 mNms a 6000 rpm	220 g (1 RW)	1U	>3 years at 6000 rpm	4W	5 rpm on all speed range	RS 485	14V [12V-16V]

Table 4 - Comat Reaction Wheel Performances [1]

4.2.2. New Space System Magnetorquers NTCR-M012

The NMTR is mainly constituted by a winding and a ferromagnetic bar which amplifies the magnetic effect of the winding. The dipole moment generated by the NMTR is linearly proportional to the current that flows into the winding. Consequently, if the magnetorquer rod is supplied with a controlled current through a current regulator the dipole moment generated by the NMTR is independent from temperature and from the movement of the equipment in the magnetic field.

Applying controlled voltage to the magnetorquer rod will lead to a variation of the generated dipole moment with temperature, due to the variation of winding resistance, and with the movement of the magnetorquer rod within the magnetic field, due to the movement induced voltage on the winding. Three magnetorquer bars from New Space System, each one for each axis, in the inertial satellite frame.

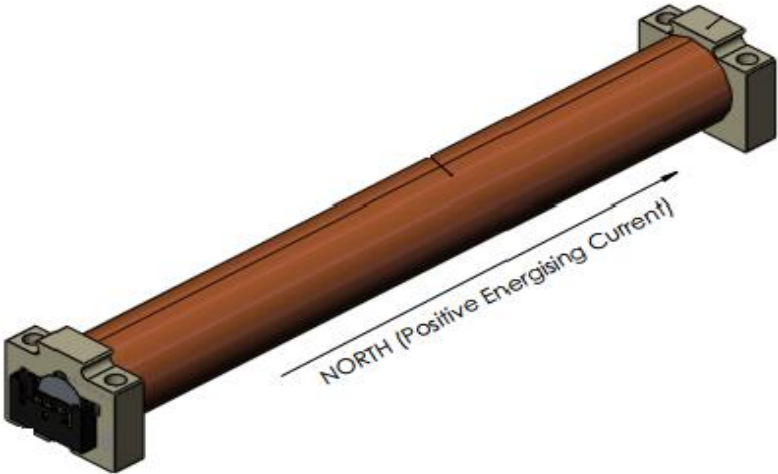


Figure 28 - NSS magnetorquer

Performances:

Nominal Dipole Moment	Nominal Resistance	Nominal Inductance	5% Linearity Limit Dipole Moment	Residual Dipole Moment	Scale Factor	Mass	Power
1.19 Am ² ± 5%	32.5 Ω ± 5%	31.5 mH ± 40%	≈1.88 Am ²	1.2 mAm ²	7.54 m ²	< 50g	<800 mW for 5V supply

Table 5 - NSS magtorquer performances [2]

The following figure shows the dipole moment variation versus current.

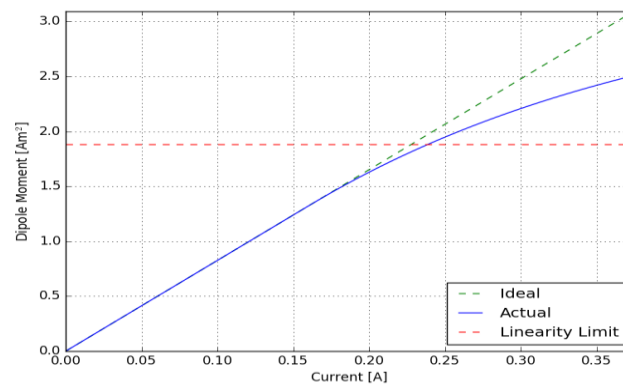


Figure 29 - The dipole moment variation versus current

4.2.3. GOM Space NanoSense FSS-4

The NanoSense FSS-4 is an ultra-compact vector sun-sensor with an I2C interface designed especially for CubeSats with high ADCS requirements. Five sun sensors are placed on each satellite faces, except for the Y+ direction.

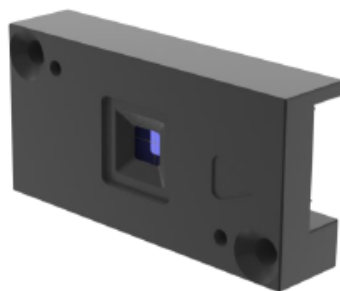


Figure 30 - GOM Space NanoSense FSS-4

Performances:

Parameter	Condition	Value
Accuracy (3σ)	FOV < 45°, No albedo	$\pm 0.5^\circ$
	FOV < 60°, No albedo	$\pm 2.0^\circ$
Sample period	Max	10 ms
Field of View	Half Angle	60°
Mass	Each one	2.2 g
Supply Voltage	Max	3.35 V

Table 6 - NanoSense performances [3]

4.2.4. ZARM AMR Magnetometer

The ZARM-Technik AMR Magnetometer is a microcontroller based Magnetometer, designed to measure the external magnetic field vector for satellite attitude determination and control. An integrated set of orthogonally arranged Anisotropic-Magneto Resistive (AMR) sensors is used to measure the magnetic field in all three directions, X, Y and Z.

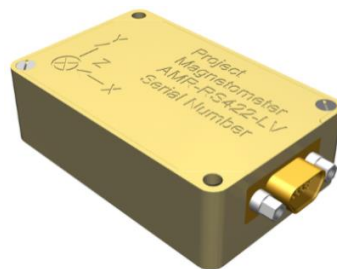


Figure 31 - ZARM AMR Magnetometer

Performances:

Number of Axes	Axial Alignment	Field Measurement Range	Scale Factor/Sensitivity	Zero Field Bias	Linearity	Accuracy	Sampling rate	Supply Voltage	Mass
Three, orthogonal	$\leq 1^\circ$	$\pm 200 \mu\text{T}$	10 nT/bit	$< \pm 350 \text{ nT}$	$< \pm 0.1\%$ (-100 to +100 μT)	$< \pm 1\%$ (-100 to +100 μT)	50,100,200 and 300 Hz	+6 V to +16 V	$\leq 60 \text{ g}$

Table 7 - AMR Magnetometer performances [4]

4.2.5. Auriga Star Tracker

A star tracker specifically designed for small satellites, it has a simple architecture, excellent robustness, fast acquisition and arcsine tracking.

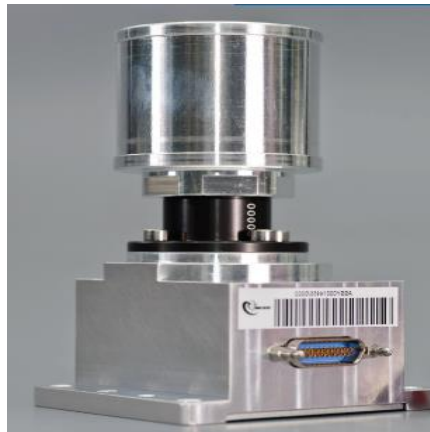


Figure 32 - AURIGA Star Tracker

Performances:

Bias	Thermo-elastic Error	FOV error	Space-time Noise XY/Z	Time from lost-in-space at EOL	Kinematics in Acq/Tracking at EOL	Full Moon in the FOV	Baffle Sun Exclusion Angle	Baffle Earth Exclusion Angle	Mass
0.03°	0.5 arcsen/°C	2/11 arcsen	6/40 Arcsen	< 11 s	Up to 0.4/3°/s according to temperature	No performance degradation	34°	29°	210 g

Table 8 - AURIGA Star Tracker performances [5]

4.3. ACDS Modes

An ADCS mode is characterized by a set of operating equipment. Thus, a transition between modes corresponds to a change of subsystem. In order to simplify the architecture, a minimum number of modes is preferable, a mode being possibly composed of different phases. A transition of phases corresponds to a change of software.

They are defined:

- Launching/End-of-Life Mode

- Safe Mode
- Mission Mode
- Standby Mode

	LM/EOL	Safe	Mission
Reaction Wheel	OFF	ON	ON
Magnetorquers	OFF	ON	ON
Sun Sensors	OFF	ON	ON
Magnetometer	OFF	ON	ON
Star Tracker	OFF	OFF	ON

Table 9 - Systems used for each Mode

4.3.1. Launch Mode and End of Life Mode (LM/EOL)

It corresponds to the launching phase, when the satellite is attached to the launcher. After the separation, an automatic transition to the safe mode shall be performed.

4.3.2. Safe Mode

After deployment from the CubeSat dispenser, the satellite has an arbitrary attitude and high angular rates due to the ejection or induced by the spinning of the launcher. During a passage to the Safe Mode the angular rates might be high and therefore the attitude arbitrary. Thus, either after the launch or in an emergency the first step is the damping of these tip-off rates.

After the damping of the angular rates, the priority is to orientate the satellite solar panels to the sun, in order to maintain stable, the vital functions of the satellite (power, thermal ...). In the first case this allows performing a set up recharge before going forward with the operations and guarantees energy availability to keep vital systems alive while failure detection and recovery is going on.

Typically, two different modes are defined for acquisition after launching and safe mode. Nevertheless, given the similarity of modes and the simplification that a minimization of the number of modes might bring it is preferable to select a single mode for these functions.

In synthesis, the two main goals of the acquisition and safe mode are:

- Damping phase: damping of the high angular rates;
- Sun pointing with lowest possible spin around the axis perpendicular to the solar panels.

4.3.3. Mission Mode

After the stabilization, the satellite has to complete the mission, that means to point regularly, each orbit, towards the:

- Auroras observation
- Air nightglows observation
- Potential transmission to the ground
- Stand-by Mode

During all these phases I had to take into account the charge of batteries as much as possible, because it cost a lot use all the equipment.

Indeed, during this phase I can use all the Reaction Wheels and Star Tracker, that allows to obtain a high level of accuracy in term of pointing, and also a higher agility to reach all the several positions.

A possible example of the orbit in mission mode it should be like that:

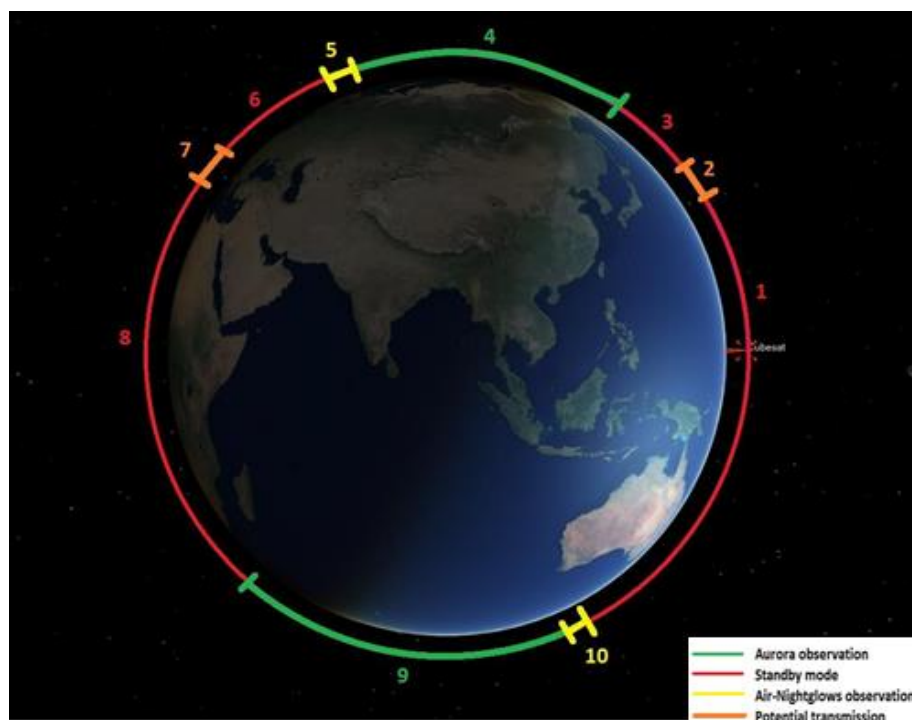


Figure 33 - Mission phases profile

4.4. ADCS Control Laws

Main part of the work was to define the control laws for each mode of the mission; it consisted into consider all the equations of motion, taking into account inputs and output variable of the whole system. So, for the development of a mathematic model is extremely useful a system block diagram to which the model refers. This diagram is a graphic representation of the cause-effect relations existents between the several quantities of the system, and what allows to have a general view of present connections between the different parts constituting it. Each block of the diagram represents a subsystem or a component, and it is built with a rectangle containing an existent functional relation between output and input variables.

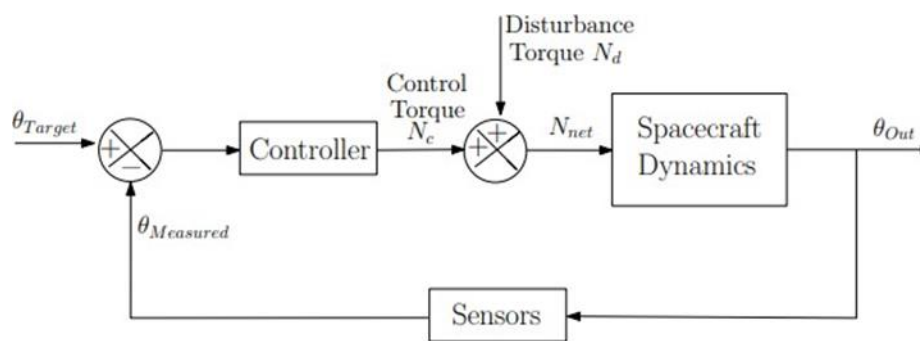


Figure 34 - Simplified dynamic feedback loop for spacecraft attitude control

As well, in these cases, it's almost mandatory to use a close-loop control scheme (Figure 18), because it measures, directly or indirectly, the controlled variables and uses the results of these measures to generate the control variables. In other words, in these systems the output is measured continuously (or periodically) and the result of the measurement is compared with the desired value that the measured quantity should take; the difference between the actual measured value and the desired one, that is the system error, is used to correct the value of an input in the direction necessary to reduce the error. In this way the measured quantity - or some other output from this employee - is forced to follow a predetermined cycle of values.

So, considering the output and input of the system, that means in our case, the data measured by the sensors (Magnetometer, Sun Sensor and only for Mission Mode the Star Tracker), the control on the actuators (Reaction Wheels and Magnetorquers), and dynamic of satellite, we can evaluate which is the best setting for the control, in order to reach the objective.

There are several ways to define the attitude of a satellite. A three-parameter set such as the Euler angle set – analogous to roll, pitch, and yaw – is attractive as it contains as many variables as degrees of freedom and is therefore easy to visualize. However, like any three-parameter set, Euler angles are subject to singularities. By contrast, Euler parameters – also known as quaternions – are a four-parameter set used to describe

spacecraft attitude. They originate from Euler's theorem that states: the most general motion of a rigid body with one point fixed is a rotation about an axis through that point. Euler parameters are advantageous for describing spacecraft attitude in that they avoid the singularities encountered with the use of three-parameter sets. They are also much more computationally efficient as they avoid complex trigonometric routines. For this reason, Euler parameters are of great interest in the field of spacecraft attitude dynamics and are used to describe the attitude. [6]

4.4.1. Euler parameter

Any two independent orthonormal coordinate frames can be related by a sequence of rotations (not more than three) about coordinate axes, where no two successive rotations may be about the same axis [7]. The angles of these three rotations are commonly defined as Euler Angles and the axes of rotation designated as axes 1, 2, and 3 or x, y, and z. The order in which the axes of rotation are taken in referred to as the Euler rotation sequence; there are twelve of these sequences: 1-2-3(x, y, z), 3-2-1 (z, y, x) and so on including all combination with no two succeeding rotations about the same axis.

Euler angles as applied to the Aerospace industries are often called the roll or bank angle, about the x axis, the pitch or attitude angle, about the y axis, and the yaw or heading angle, about the z axis; the reference, or initial, coordinate frame is frequently z axis positive down, x axis horizontal North and the y axis located to form a right handed coordinate frame. For the satellite:

- φ is roll, the rotation around the x_0 -axis.
- θ is pitch, the rotation around the y_0 -axis.
- ψ is yaw angle, the rotation around the z_0 -axis.

As such, they provide a certain level of intuitive understanding; however, they also have two inherent disadvantages:

- I. **Ambiguity** - For small values of Euler angles the Euler Rotation Sequence may not be important. However, for large angles, the rotation sequence becomes critical; for example, for a given set of three Euler angles, the result of a 1-2-3 rotation sequence is very different from that of a 3-2-1 sequence. There is no industry accepted standard rotation sequence; thus, there is an inherent risk of mistaken assumption of rotation sequence in performing analysis and communicating using Euler angles. [8]
- II. **Singularities** - Any set of Euler angles where the second rotation aligns the axes of the first and third rotations causes a singularity. For an Euler Rotation Sequence where the first and third axes are the same, called a repeated axis sequence, singularities occur for second rotation angles of zero and 180

degrees; for non-repeated axis sequences singularities occur at +/- 90 degrees. At a singularity a number of potentially disastrous effects occur, including: the first and third rotations degenerate into a single rotation and the angular derivatives, or equations of motion, become infinite. However, since, in general, all attitudes are equally likely for spacecraft, Euler angles do not lend themselves well to analysis applied to astronautics or to highly manoeuvrable aircraft. [8]

4.4.2. Unit Quaternions

The representation of relative orientation using Euler angles is easy to develop and to visualize, but computationally intense. Also, a singularity problem occurs when describing attitude kinematics in terms of Euler angles and therefore it is not an effective method for spacecraft attitude dynamics. The widely used quaternion representation is based on Euler's rotational theorem which states that the relative orientation of two coordinate systems can be described by only one rotation about a fixed axis. A Quaternion is a 4x1 matrix which elements consists of a scalar part s and a vector part \vec{v} . Note the scalar part is the first element of the matrix. [9]

$$q = \begin{bmatrix} s \\ \vec{v} \end{bmatrix} = \begin{bmatrix} s \\ v_x \\ v_y \\ v_z \end{bmatrix} = \begin{bmatrix} q_s \\ q_x \\ q_y \\ q_z \end{bmatrix}$$

As seen before, according to Euler's rotational theorem a quaternion is defined by a rotational axis and a rotation angle. A quaternion representing a coordinate transformation from system A to system B, $q_{B \leftarrow A}$, is defined by:

$$q = \begin{bmatrix} q \\ q_x \\ q_y \\ q_z \end{bmatrix} = \begin{bmatrix} \cos\left(\frac{\theta}{2}\right) \\ \|\vec{e}\| * \sin\left(\frac{\theta}{2}\right) \end{bmatrix}$$

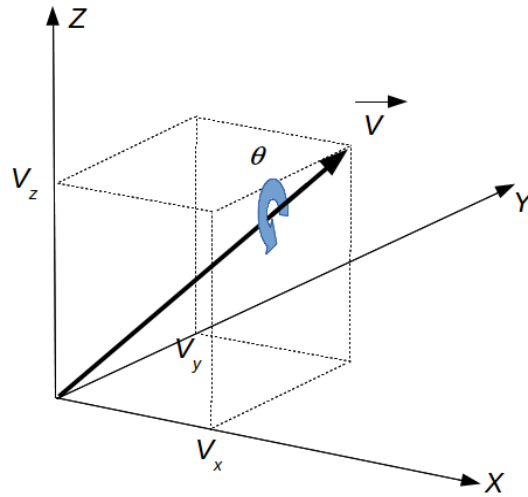


Figure 35 - Concept of Euler's rotational theorem of a quaternion

Where $||\vec{e}||$ is the normalized rotational axis and θ is not the rotational angle but the transformation angle.

4.4.2.1. Euler to Quaternion Conversion

By combining the quaternion representations of the Euler rotations, we get for the body 3-2-1 sequence, where the airplane first does yaw (Body-Z) turn during taxiing onto the runway, then pitches (Body-Y) during take-off, and finally rolls (Body-X) in the air. The resulting orientation of Body 3-2-1 sequence is equivalent to that of lab 1-2-3 sequence, where the airplane is rolled first, and then nosed up around the horizontal, and finally rotated around the vertical [10]:

$$\begin{aligned}
 q_{Eul2Quat} &= \begin{bmatrix} \cos\left(\frac{\phi}{2}\right) \\ 0 \\ 0 \\ \sin\left(\frac{\phi}{2}\right) \end{bmatrix} \begin{bmatrix} \cos\left(\frac{\theta}{2}\right) \\ 0 \\ \sin\left(\frac{\theta}{2}\right) \\ 0 \end{bmatrix} \begin{bmatrix} \cos\left(\frac{\psi}{2}\right) \\ \sin\left(\frac{\psi}{2}\right) \\ 0 \\ 0 \end{bmatrix} = \\
 &= \begin{bmatrix} \cos\left(\frac{\phi}{2}\right) \cos\left(\frac{\theta}{2}\right) \cos\left(\frac{\psi}{2}\right) + \sin\left(\frac{\phi}{2}\right) \sin\left(\frac{\theta}{2}\right) \sin\left(\frac{\psi}{2}\right) \\ \sin\left(\frac{\phi}{2}\right) \cos\left(\frac{\theta}{2}\right) \cos\left(\frac{\psi}{2}\right) - \cos\left(\frac{\phi}{2}\right) \sin\left(\frac{\theta}{2}\right) \sin\left(\frac{\psi}{2}\right) \\ \cos\left(\frac{\phi}{2}\right) \sin\left(\frac{\theta}{2}\right) \cos\left(\frac{\psi}{2}\right) + \sin\left(\frac{\phi}{2}\right) \cos\left(\frac{\theta}{2}\right) \sin\left(\frac{\psi}{2}\right) \\ \cos\left(\frac{\phi}{2}\right) \cos\left(\frac{\theta}{2}\right) \sin\left(\frac{\psi}{2}\right) - \sin\left(\frac{\phi}{2}\right) \sin\left(\frac{\theta}{2}\right) \cos\left(\frac{\psi}{2}\right) \end{bmatrix}
 \end{aligned}$$

Other rotation sequences use different conventions.

4.4.2.2. Quaternion To Rotation Vector Conversion

On the other way the Euler angles can be obtained from the quaternions via the relation:

$$\vec{v}_{Rot} = 2 * atan2(|\vec{v}|, q_s) * \frac{\vec{v}}{|\vec{v}|}$$

Considering that if the scalar part is negative, we take the conjugate quaternion, and if it is equal to 1, we consider \vec{v}_{Rot} as zero vector.

4.4.2.3. Rotation between Frames

Note that canonical way to rotate a three-dimensional vector \vec{v} by a quaternion q defining an Euler rotation is via formula:

$$p' = qpq^*$$

Where $p = (0, \vec{v}) = 0 + iv_1 + jv_2 + kv_3$ is a quaternion containing the embedded vector \vec{v} , q^* is a conjugate quaternion, and $p' = (0, \vec{v}')$ is the rotated vector \vec{v}' . In computational implementations this requires two quaternion multiplications. An alternative approach is to apply the pair of relations

$$\vec{t} = 2\vec{q} \times \vec{v}$$

$$\vec{v}' = \vec{v} + q_0\vec{t} + \vec{q} \times \vec{t}$$

Where \times indicate a three dimensional vector cross product. This involves fewer multiplications and is therefore computationally faster. Numerical tests indicate this latter approach may be up to 30% faster than the original for vector rotation.

4.4.3. Reference Frame

4.4.3.1. Inertial Frame J₂₀₀₀ (IR)

This reference point is the inertial reference point for the ATISE mission. It is in this J₂₀₀₀ reference point that the absolute orientation instructions for the nanosatellite (quaternions of passage) will be calculated.

The benchmark J₂₀₀₀, noted R_{J2000} = (O_{J2000}, X_{J2000}, Y_{J2000}, Z_{J2000}) is by definition the average celestial benchmark from January 1, 2000 to noon (TU1).

Its origin is at the Earth's centre of mass O_{J2000} and its axes are defined as follows:

- Z_{J2000} passes through the average pole of the date 01/01/2000 (pole without Bradley and Newton nutations)

- X_{J2000} is directed towards the mean vernal point of the date 01/01/2000, i.e. the intersection between the equatorial plane (mean) and the ecliptic plane (mean). To simplify, we will say that X_{J2000} is in the direction of the spring equinox on January 1st, 2000 at 12h.
- Y_{J2000} is in the equatorial plane (mean) and completes the trihedron such that R_{J2000} is direct.

The J_{2000} marker is inertial at better than 1" arc per year. The J_{2000} benchmark is also called the EME₂₀₀₀ benchmark (Earth Mean Equator and Equinox at epoch $J_{2000.0}$).

The position of a satellite in its orbit is characterized by 6 orbital parameters. These 6 parameters are usually:

- The half major axis **a**;
- The inclination **i**;
- The eccentricity **e**;
- The right ascension of the ascending node **Ω** ;
- The perigee argument **ω** ;
- The average anomaly **M**.

In this figure, the angles are marked with respect to the inertial mark (O, X_I , Y_I , Z_I). The one used is J_{2000} and will be defined later in this note.

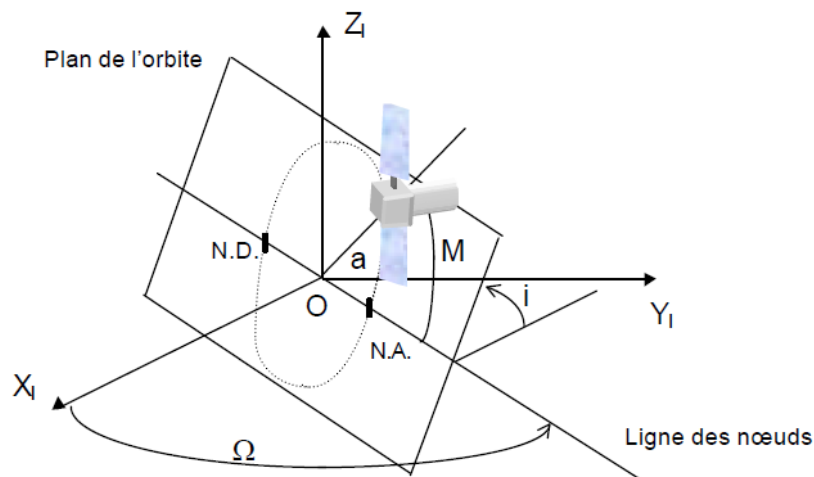


Figure 36 - Illustration of orbital parameters

In the case of a quasi-circular orbit, the eccentricity and perigee argument can be replaced by more adapted parameters:

$$e_x = e * \cos\omega, \text{ and } e_y = e * \sin\omega$$

In the case of ATISE, the eccentricity will be low ($< 5 * 10^{-3}$) and the perigee argument will be fixed at 0° . The e_x and e_y parameters are therefore negligible in the first order for satellite orientation studies.

The other parameters are:

- The right ascension of the ascending node, which is the angle measured around the vector ZI, between the XI axis of the inertial reference frame and the intersection of the plane of the orbit with the equator when the satellite goes from the southern hemisphere to the northern hemisphere (this intersection is called the "ascending node").
- The inclination i , which is the angle between the plane of the equator and the plane of the orbit. This angle is measured around the node axis, oriented from the descending node to the ascending node.
- The mean anomaly M , which in this case is equivalent to the "orbital position" (PSO), and which is the angle between the ascending node and the satellite, measured around the axis perpendicular to the orbital plane and increasing with time
- A distance: the radius of orbit a .

The orbit currently envisaged for the ATISE mission expressed in the EME₂₀₀₀ benchmark is:

Altitude	650 km
Semi-major axis	7028 km
Inclination	80°
Eccentricity	$5 * 10^{-3}$

Table 10 - Orbit configuration

4.4.3.2. Satellite Frame (SR)

The satellite frame has the X_{Sat} normal to the solar panels, that means faced to the sun there is $-X_{Sat}$.

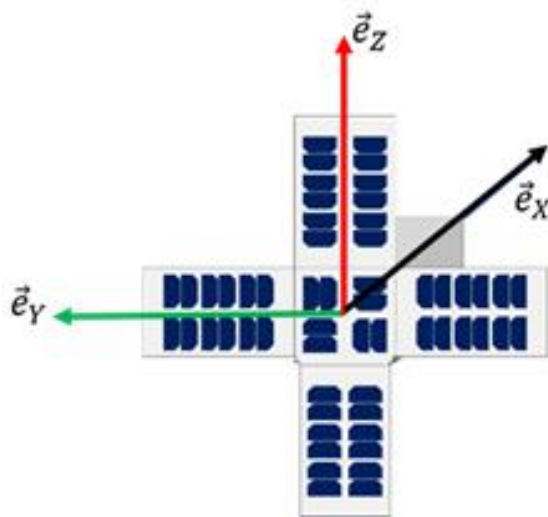


Figure 37 - Inertial Reference

4.4.3.3. Orbital Frame (OR)

The Orbital Reference is defined:

- Z_{OR} direct to the Earth
- X_{OR} is parallel with a satellite linear speed
- Y_{OR} defined by the others two

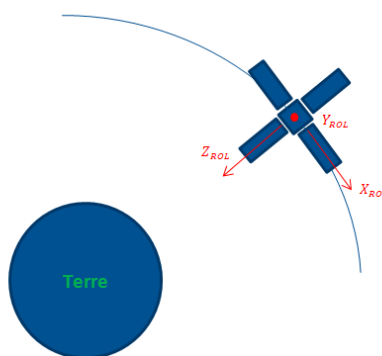


Figure 38 - Orbital Reference

4.4.4. Safe mode Dynamic

First of all, I studied the system with the dynamic equations following the kinetic momentum theory, linearizing the system, considering the state condition of satellite, it means the possibility to measure the magnetic field of the satellite, and to control it with magnetorquers; everything taking into account the different reference frame to deal with. Thanks to that I realized a approximative set of gain and parameters to build the controller.

We define $[I_{sat}]$ satellite inertial matrix at the centre of gravity, taking into account just the diagonal's term, because the other are negligible, $\vec{\omega}_{sat_{SR}}$ satellite rotation speed referenced to the inertial frame, \vec{H} kinetic momentum, \vec{C} extern perturbation torques resultant and command torques applied on the satellite.

$$[I_{sat}] = \begin{bmatrix} I_{XX} & 0 & 0 \\ 0 & I_{YY} & 0 \\ 0 & 0 & I_{ZZ} \end{bmatrix} \quad \vec{\omega}_{sat_{IR}} = \begin{bmatrix} p \\ q \\ r \end{bmatrix}_{SR} \quad \vec{H} = \begin{bmatrix} H_x \\ H_y \\ H_z \end{bmatrix}_{SR} \quad \vec{C} = \begin{bmatrix} C_x \\ C_y \\ C_z \end{bmatrix}_{SR}$$

- The kinematic momentum theory:

$$[I_{sat}] \left(\frac{d\vec{\omega}_{sat_{SR}}}{dt} \right)_{SR} + \vec{\omega}_{sat_{SR}} \wedge ([I_{sat}] \vec{\omega}_{sat_{SR}} + \vec{H}) = \vec{C} + \dot{\vec{H}}$$

Then we get an equations system in IR (Inertial Reference):

$$\begin{cases} I_{XX} * \dot{p} + (I_{ZZ} - I_{YY})q * p + q * H_z - r * H_y = C_x - \dot{H}_x \\ I_{YY} * \dot{q} + (I_{XX} - I_{ZZ})p * r + r * H_x - p * H_z = C_y - \dot{H}_y \\ I_{ZZ} * \dot{r} + (I_{YY} - I_{XX})p * q + q * H_y - r * H_x = C_z - \dot{H}_z \end{cases}$$

In our case study, $\dot{H}_x = \dot{H}_y = \dot{H}_z = 0$ and $\vec{H} = \begin{bmatrix} H \\ 0 \\ 0 \end{bmatrix}_{SR}$

- At this point we have to define p, q and r, using the satellite inertial reference and orbital reference, that means:

$$\vec{R} = \begin{bmatrix} \alpha \\ \beta \\ \gamma \end{bmatrix}_{SR}$$

With α , β , and γ are the Cardan angles, which allow to transport the reference from the IR to the OR (Orbital Reference).

In the literature we can find that:

$$\begin{cases} p = \dot{\alpha} - \omega_0 * \gamma \\ q = \dot{\beta} - \omega_0 \\ r = \dot{\gamma} + \omega_0 * \alpha \end{cases}$$

With ω_0 the orbital rotation speed.

- After the rotation, we have:

$$\begin{bmatrix} X_{OR} \\ Y_{OR} \\ Z_{OR} \end{bmatrix} = \begin{bmatrix} 1 & -\gamma & \beta \\ \gamma & 1 & -\alpha \\ -\beta & \alpha & 1 \end{bmatrix} \begin{bmatrix} X_{SR} \\ Y_{SR} \\ Z_{SR} \end{bmatrix}$$

This matrix allows passing between the two orthonormal references, because it is orthogonal, and its inverse is the transposed:

$$\begin{bmatrix} X_{SR} \\ Y_{SR} \\ Z_{SR} \end{bmatrix} = \begin{bmatrix} 1 & \gamma & -\beta \\ -\gamma & 1 & \alpha \\ \beta & -\alpha & 1 \end{bmatrix} \begin{bmatrix} X_{OR} \\ Y_{OR} \\ Z_{OR} \end{bmatrix}$$

According with the normalized magnetic field in OR:

$$\vec{b} = \begin{bmatrix} \cos(\omega_0 t) \\ 0 \\ \sin(\omega_0 t) \end{bmatrix}_{OR}$$

$$\vec{b}_{SR} = \begin{bmatrix} 1 & \gamma & -\beta \\ -\gamma & 1 & \alpha \\ \beta & -\alpha & 1 \end{bmatrix} \vec{b}_{OR}$$

$$\vec{b}_{SR} = \begin{bmatrix} \cos(\omega_0 t) - \beta \sin(\omega_0 t) \\ -\gamma \cos(\omega_0 t) + \alpha \sin(\omega_0 t) \\ \beta \cos(\omega_0 t) + \sin(\omega_0 t) \end{bmatrix}_{SR}$$

$$\dot{b}_{SR} = \begin{bmatrix} -\omega_0 \sin(\omega_0 t) - \dot{\beta} \sin(\omega_0 t) - \beta \omega_0 \cos(\omega_0 t) \\ -\dot{\gamma} \cos(\omega_0 t) + \gamma \omega_0 \sin(\omega_0 t) + \dot{\alpha} \sin(\omega_0 t) + \alpha \omega_0 \cos(\omega_0 t) \\ \dot{\beta} \cos(\omega_0 t) - \beta \omega_0 \sin(\omega_0 t) + \omega_0 \cos(\omega_0 t) \end{bmatrix}_{SR}$$

$$\dot{b}_{SR} = \begin{bmatrix} -\sin(\omega_0 t) [\omega_0 + \dot{\beta}] + [\beta \omega_0] \cos(\omega_0 t) \\ \cos(\omega_0 t) [-\dot{\gamma} + \alpha \omega_0] + \sin(\omega_0 t) [\gamma \omega_0 + \dot{\alpha}] \\ \cos(\omega_0 t) [\dot{\beta} + \omega_0] + \sin(\omega_0 t) [\beta \omega_0] \end{bmatrix}_{SR}$$

In that case, with a control lead by the magnetorquers, we will have a momentum:

$$\vec{M}_0 = -[K]\vec{B}$$

$$\text{with } [K] = \begin{bmatrix} k_{xz} & 0 & 0 \\ 0 & k_y & 0 \\ 0 & 0 & k_{xz} \end{bmatrix}_{SR}$$

Especially at the end of this study, we can consider equal values $k_{xz} = k_y$. We will keep the matrix to be conform with the vectorial form.

In this case is important just the magnetic field direction, so it is possible to use a normalized magnetic field:

$$\vec{b} = \frac{\vec{B}}{||\vec{B}||} \quad \dot{\vec{b}} = \frac{d}{dt} \left(\frac{\vec{B}}{||\vec{B}||} \right) \quad \vec{M}_1 = -[K]\vec{b}$$

The command torque will be:

$$\vec{C}_{com} = \vec{M}_{com} \wedge \vec{B} = -\frac{[K]}{||\vec{B}||} \vec{b} \wedge \vec{B}$$

At this point we can optimize the command line in the controller taking just the collinear component with the magnetic field:

$$\vec{M}_{com} = \vec{M}_2 - (\vec{M}_2 \cdot \vec{b}) \vec{b}$$

So, our command should be:

$$\vec{C}_{com} = \vec{M}_{com} \wedge \vec{B} = -\left(\frac{[K]}{||B||} \dot{\vec{b}} - \left(\frac{[K]}{||B||} \dot{\vec{b}} \cdot \vec{b}\right) \vec{b}\right) \wedge \vec{B} = -\frac{[K]}{||B||} \dot{\vec{b}} \wedge \vec{B} = [K] \dot{\vec{b}} \wedge \vec{b}$$

$$\text{and } \left(\frac{[K]}{||B||} \dot{\vec{b}} \cdot \vec{b}\right) \vec{b} \sim 0$$

Considering terms not over the first order, we know:

$$\begin{cases} \cos^2(\omega_0 t) \approx \frac{1}{2} \\ \sin^2(\omega_0 t) \approx \frac{1}{2} \\ \cos(\omega_0 t) * \sin(\omega_0 t) \approx 0 \end{cases}$$

As consequence:

$$\vec{C}_{com} = \begin{bmatrix} -\frac{1}{2} k_y (\gamma \omega_0 + \dot{\alpha}) - \frac{1}{2} k_{xz} \gamma \omega_0 \\ -k_{xz} (\dot{\beta} + \omega_0) \\ \frac{1}{2} k_{xz} \alpha \omega_0 - \frac{1}{2} k_y (\alpha \omega_0 - \dot{\gamma}) \end{bmatrix}_{SR}$$

Now adding this result to the kinematic momentum equations:

$$\begin{cases} I_{XX}\ddot{\alpha} - [(2I_{XX} - I_{YY})\omega_0 + H]\dot{\gamma} - [(I_{XX} - I_{YY})\omega_0 + H]\omega_0\alpha = -\frac{1}{2}k_y(\gamma\omega_0 + \dot{\alpha}) - \frac{1}{2}k_{xz}\gamma\omega_0 & (1) \\ I_{YY}\ddot{\beta} = -k_{xz}(\dot{\beta} + \omega_0) & (2) \\ I_{XX}\ddot{\gamma} + [(2I_{XX} - I_{YY})\omega_0 + H]\dot{\alpha} - [(I_{XX} - I_{YY})\omega_0 + H]\omega_0\gamma = \frac{1}{2}k_{xz}\alpha\omega_0 + \frac{1}{2}k_y(\alpha\omega_0 - \dot{\gamma}) & (3) \end{cases}$$

4.4.4.1. Dynamic during the detumbling

Using the Laplace domain, and the second kinematic moment equation:

$$I_{YY}\beta s^2 = -k_{xz}(\beta s + \omega_0)$$

$$\beta = \frac{\frac{\omega_0}{s} k_{xz}}{I_{YY}s + k_{xz}}$$

$$\dot{\beta} = \frac{\omega_0 k_{xz}}{I_{YY}s + k_{xz}}$$

Then the cut off frequency will be:

$$\omega_c = \frac{k_{xz}}{I_{YY}}$$

And the time constant:

$$\tau_{xz} = \frac{1}{\omega_c}$$

As well for the orbital rotation speed ω_0 and the orbital period T_0 :

$$T_0 = \frac{1}{\omega_0} \approx 1,164 * 10^3 \quad \text{with } \omega_0 \sim 0,05 \text{ } ^\circ/\text{s} = 8,722 * 10^{-4} \frac{\text{rad}}{\text{s}}$$

To have a convergent command, it's necessary to take τ_{xz} as a little part of the T_0 . Thus, the gain k_{xz} will depends on τ_{xz} :

$$k_{xz} = \frac{I_{YY}}{\tau_{xz}} \quad \text{with } 0 < \tau_{xz} < 150 \text{ s}$$

But after all, it will be clarified that it is marginal as parameter, because during all this phase the magnetorquers are completely saturated, it means that we can't really have a control.

4.4.4.2. Dynamic during the sun pointing

Different situation during the sun pointing, with which we can have more control; and there is one more variable to consider, the inertial momentum from the reaction wheel. First of all:

$$H \gg (2I_{XX} - I_{YY})\omega_0 \quad H \gg (I_{XX} + I_{YY})\omega_0$$

Then, from the other two kinematic equations we have:

$$I_{XX}s^2\alpha - H\omega_0\alpha - \frac{1}{2}k_y s\alpha = Hs\gamma - \frac{1}{2}\gamma(k_y + k_{xz})\omega_0 \quad (1)$$

$$I_{XX}s^2\gamma - H\omega_0\gamma - \frac{1}{2}k_y s\gamma = -Hs\alpha + \frac{1}{2}\alpha(k_y + k_{xz})\omega_0 \quad (2)$$

To obtain k_y , one needs to simplify the equation system:

$$\alpha * (1) + \gamma * (2)$$

$$(\alpha^2 + \gamma^2) * (I_{xx}s^2 + \frac{k_y}{2}s - H\omega_0) = 0$$

To obtain an equation in term of k_y , it is the formula with the cut off frequency ω_c :

$$I_{xx}\omega_c^2 + \frac{k_y}{2}\omega_c - H\omega_0 = 0$$

As we can suppose, for a second-grade dynamic equation, an optimized solution is between three and four times the orbital speed ω_0 , and for sure it will be between:

$$6\omega_0 > \omega_c > \omega_0$$

And we can ignore the $I_{xx}\omega_c^2 \sim 0$, because the orbit speed order is very small; we obtain:

$$k_y = \frac{2H\omega_0}{\omega_c} = \frac{2H}{N_y} \quad 6 > N_y > 1$$

Based on the angular momentum that we want to use during the safe mode, and N_y for example:

$$\omega_{RWS_{SafeMode}} = 300 \frac{rad}{s} \rightarrow H_{RWS} = 1.44 * 10^{-2} \frac{kg * m}{s^2} \quad N_y \approx 3.79$$

$$k_y = K_2 = 7.6 * 10^{-3}$$

4.4.4.3. Regulation Reaction Wheel Kinetic Momentum

First requirement is that the reaction wheel kinetic momentum would be higher than satellite one:

$$\vec{H}_{Tot} = \vec{H}_{Sat} + \vec{H}_{RWS} \approx \vec{H}_{RWS}$$

And it is usually true, also because the system needs to be stable.

Second requirement is that the \vec{H}_{Sat} and \vec{H}_{RWS} have the same direction.

According to these requirements, and taking into account, I_{YY} of satellite around the reaction wheel axes, and I_{XX} inertia around the other two axes. Considering again the kinetic momentum equations:

$$I_{XX}\ddot{\alpha} - [(2I_{XX} - I_{YY})\omega_0 + H]\dot{\gamma} - [(I_{XX} - I_{YY})\omega_0 + H]\omega_0\alpha = -\frac{1}{2}k_y(\gamma\omega_0 + \dot{\alpha}) - \frac{1}{2}k_{xz}\gamma\omega_0 \quad (1)$$

$$I_{XX}\dot{\gamma} + [(2I_{XX} - I_{YY})\omega_0 + H]\dot{\alpha} - [(I_{XX} - I_{YY})\omega_0 + H]\omega_0\gamma = \frac{1}{2}k_{xz}\alpha\omega_0 + \frac{1}{2}k_y(\alpha\omega_0 - \dot{\gamma}) \quad (3)$$

But this time, in static equilibrium of satellite:

$$-[(I_{XX} - I_{YY})\omega_0 + H]\omega_0\alpha = -\frac{1}{2}k_y\gamma\omega_0 - \frac{1}{2}k_{xz}\gamma\omega_0 \quad (1)$$

$$-[(I_{XX} - I_{YY})\omega_0 + H]\omega_0\gamma = \frac{1}{2}k_{xz}\alpha\omega_0 + \frac{1}{2}k_y\alpha\omega_0 \quad (3)$$

Knowing that $k_{xz} = k_y$, we can resolve the system and obtain the H_{Sat} :

$$\alpha * (1) + \gamma * (3)$$

As consequence:

$$-2[(I_{XX} - I_{YY})\omega_0 + H] = 0$$

$$H = H_{Sat} = 2(I_{XX} - I_{YY})\omega_0$$

As well the total kinetic momentum should be:

$$H_{Tot} = 2(I_{XX} - I_{YY})\omega_0 + H_{RWS}$$

we can define three different positions:

\vec{H}_{RWS} parallel to \vec{N}_{orb} (Orbit Normal)

$$H_{Tot1} = 2\omega_0 I_{YY} + H_{RWS}$$

Inverse position($-\vec{N}_{orb}$)

$$H_{Tot2} = 2\omega_0 I_{YY} - H_{RWS}$$

Trasverse position (x_{sat})

$$H_{Tot3} = 2\omega_0 I_{XX}$$

At this point to respect the second requirement, it's necessary that in the position parallel to the normal orbit direction, we have the higher kinetic moment:

$$H_{Tot1} > H_{Tot3} > H_{Tot2}$$

It means:

$$2\omega_0 I_{YY} + H > 2\omega_0 I_{XX} > 2\omega_0 I_{YY} - H$$

To respect also the first requirement, and with obviously $H > 0$, it need:

$$H > |2\omega_0(I_{XX} - I_{YY})|$$

As consequence we obtain the minimum value below which the satellite is instable:

$$H_{min} = 1.02 * 10^{-5} Nms$$

And the maximum it will be given by the specific datasheet of our reaction wheel:

$$H_{max} = 3 * 10^{-2} Nms$$

The final value it will be between these two constraints; if H will be too much high, the alignment time could be increased, but on the other side, if H will be too low, we could have stability issues.

Probably the right value during the optimization it will be closer to the H_{max} , because we need mainly the stability.

4.4.4.4. Final Result

According with the previous evaluations and the initial condition mainly influenced by the launcher ejection; after a long iteration, we obtained:

H_{RWS} (Nms)	1.44*10 ⁻²
τ_{xz} (s)	50
N_y	3.79

Table 11 - Final gains for safe mode control law

4.4.5. Mission Mode Dynamic

In this phase, the mathematical model is the same, but there is the intervention of three Reaction Wheels, and the determination attitude compute by the Star Tracker. As well, it need to consider the necessity of an estimator due to the presence of several sensors, which send data about the satellite condition, and with which I compute a weighted average for the speed, using also a filter for each signal. The diagram of the reaction wheel control loop is given below. The different blocks are detailed below:

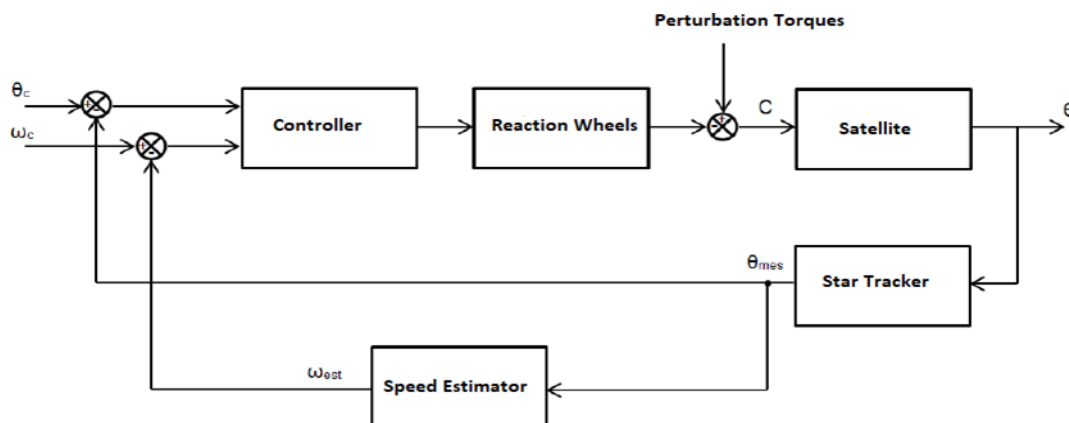


Figure 39 - Mission Mode Loop Scheme

The main role of this Controller is to allow a score with a minimum accuracy of 0.25° (Table 3). Given the low level of requirement required, we will choose to take a margin on this value because the quality of the shots will depend on this precision. Thus, we will make the adjustments in order to obtain accuracy necessarily better than that of the stellar sensor, i.e. 0.005°. Indeed, whatever the stellar sensor chosen in the end, this value will be smaller than the measurement noise of the sensor.

I decided that the first control had to involve the sun pointing, with inputs the quaternion from the Star Tracker and the speed estimated from the Estimator (it will be presented below). As well, we still have the sun direction compute by sun sensors, magnetic field from magnetometers. The law chosen for the reaction wheels is a control PID; it means Proportional-Integrative-Derivative, which received the position and speed errors, and giving as output the command torque. At the same time, I chosen to use, as always, a B_{point} control law to help the system in case of wheels saturated, or high perturbation, or high-speed cause by a manoeuvre.

But first of all, the satellite block corresponds to the rigid dynamics of the satellite without taking into account the actuators. It is then a simple double integrator. Indeed, the fundamental principle of dynamics gives us:

$$J\ddot{\theta} = C$$

The transfer function of the rigid satellite is therefore given by:

$$\frac{\theta}{C} = \frac{1}{Js^2}$$

With J the inertia of the deployed satellite and C the resultant of the disturbance and control torques. It may also be important to take into account the satellite's Mission Modes, which correspond to the deployed appendices. Generally, these are antennas and solar panels, and the only Mission Modes correspond to the panels since in the current configuration the antennas are not masts, but kind of discs stuck on the box. Mission Modes are potentially disturbing if they are not high enough in frequency to be attenuated in gain by a corrector that section. Usually, they are expected to be disturbing if there is less than a decade between the band loop and the frequency of the Mission Mode.

Nevertheless, to ensure that our system is robust to Mission Modes, we model the satellite by taking into account the Mission Modes as follows:

$$J\ddot{\theta} - C_s = C$$

With

$$C_s = \frac{J_s s^2}{s^2 + 2\zeta\omega_s s + \omega_s^2} \ddot{\theta}$$

With the inertia J of the flexible mode approximated by $J_s = J_{GS}$, with J_{GS} the equivalent inertia of the panels at the satellite's centre of gravity. The transfer function corresponding to the Mission Mode will therefore be obtained via:

$$\left(J - \frac{J_s s^2}{s^2 + 2\zeta\omega_s s + \omega_s^2} \right) \theta s^2 = C$$

So, the transfer function is:

$$\frac{\theta}{C} = \frac{s^2 + 2\zeta\omega_s + \omega_s^2}{(J - J_s)s^4 + 2J\zeta\omega_s s^3 + J\omega_s^2 s^2}$$

The corrector settings will be based on the dynamics of the rigid satellite for reasons of simplicity of calculation. On the other hand, stability studies will be carried out with both models in order to see the impact of flexible modes on the system and ensure its proper functioning. [11]

4.4.5.1. Star Tracker Computation

I developed a model for the Star Tracker using the concept of measure delay and adding the noise and bias due to the instrument error. Obviously, it sends a quaternion to obtain the estimate position of the satellite; so, the input of the sensor it should be the quaternion of the satellite real position delayed multiple by its properties.

$$q_{sat} * q_{Bias} = \begin{bmatrix} q_{sat0} & -q_{sat1} & -q_{sat2} & -q_{sat3} \\ q_{sat1} & q_{sat0} & -q_{sat3} & q_{sat2} \\ q_{sat2} & q_{sat3} & q_{sat0} & -q_{sat1} \\ q_{sat3} & -q_{sat2} & q_{sat1} & q_{sat0} \end{bmatrix} \begin{pmatrix} q_{Bias0} \\ q_{Bias1} \\ q_{Bias2} \\ q_{Bias3} \end{pmatrix} = q_1$$

With

$$q_{Bias} = \begin{pmatrix} \cos\left(\frac{\theta}{2}\right) \\ \vec{u}_1 * \sin\left(\frac{\theta}{2}\right) \\ \vec{u}_2 * \sin\left(\frac{\theta}{2}\right) \\ \vec{u}_3 * \sin\left(\frac{\theta}{2}\right) \end{pmatrix}$$

With θ the Bias value of the star tracker. As well, to add the noise we use the same procedure:

$$q_1 * q_{noise} = q_{st}$$

4.4.5.2. Speed Estimator Filter

Thanks to the star tracker, we can evaluate the speed of the satellite, using the quaternion; indeed, the angular velocity is the rotation axis, normalized, multiplied by the rotation speed in radians:

$$q_s = \frac{q_{st}q_{st}^*}{|q|^2} = q_{st}q_{st\text{invers}}$$

At this point, we can evaluate the rotation axis, as I already explain in 4.4.2.2. [12]

Another point that I took into account is to implement a filter based on the theory of Discrete State-Space:

$$x(n + 1) = Ax(n) + Bu(n)$$

$$y(n) = Cx(n) + Du(n)$$

With four vectors related on initial condition, cut-off angular frequency and damping parameter.

As well, I decided to use also the output of the magnetometer to compute a second value of the satellite speed based on the magnetic field variation, as in the safe mode way. That conducts to an average weighted between the two signals inside the estimator.

$$\omega_{est} = \frac{(a_1\omega_{q_s} + a_2\omega_{Bsat})}{a_1 + a_2}$$

With $a_1 = 1.20$ and $a_2 = 1.05$.

4.4.5.3. Reaction Wheels Control PID

The purpose of the Reaction wheels is to reach equilibrium between the pointing accuracy and maneuverability; in order to get this objective; we need a more complex control than the safe mode. As far as we consider a control very competitive, I chosen a PID controller, because we faced with instability and command saturation. Adding a integrative control, there is:

$$U_I(s) = \frac{K_p}{T_I s} E(s)$$

With K_p the proportional gain, and T_I the integration period. The integrator has the ability to guide the control variable U to the set-point; also, it can be defined like a dispositive for the error zeroing that means high accuracy without influencing the stability.

Adding a derivative action, I get a higher stability of closed loop system.

$$U_D(s) = \frac{K_p T_D}{1 + \frac{T_D}{N} s} E(s)$$

The derivation give as output the derivate respect the time of error e_t , and for that reason the derivative controller is also called speed controller.

Taking advantage of these implementations, we get:

$$PID(s) = \frac{U(s)}{E(s)} = K_p + \frac{K_p}{T_I s} + \frac{K_p T_D s}{1 + \frac{s T_D s}{N}} = P(s) + I(s) + D(s)$$

At this point, it's necessary to tune the controller gain, and I used the Ziegler-Nichols method for closed loop; The Ziegler-Nichols rule is a heuristic PID tuning rule that attempts to produce good values for the three PID gain parameters:

- K_p - the controller path gain;
- T_I - the controller's integrator time constant;
- T_d - the controller's derivative time constant.

Given two measured feedback loop parameters derived from measurements:

- the period T_u of the oscillation frequency at the stability limit;
- the gain margin K_u for loop stability;

With the goal of achieving good regulation (disturbance rejection). [13]

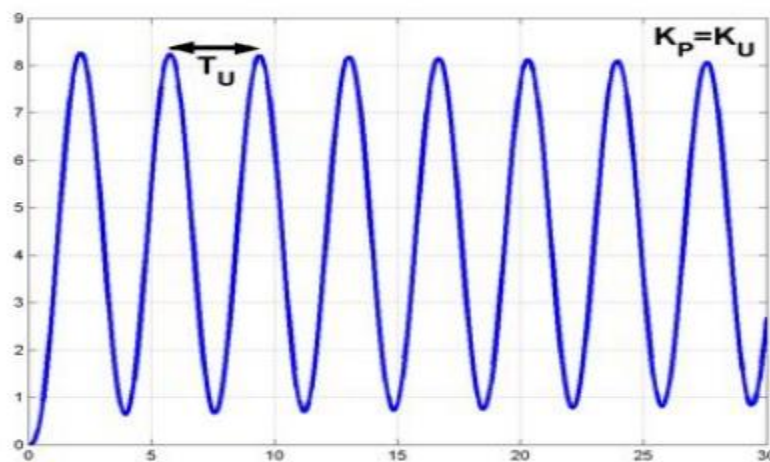


Figure 40 - Oscillation Frequency at the stability limit

Applying this procedure, with a $K_p = 5,86 * 10^{-4}$, I found out:

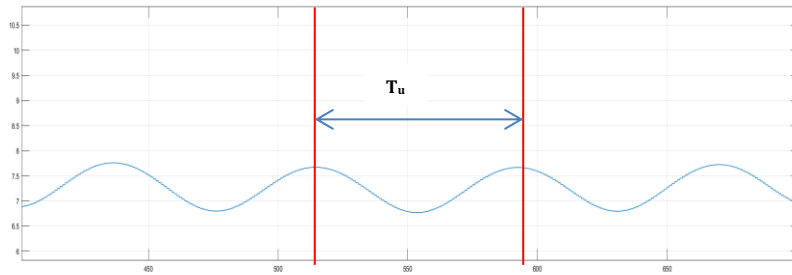


Figure 41- Oscillation stability limit in our controller

With $T_u = 77s$. Now using the tuning rule table of Ziegler-Nichols for PID controller, and knowing $K_p = K_u$ we obtain:

	K_I	T_I	T_D
PID controller	$0.6K_u = 9.7 * 10^{-6}$	$\frac{T_u}{2} = 38.5 s$	$\frac{T_u}{8} = 9.7 s$

Table 12 - Ziegler-Nichols PID tuning table

Easily we can calculate all the PID gains for our controller, getting:

$$K_p = 5.86 * 10^{-4} \quad K_I = 9.7 * 10^{-6} \quad K_D = 0.0032$$

Actually the final gains set in the final model are slightly different, probably due to the complexity of the system, and disturbances coming from sensors and environment. Finally I got the final gains, based the simulation, and an iterative approach.

$$K_p = 5.86 * 10^{-4} \quad K_I = 1 * 10^{-7} \quad K_D = 0.0302$$

4.4.5.4. Magnetorquers Control Law

According to the laws of dynamics applied to the satellite, we have:

$$\frac{d\vec{H}_{tot}}{dt} = \vec{C}_{ext}$$

With \vec{H}_{tot} the satellite total kinetic moment, sum of the kinetic moment of the satellite body \vec{H}_{sat} and that of the reaction wheels \vec{H}_{RWS} , and \vec{C}_{ext} the sum of the perturbing couplers. With perturbations, \vec{H}_{tot} changes. Without wheel control, \vec{H}_{RWS} don't move, we have a variation just of \vec{H}_{sat} . The purpose of the wheel control is to reduce to its value of command H_{cons} .

For a geocentric pointing for example, H_{cons} is nil along the roll and yaw axes and is $-\omega_{orb}I_{YY}$ along the pitch axis.

Thus, the wheel control will modify \vec{H}_{RWS} , in order to correct the variation of \vec{H}_{sat} . In the end, the perturbation followed by correction therefore vary \vec{H}_{RWS} . If it repeats itself like that, \vec{H}_{sat} will reach its saturation value and control will no longer be possible, hence the interest of "desaturation" the wheels before this only happens.

The goal is therefore to generate a command in order to make \vec{H}_{tot} to H_{cons} , in order to "absorb" it the variation of \vec{H}_{tot} which in fact corresponds almost to the variation of \vec{H}_{RWS} once the order of the wheels realized. Thus, the wheels are allowed to recover a capacity of variation in kinetic momentum' and so a greater capacity for action. The desaturation torque control must therefore be of the form:

$$\vec{C}_{des} = -K_{MTB}(\vec{H}_{tot} - \vec{H}_{cons})$$

So, known $\overrightarrow{M_{comMTB}}$ the command momentum of the magnetorquers, and \vec{B} the environment magnetic field, and the torque delivered to the magnetorquers is:

$$\vec{C}_{MTB} = \overrightarrow{M_{comMTB}} \wedge \vec{B}$$

So, knowing the torque desired, the equation for the command momentum should be:

$$\overrightarrow{M_{comMTB}} = \frac{\vec{B} \wedge \vec{C}_{des}}{B^2}$$

By neglecting the disturbing torques, the equations of dynamics give us:

$$\frac{d\vec{H}_{tot}}{dt} = \vec{C}_{des} = -K_{MTB}(\vec{H}_{tot} - \vec{H}_{cons})$$

In the Laplace domain this equation becomes:

$$H_{tot}s = -K_{MTB}(H_{tot} - H_{cons})$$

So, the transfer function between H_{tot} and H_{cons} :

$$\frac{H_{tot}}{H_{cons}} = \frac{K_{MTB}}{K_{MTB} + s} = \frac{1}{1 + \frac{1}{K_{MTB}}s}$$

And we can visualize the transfer function of first order $\frac{1}{1+\tau s}$, that means the cut-off pulsation is $\omega_c = \frac{1}{\tau} = K_{MTB}$.

For the magneto torque control loop to be effective, it must be slow enough in front of the jet wheel control loop, since it must not interfere with it at the risk of disrupting the main control. Usually, a convergence time around an orbit is chosen for the

magneto torque control loop, which is sufficient for the desaturation of the wheels. It is also ensured that there is about two decade-gap between the frequency of the magneto torque control loop and that of the wheels, which corresponds to the number of "stages" in the total servo system between these two loops.

Thus, remembering that the convergence time of a first-order system is 3τ , that means:

$$3\tau = T_{orb} = \frac{2\pi}{\omega_{orb}}$$

With $\omega_{orb} \sim 0,05 \text{ } ^\circ / \text{s} = 8,722 * 10^{-4} \frac{\text{rad}}{\text{s}}$

So, we obtain:

$$\frac{3}{K_{MTB}} = \frac{2\pi}{\omega_{orb}}$$

Thus:

$$K_{MTB} = \frac{3}{2\pi} \omega_{orb} = 4.166 * 10^{-4} \text{s}^{-1}$$

Just to verify, the cut-off frequency of the loop control is:

$$f_c = \frac{\omega_c}{2\pi} = \frac{K_{MTB}}{2\pi} = 6.634 * 10^{-5} \text{Hz}$$

Since the wheel control loop has a frequency of about a minimum $\approx 10^{-2}$ (lowest frequency for the adjustment corresponding to an accuracy of 0.1°), there is a difference of about two decades. To definitively validate the setting of the magneto torques control loop, a scan of K_{MTB} will be carried out around the value determined here once the simulator has been carried out. [11]

4.5. ADCS Simulation

The ADCS can be studied using a powerful software as Matlab-Simulink, building models for each mission mode, it means Safe Mode, Mission Mode, etc..., and taking advantage of the PILIA library. Inside PILIA we can find all the different models for each need:

- Actuators and Sensors like reaction wheel model or a sun sensor model;
- Environment models, for example a model able to simulate external perturbation present in space as magnetic torque or aerodynamic torque;
- Controller models, maybe the most important, with which we can define and implement our command control for the whole system in all different case;
- Other models, manly support models which help us to build a better simulator.

Important to know, all the models are modular, it means that we are sufficiently helped and free to build the simulator.

Exactly at this point, it shows up the second objective, that is the development of PILIA's models; according with the lack of system models and pertinence with reality, I built a development plan:

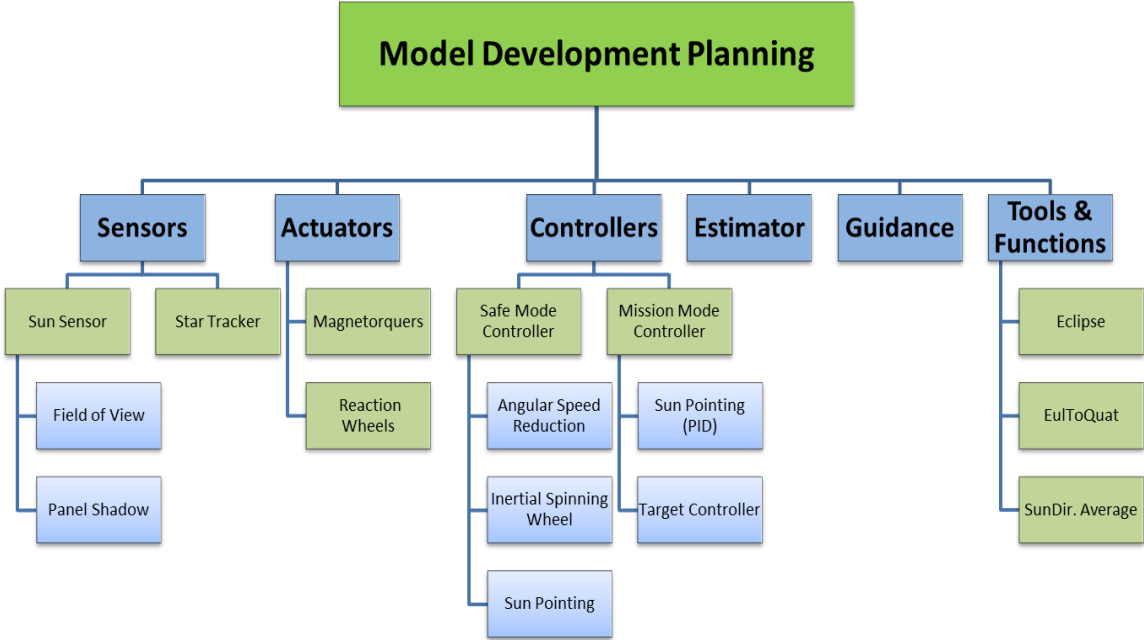


Figure 42 - Models Development Plan

4.5.1. Orbit and Environment

In order to consider a sufficiently real back up, on which base all our simulations, we use a time and position reference, which is the exact moment (time, day, month, year), and coordinates on earth reference; and it's possible thanks to PILIA, which contains already in its library these models.

- Date and Orbit block is able to give them, using some data that we set up in Matlab files before the simulation, and depending on the project. Other data relative to the orbit allows calculating speed and position with the earth inertial frame, in a Keplerian theory.

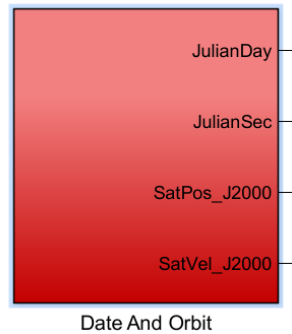


Figure 43 - Data and Orbit Block

- Environment block is able to evaluate Sun position, as well in earth frame, using the first two outputs from Data and Orbit, JulianDay and JulianSec, and earth dipole magnetic field composition, using exactly satellite position.

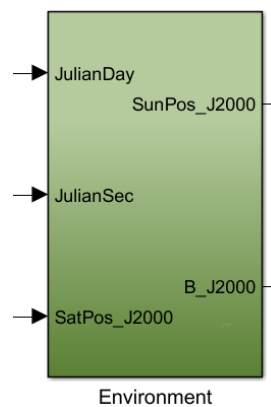


Figure 44 - Environment Block

4.5.2. Space Perturbations

Even if the space looks like empty, there are a lot perturbation which can disturb and compromise the attitude control; they are torques, which push and move for several reasons the satellite. We have:

- Aerodynamic Torque due to the tiny existent density of the atmosphere
- Sun Torque due to the solar pressure caused by the solar wind.
- Gravity Gradient Torque due to the earth mass, as consequence gravity attraction.
- Magnetic Torque due to the influence by earth magnetic field.

To evaluate the torques, in inputs we have Orbit and Environment outputs, plus the feedback of satellite quaternion frame to get how it is positioned in term of space and time.

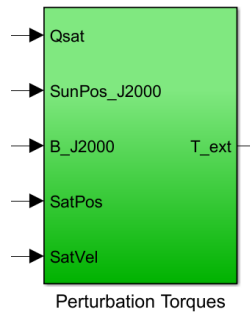


Figure 45 - Perturbations Block

All these perturbations are synthetized as External Torque:

$$T_{ext} = T_a + T_s + T_g + T_m$$

So, the model it will be:

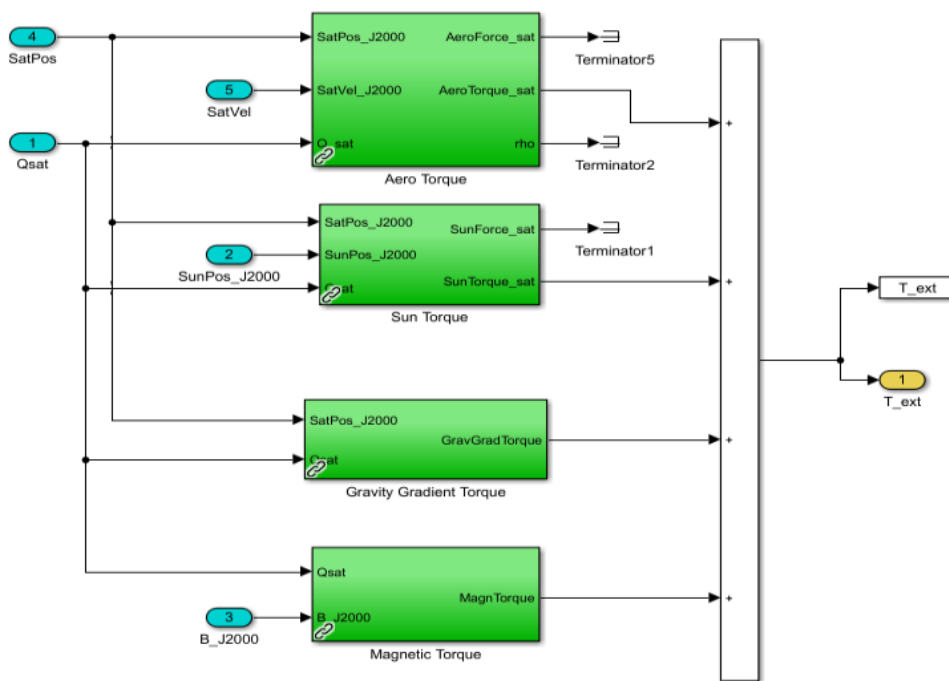


Figure 46 - External Torques Calculation

Besides the External Torque, we could take in account Internal Disturbs, which come from our instruments, for example actuators; but in that case, we don't consider them.

4.5.3. Safe Mode Simulator

First control mode in a satellite mission, the safe mode starts the de-tumbling phase, which aims at stopping the high rotation speeds due to the launcher ejection; then runs one reaction wheel to obtain a gyroscopic rigidity, and at the end, points the solar panels in sun direction. As sensors we have a magnetometer and five sun sensors

placed over each face of satellite, except for Y+ direction. As actuators we have 3 axis magnetorquers and 3 reaction wheels, but we only use one of the latest. So, the whole model will have the following configuration:

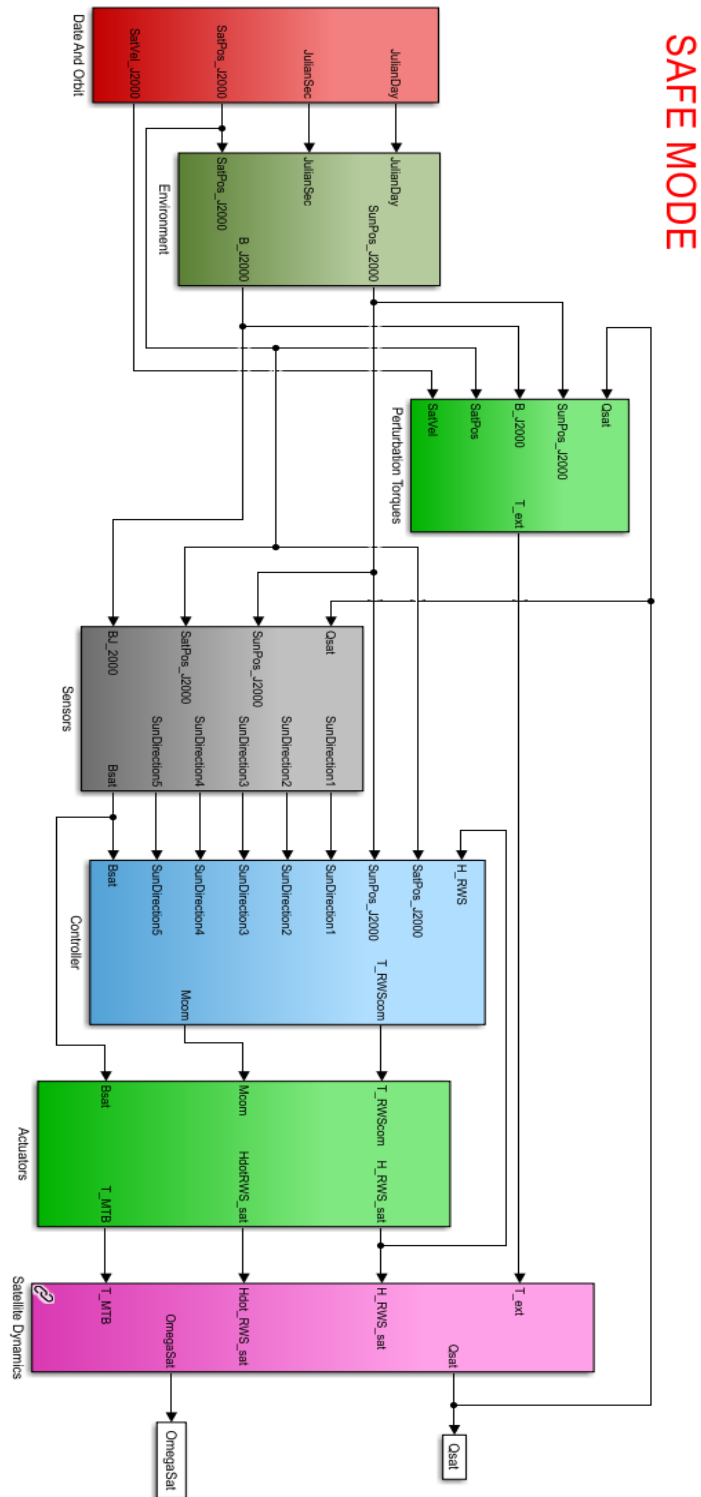


Figure 47-Safe Mode Simulink Model

4.5.3.1. Sensors

On ATISE we have 5 Sun Sensors and one Magnetometer, but it could be a different configuration. We need them, because the magnetometer allows to compute the direction of the magnetic field of satellite in its reference, taking in account the variation of the satellite's position in quaternion frame, and the sun sensors give the sun direction useful for pointing phase.

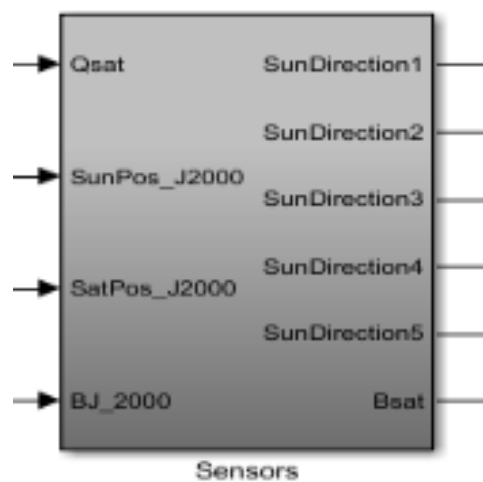


Figure 48 - Sensors Model

4.5.3.1.1. Magnetometer

Inside the Sensors Model we find the Magnetometer Model. As explained before, we need just two inputs, Qsat and B, the magnetic dipole field; the first is given as feedback after all the command line which takes into account every parameter; the second is given by the calculation did by Environment and Date and Orbit blocks.

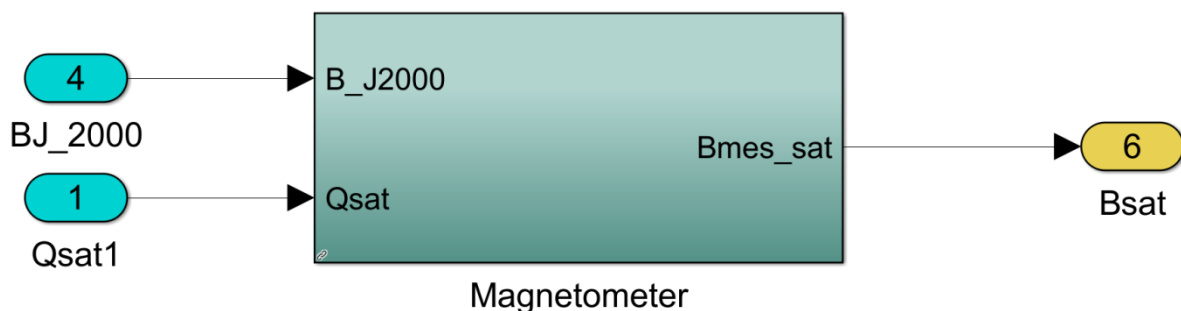


Figure 49-Magnetometer

This block is built easily, but it is necessary to consider other parameters, which allows to have a more realistic model; thus, it should put magnetometer position in satellite reference frame, Scale Factor and Misalignment (which during the development can influence this calculation even if they are few grades), Bias and Noise related and given by the producer. All data can be loaded on the Matlab file of the magnetometer; though one must pay attention to the units of the variables.

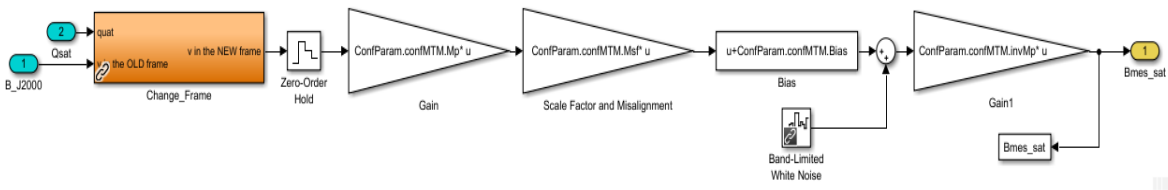


Figure 50-Magnetometer inside the Simulink Model

As result we obtain the magnetic field of the satellite, B_{sat} ; here is an example graph of a magnetic field:

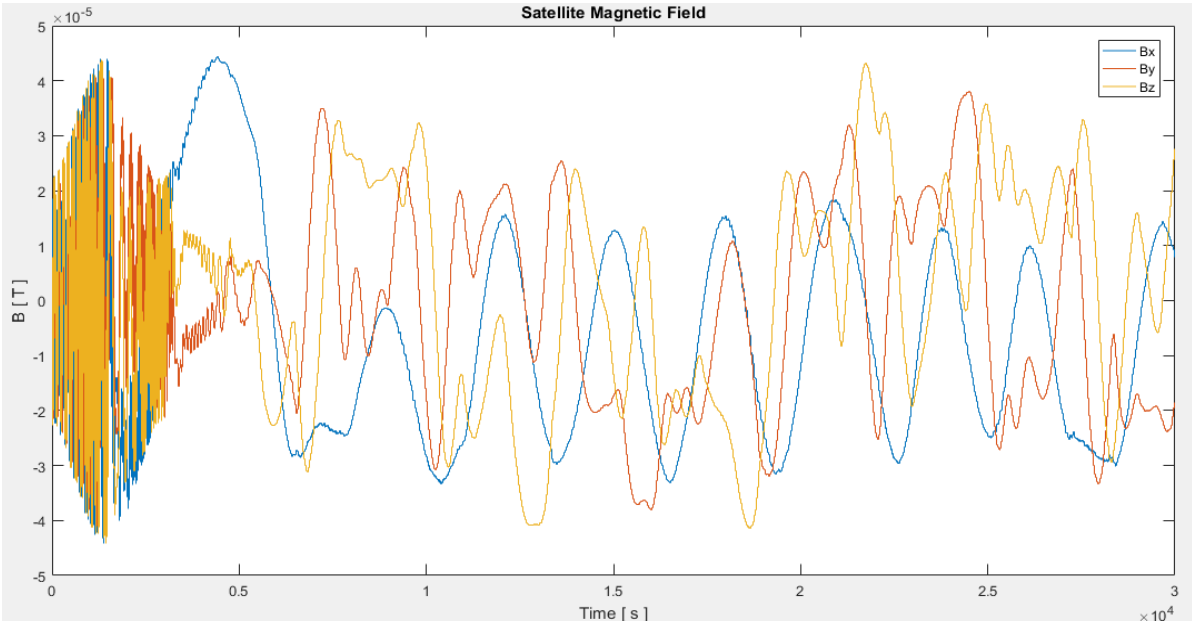


Figure 51 - Satellite Magnetic Field

4.5.3.1.2. Sun Sensor

In this case we need three inputs to build the sun sensor model, which are Sun Position, Satellite Position and, as always, the feedback Qsat; the output is the Sun Direction: and in the case of ATISE we will have five different Sun Direction computations.

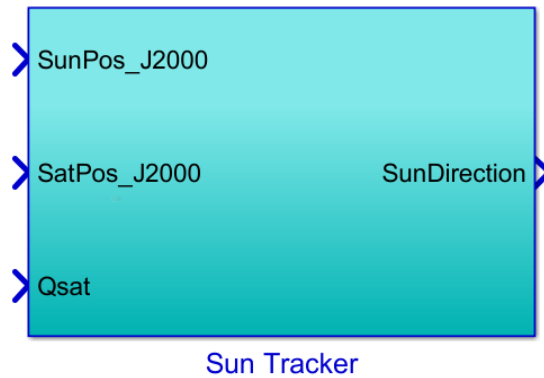


Figure 52 - Single Sun Sensor Block

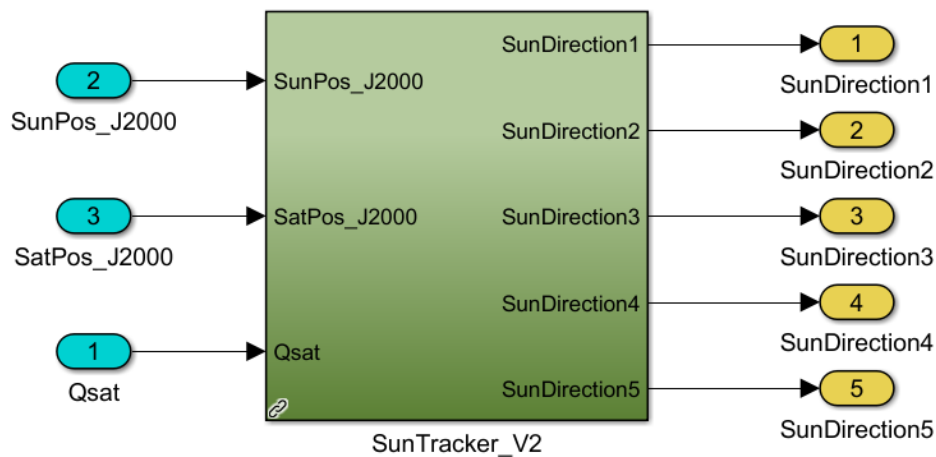


Figure 53 - Multiple Sun Sensor Block

4.5.3.1.3. Single Sun Sensor

Depending on your project or need, a basic sensor tracker system is the single version (Figure 10); in that case with just one sensor, on the Single Sun Sensor file, the first step should be to write in the Sensor Direction to allow the model to evaluate the position and direction of the Sensor frame; and other parameters as Bias, White Noise, Field of View, Accuracy, Frequency have to be written as well. Indeed, inside the model we see:

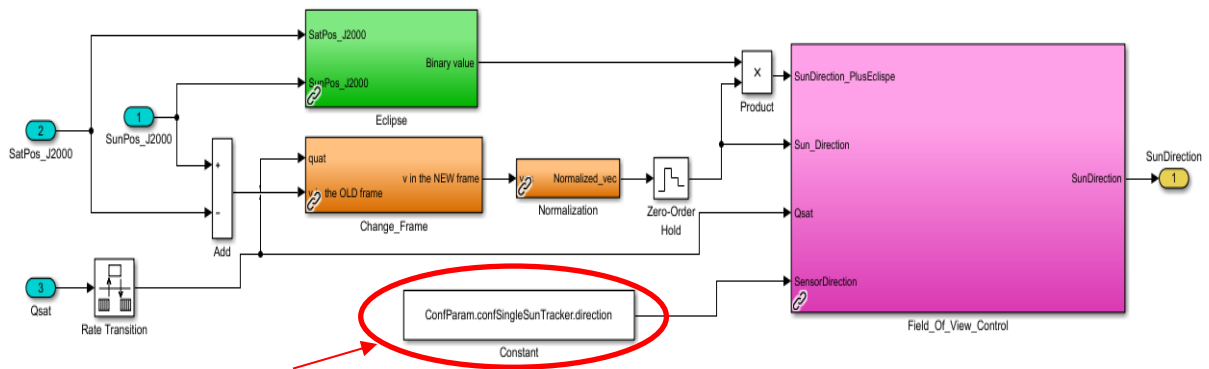


Figure 54 -Inside the Single Sun Sensor Model

As well, there is a computation of Sun Direction vector making the vectoral difference between SatPos and SunPos, and then it changes frame into satellite frame using the quaternion data from the feedback; but it is not all, there are others important evaluations to perform before going on: the Eclipse, the Field of View of Sensor and the influence of Panel Shadow.

ECLIPSE MODEL

It is easy to notice also a block called Eclipse, in which both SatPos and SunPos are taken as input; we use them to consider eclipse periods during the orbit around the earth.

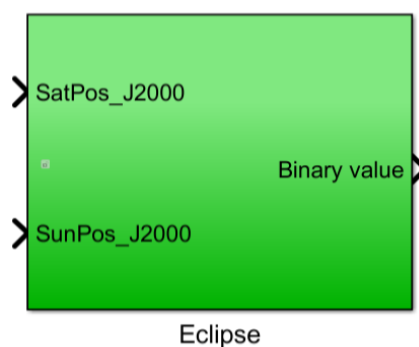


Figure 55 - Eclipse Block

Indeed, it will not be possible to see the sun at every moment, probably there will be some period of eclipse, in which the model must give a null direction; with this block we obtain a Binary Value as output, which will be 0 during an eclipse, and 1 if not.

Then the Binary Value is multiplied by the Sun Direction.

To evaluate this situation inside the block, two angles are calculated, Angle Sat-Earth and Angle Sun-Sat. We calculate the difference between them: if it is less than zero we are in eclipse.

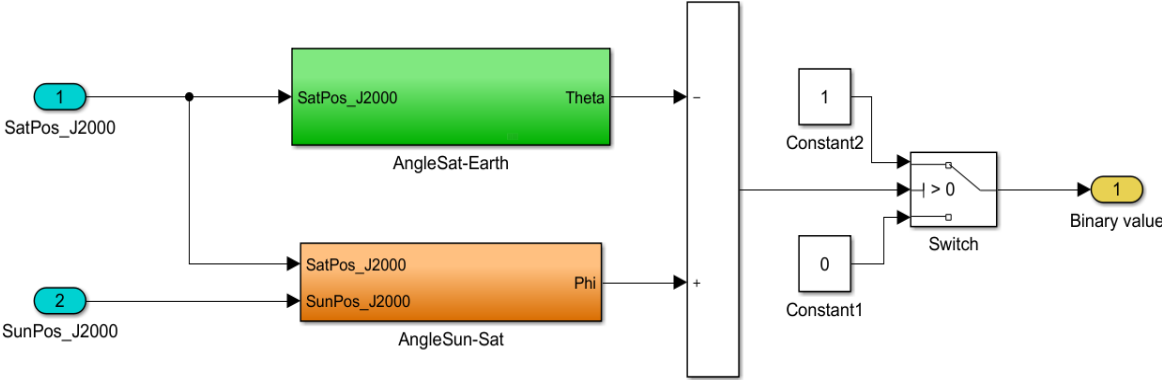


Figure 56 - Eclipse Model

The angle Sat-Earth is between satellite position in inertial frame and the radius of earth, and the Sat-Sun between satellite and sun position. An example about what happens:

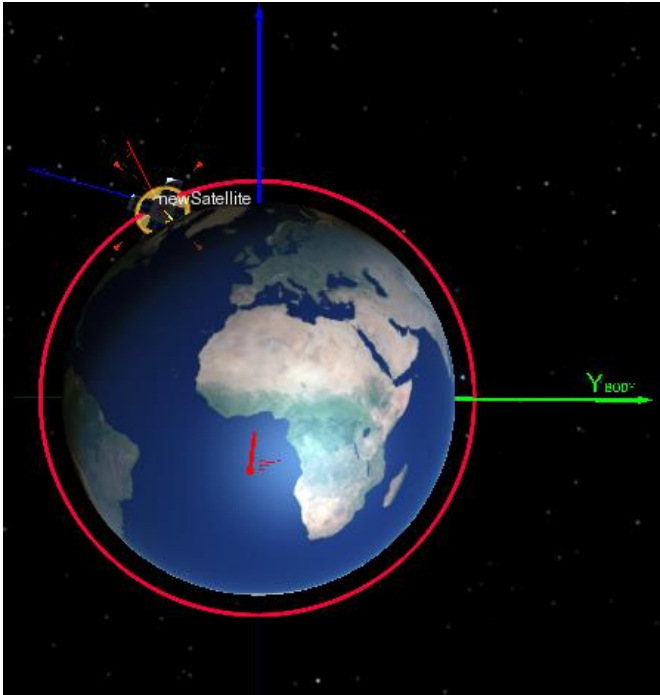


Figure 57 - During the eclipse



Figure 58 - Out the eclipse

FIELD OF VIEW CONTROL

Eclipse period is not the only issue that we have to consider in this model, indeed there is the Field of View which must be considered, because the sensor has a limitation in term of degree. That means we have to take into account if the sun direction is inside this field. After that, it is necessary to see if the solar panels influence the sensors due to the shadow.

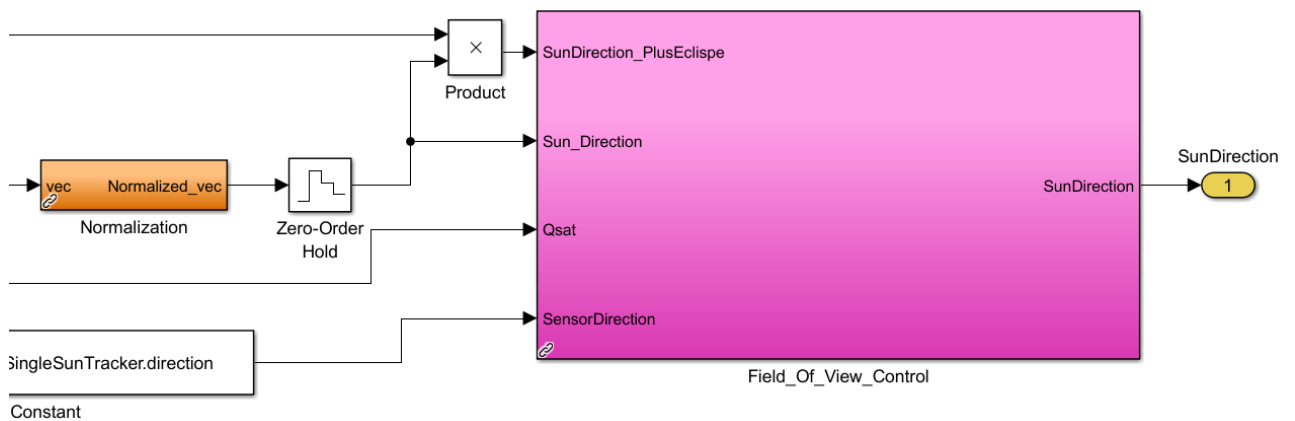


Figure 59 - Field of View Block

We used four inputs: Sun Direction, Q_{sat} , Sun Direction taking into account the eclipse, and Sensor Direction; and as output we obtain just the Sun Direction, which will be a zero vector in case of shadow, eclipse, or just it is not in the FOW.

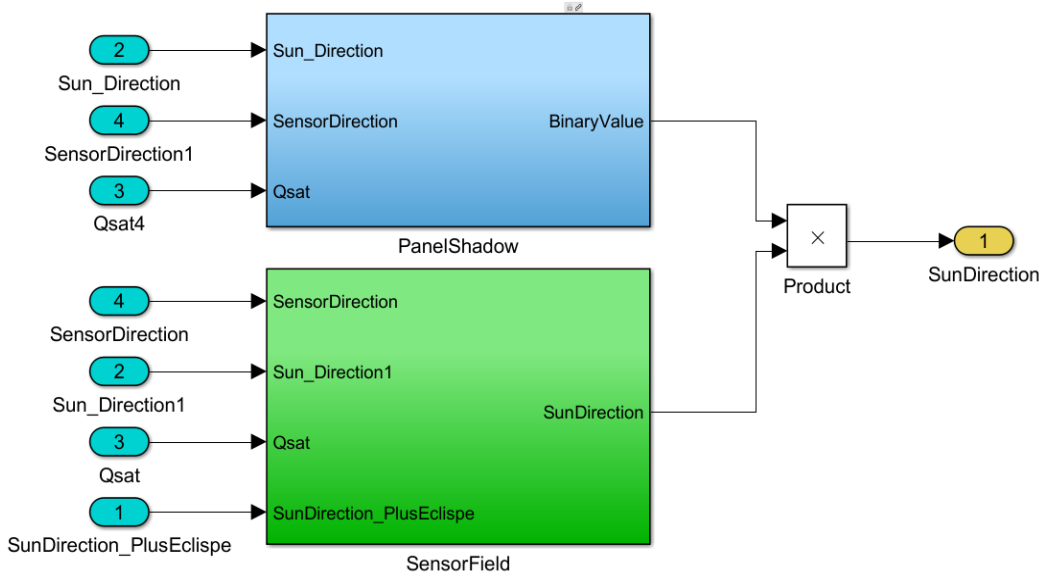


Figure 60 - Inside the FOW Model

SENSOR FOW

The computation is similar to the eclipse, with a binary value multiplied by the Sun Direction; in particular to simulate the sensor cone, it calculates the angle between the sun vector and sensor direction, and then adds Bias and White Noise, to verify if it is within the instrument limitation.

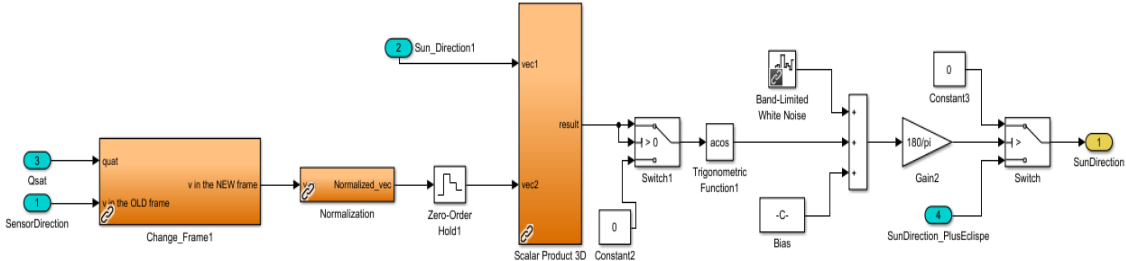


Figure 61 - Sensor Field Model

Obviously, we need to consider at each step the variation of satellite position, thus we need to change frame for the sensor direction. To visualize the result, we can use a VTS simulation:

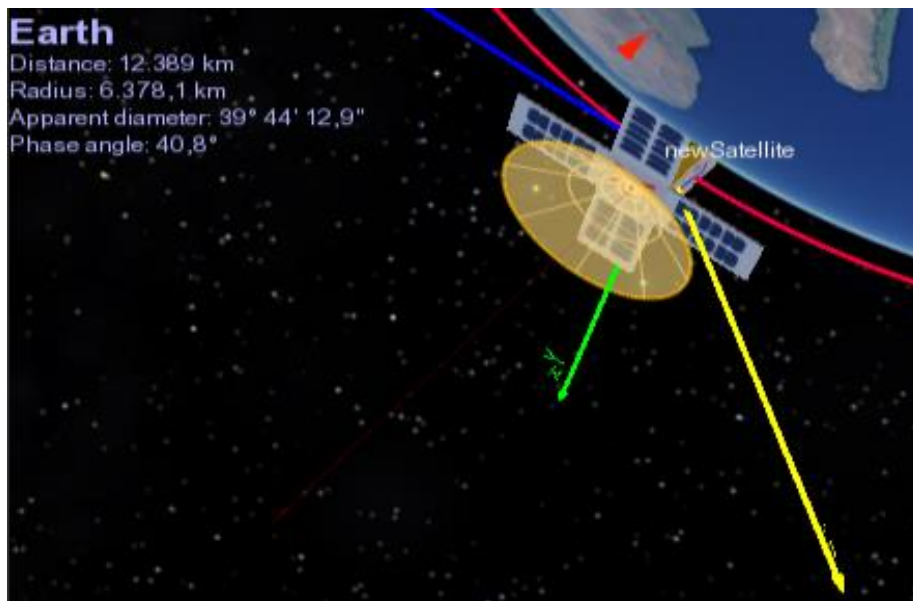


Figure 62 - Test Sun Direction out FOW

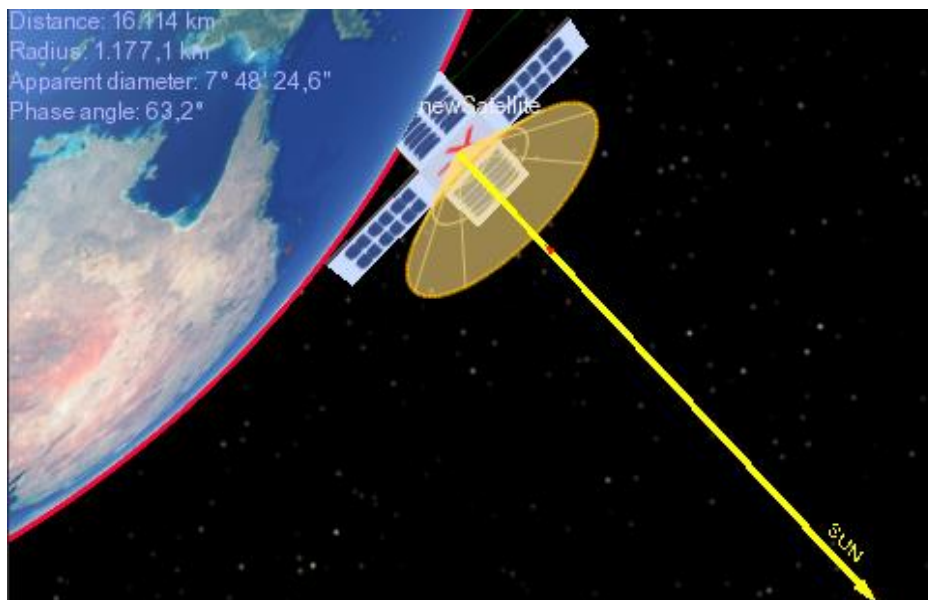


Figure 63 - Test Sun Direction in FOW

PANEL SHADOW

The second block, which evaluates if the shadow of panels influences or not our sensors, uses almost the same inputs. In that case we have to consider a region in the space that could cover the sensor view, which means a solid angle build from the sensor

to the panel borders; thus, three angles are measured using the panel geometry and sensor position: Omega-, Omega+ on sensor face plan and Teta on sensor direction plan. The PanelShadow block uses two projections of the sun direction, one on the sensor direction plan, and the second on the plan where the sensor is placed; then two angles are measured: Alfa and Beta, both between sun direction projections and panel direction.

At this point it is necessary just to verify if Alfa and Beta are smaller than Omega-, Omega+ and Beta. If they are smaller, the sensor cannot see the sun.

All data about panel geometry, sensor position and Panel Direction have to be written in the Satellite Features file.

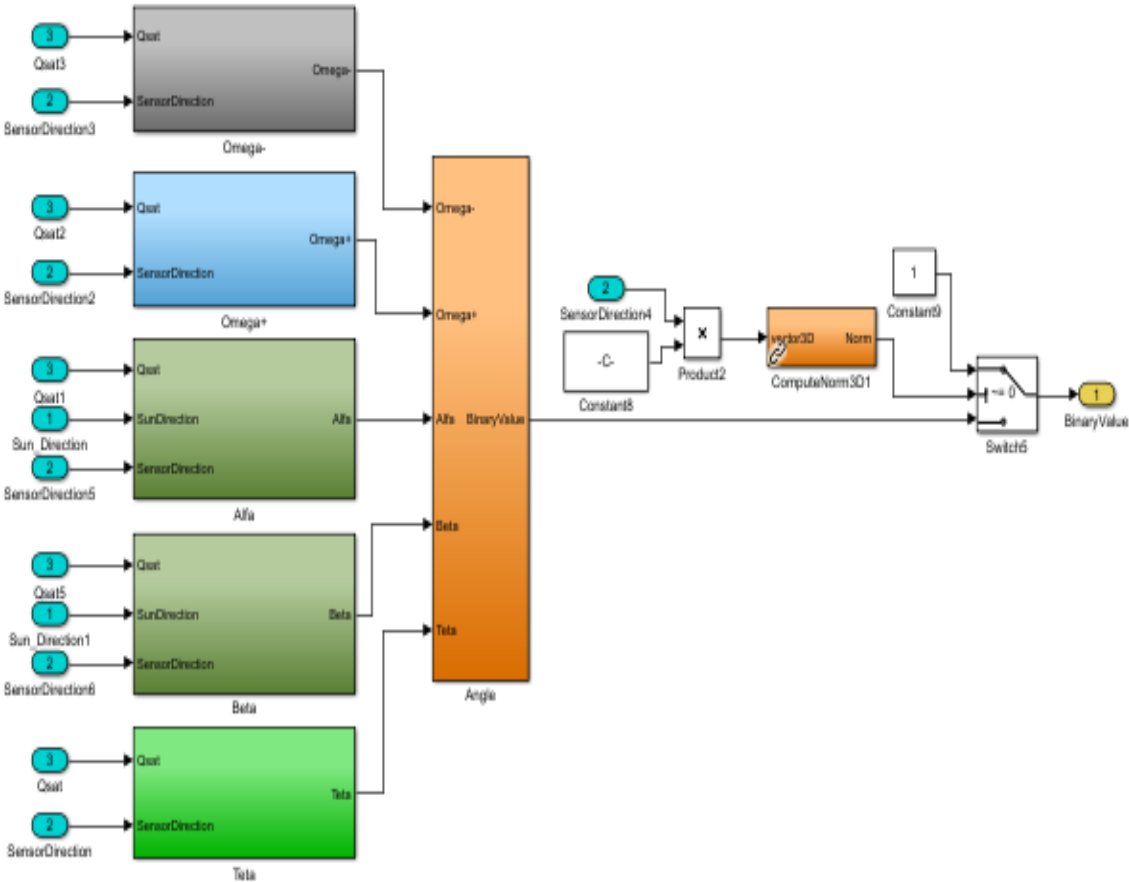


Figure 64 - Panel Shadow Model

For example, considering the sensor on the -Y face, we can see how the panel is covering the Sun Direction (Yellow vector).

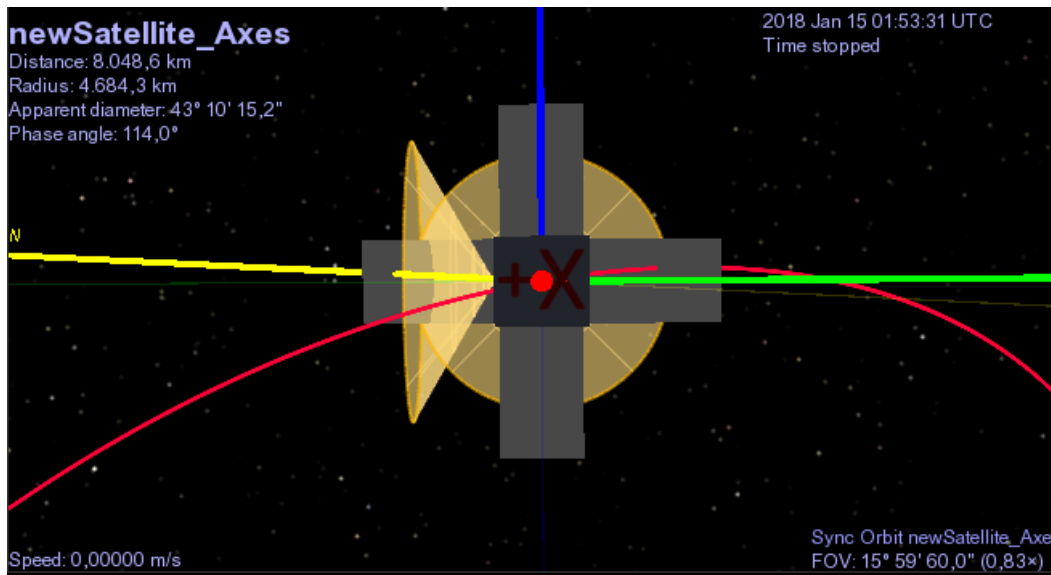


Figure 65 - Simulation of Shadow Problem

Indeed, changing the view to the sensor view, we can see that part of the panel is obstructing the FOW.

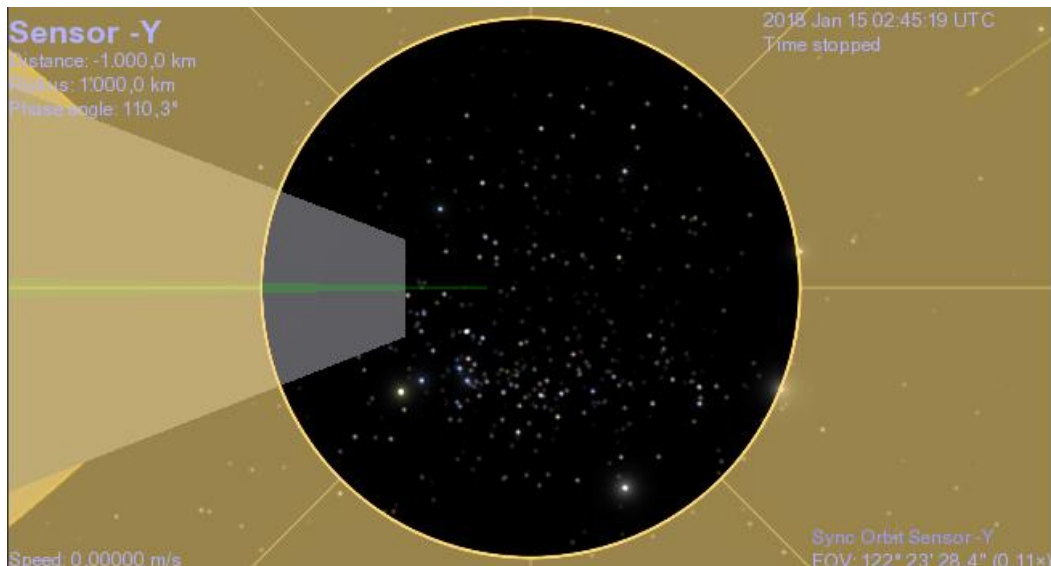


Figure 66 - View of the Sensor -Y direction

4.5.3.1.4. Multiple Sun Sensors

On a satellite we can have more than just one sun sensor, like ATISE where we have five of them. It is then necessary to identify the direction and position of each sensor, with a new version of the sun sensor model:

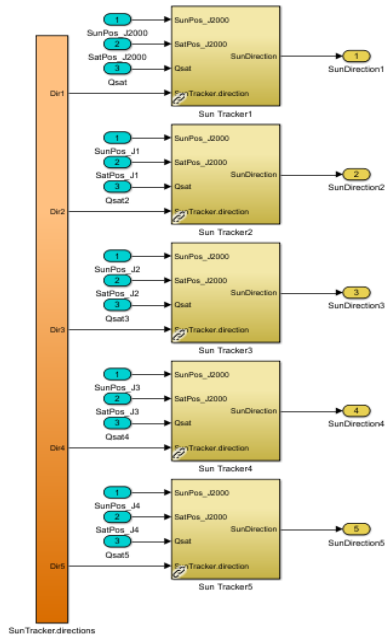


Figure 67 - Multiple Sun Sensor Model

We have five single sensors put together in the same block, as always with the same inputs. All sun sensor directions have to be written in the Multiple Sun Sensor file, as a vector, and all the rest will be the same as the single version. It is possible to use this version even if the satellite has less than five sensors; it just has to write a zero vector in the unused sensors vector directions.

As verification mean we can build a hybrid model, with a reference mode to simulate a random scenario, and check the behaviour of the sensors.

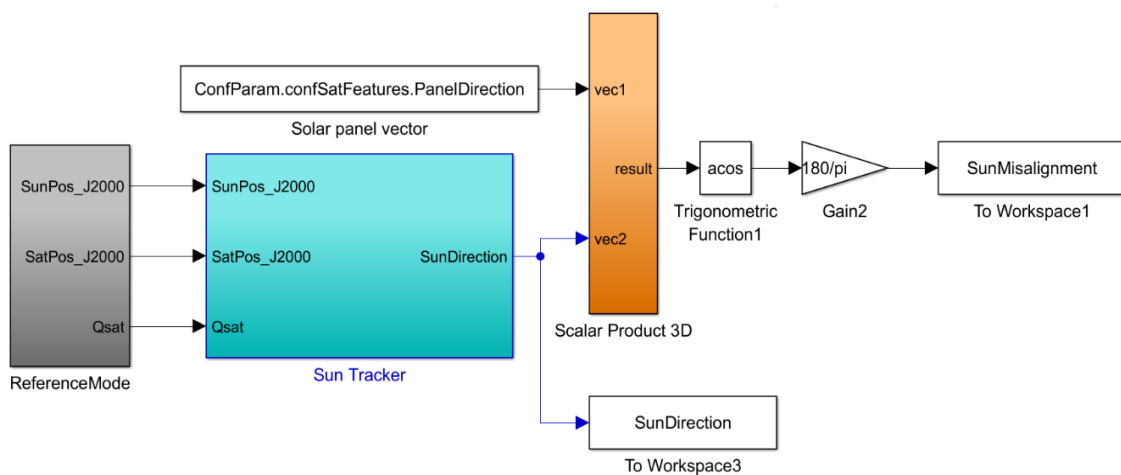


Figure 68 - Validation Sun Sensor Model

4.5.3.2. Safe Mode Controller

To stabilize the attitude and charge the batteries of our satellite, three phases are performed:

- an angular speed reduction after going out of the launcher for each axis with the magnetorquers
- induction of inertial kinetic moment with the wheel spinning, alignment of the wheel axis with the orbital normal
- rotation of satellite to point the solar panels towards the sun, again using the magnetorquers

First of all, our inputs are all the sensors data and a feedback from a reaction wheel in term of kinetic moment; while our outputs will be a command torque for the reaction wheel, and a command magnetic moment for the magnetorquers.

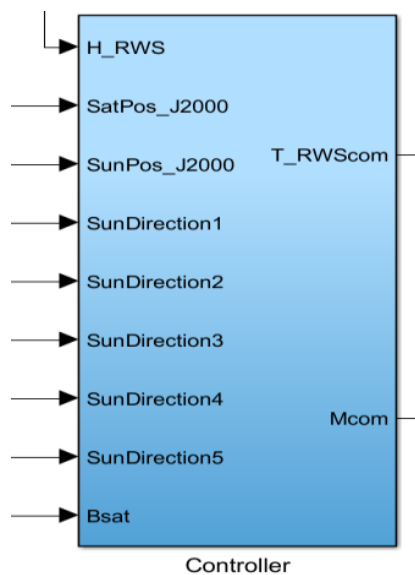


Figure 69 - Controller Block

4.5.3.2.1. Precaution Controllers

Before talking about command laws, we should mention a couple of particular solutions, because in that case we only use Sun Sensors.

- First problem, we have to consider how the controller has to react during a particular moment as an eclipse or a shadow panel situation; during these periods we receive as output:

$$\text{Sun Direction} = [0 \ 0 \ 0]$$

But if the controller receives this value, it could interpret it as a direction and try to reach it; easily the code could not compute properly the simulation. For that reason, during an eclipse or shadow case, it is necessary to introduce a controller able to maintain as input the last direction that a sun sensor has sent before entering one of these cases.

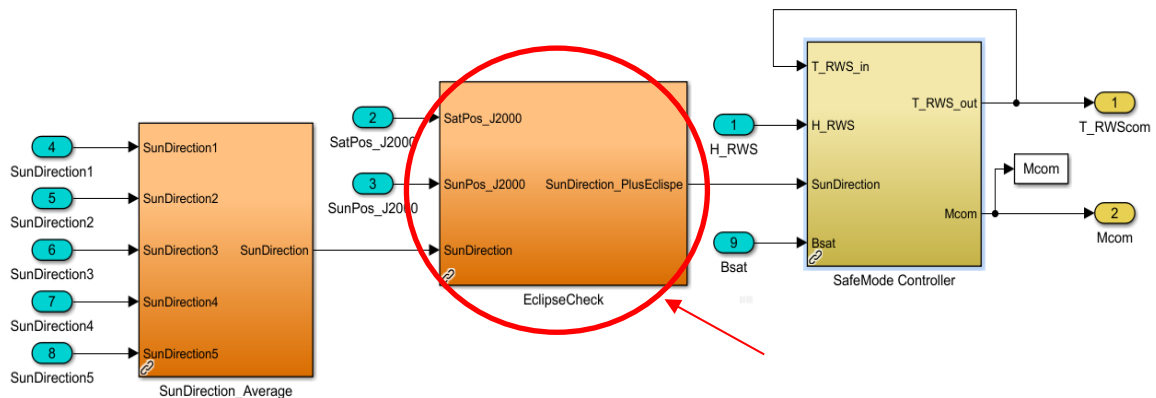


Figure 70 - Controller Model

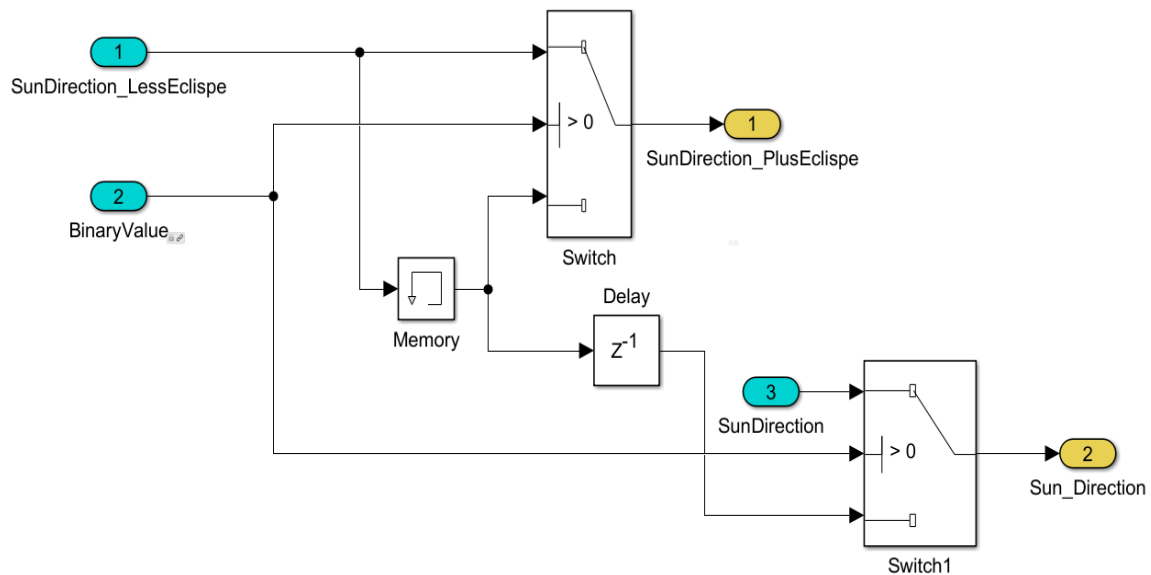
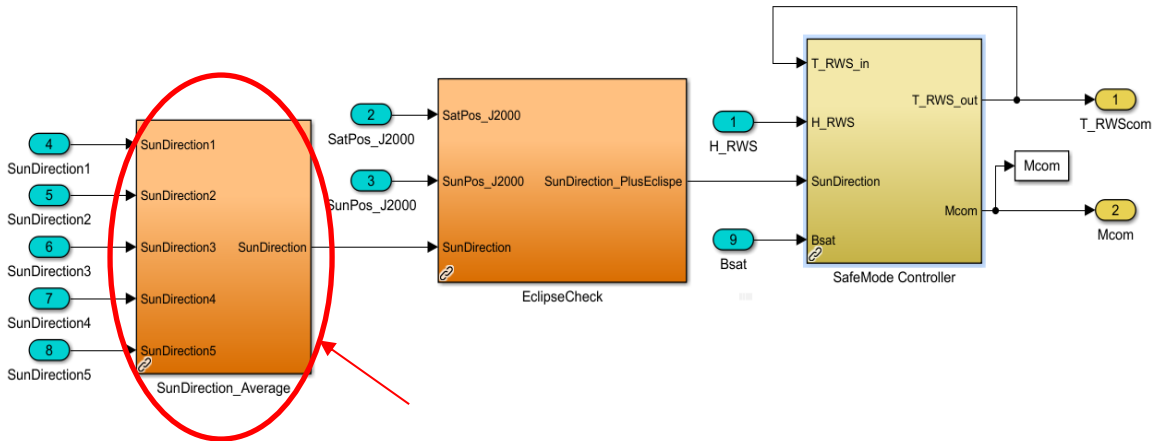


Figure 71 - Eclipse Check Model

Thanks to the binary value, and a Memory block we can keep last direction calculated.

- Another issue could be how to choose which direction to take between five, because the accuracy could be low, and with more than one sensor seeing the

sun, it should be better to do an average between all directions, getting just one information.



It will take into account this average, and a gain as Accuracy of the instrument:

$$y = \frac{a_1 * x_1 + a_2 * x_2 + a_3 * x_3 + a_4 * x_4 + a_5 * x_5 \dots}{a_1 + a_2 + a_3 + a_4 + a_5 \dots}$$

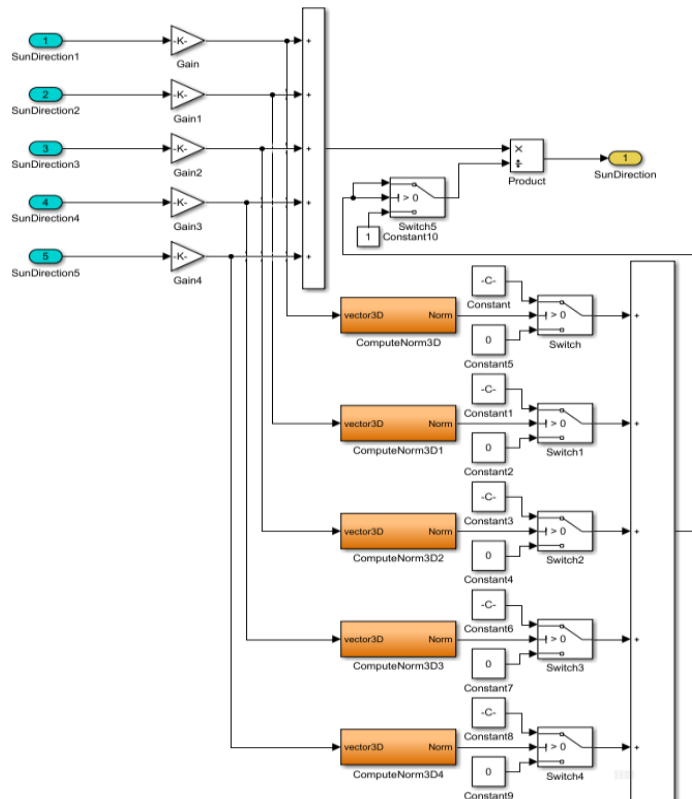


Figure 72 - Sun Direction Average Model

After these precautions, we can go deeper into the Safe Mode Controller, which is divided in three phases, with a check on the speed that allows switching between them.

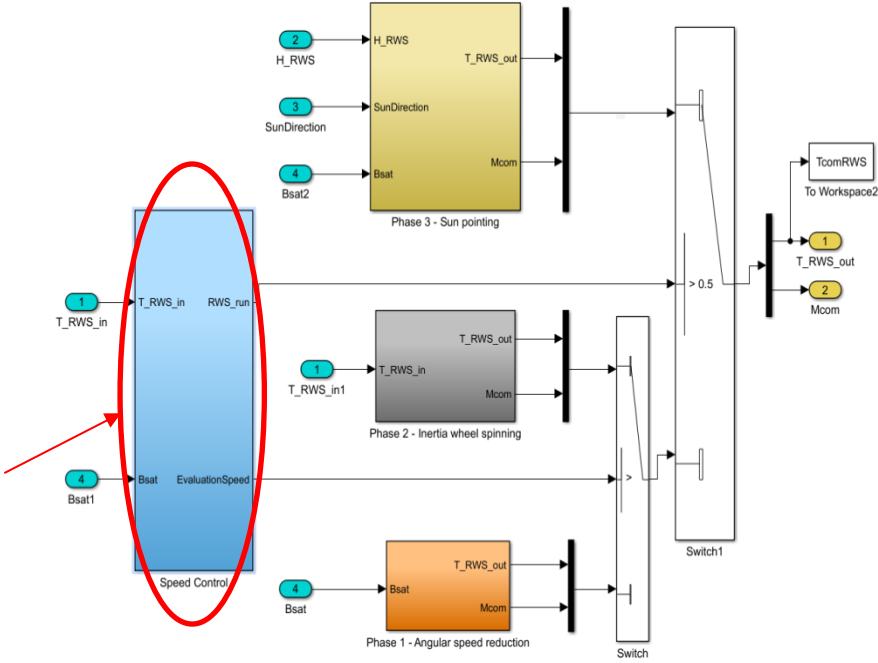


Figure 73 - Safe Mode Controller Model

There is a first check about the magnetic field speed variation: if it is higher than a determinate value, we use the magnetorquers to reduce it. A second check is performed on the reaction wheel speed: if it reaches its maximum, we can start the third phase with Sun Pointing.

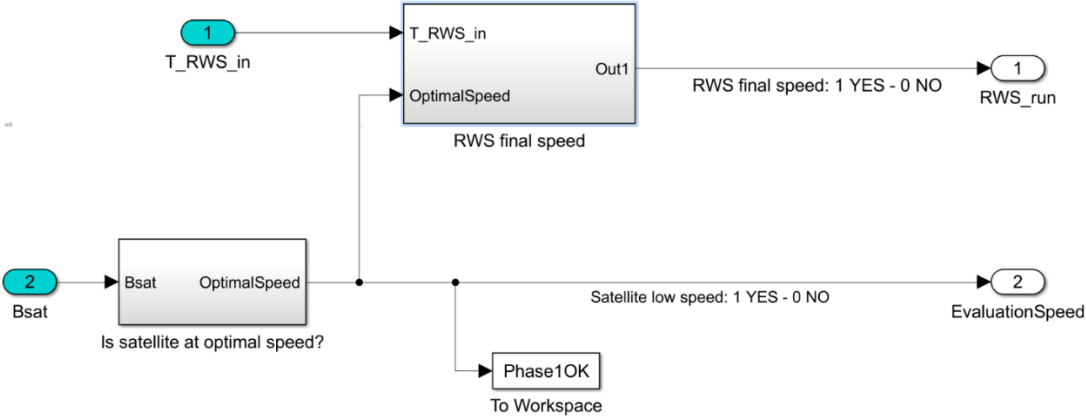


Figure 74 - Speed Check Model

As we can see, the first phase is always ready to reduce the angular speed, while the second phase passes to the pointing phase after the RW reaches its maximum speed.

4.5.3.2.2. Angular Speed Reduction

As already discuss in the Safe Mode Dynamic section, the command torque will be:

$$\vec{C}_{com} = \vec{M}_{com} \wedge \vec{B} = -\frac{[K]}{\|\vec{B}\|} \vec{b} \wedge \vec{B}$$

At this point we can optimize the command line in the controller taking just the colinear component with the magnetic field:

$$\vec{M}_{com} = \vec{M}_2 - (\vec{M}_2 \cdot \vec{b}) \vec{b}$$

However, it is already collinear in our case. Below that, our model should be built, generating an error:

$$\vec{M}_{com} = \frac{\frac{\vec{B}_{t1} - \vec{B}_{t0}}{dt}}{\left\| \frac{\vec{B}_{t1} - \vec{B}_{t0}}{dt} \right\|} \left(-\frac{[K]}{\|\vec{B}\|} \right) \quad \text{with} \quad dt = \frac{1}{f} \quad f = \text{frequency}$$

And considering $[K] \approx k_{xz}$ mentioned previously in the dynamic dissertation.

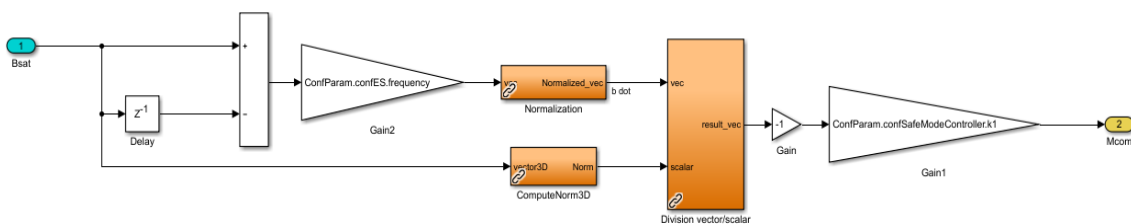


Figure 75 - Reduction Angular Moment Model

4.5.3.2.3. Inertia Wheel Spinning

After the first phase, the de-tumbling, we can start to run the only reaction wheel chosen:

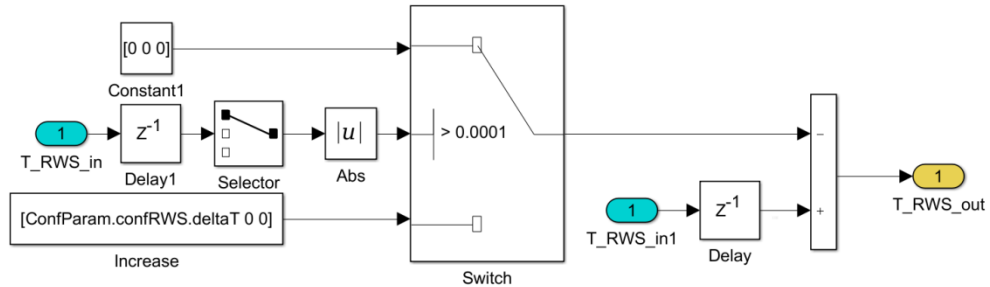


Figure 76 - Inertia Wheel Spinning Model

Starting with a default value of zero, we set a maximum torque available just for the safe mode, and a ΔT_{RWS} , with which reaches the maximum speed, by generating an error:

$$T_{RWS_{out}} = T_{RWS_{error}} = T_{RWS_{max}} - T_{RWS_{t1}}$$

When the Speed Control Model decides that we reached the maximum speed allowed in the safe mode, we switch to the last phase.

4.5.3.2.4. Sun Pointing

For the last phase of the safe mode controller, we have to turn the solar panels towards the sun direction using the data from the five sun sensors already shown. In that phase we use the magnetorquers and restrain them to their Nominal Magnetic Moment.

The command law takes into account the magnetic field variation making to make an estimation of speed, and multiplies it by the satellite inertia matrix, obtaining the inertial moment of satellite:

$$\vec{H}_{I_{sat}} = -\vec{\omega}_{sat} * I_{sat}$$

As feedback from the actuators model, we get the inertial moment of the reaction wheel:

$$\vec{H}_{pos} = \vec{H}_{I_{sat}} + \vec{H}_{RWS}$$

At this point the Sun Direction is:

$$\vec{H}_{sun_{dir}} = \overline{Sun}_{dir} * \|\vec{H}_{pos}\|$$

And the model generates a target error:

$$\vec{H}_{target} = \vec{H}_{sun_{dir}} - \vec{H}_{pos}$$

Now we need to follow the same command law as for the angular speed reduction:

$$\vec{M}_{com} = -K_2 * \frac{\vec{H}_{target}}{\|\vec{B}\|}$$

With $K_2 = k_y = \frac{2H}{N_y}$.

Then we can build the model and add saturation just before the output, using the Nominal value:

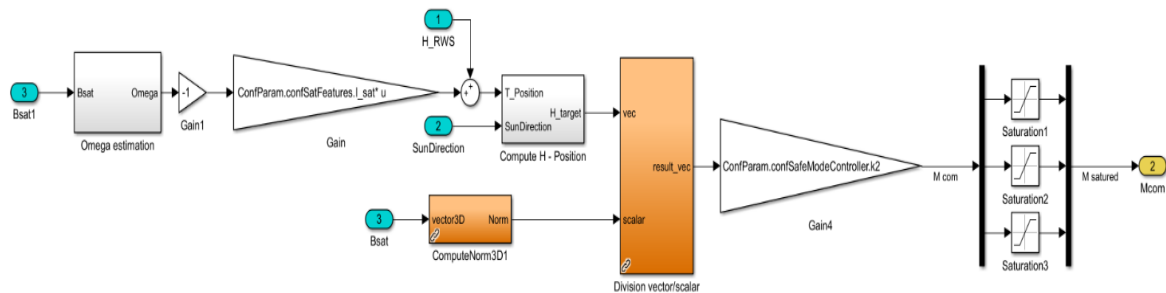


Figure 77- Sun Pointing Model

4.5.3.3. Actuators

As we have something to capture the status of the satellite, we have something to move it, which are the Actuators. In safe mode we use 3 magnetorquers, one on each axis and just one out of three reaction wheels in the panel direction, to de-tumble and stabilize the satellite. Thanks to Magnetorquers we can use the earth magnetic field to align the satellite with field lines, producing a useful torque; this makes possible to pivot the satellite around a known local gradient of magnetic field by using only electrical energy. On the other part, there is a reaction wheel on the X axis for ATISE, which induces a gyroscopic moment to stabilize the rotation of the satellite around one axis.

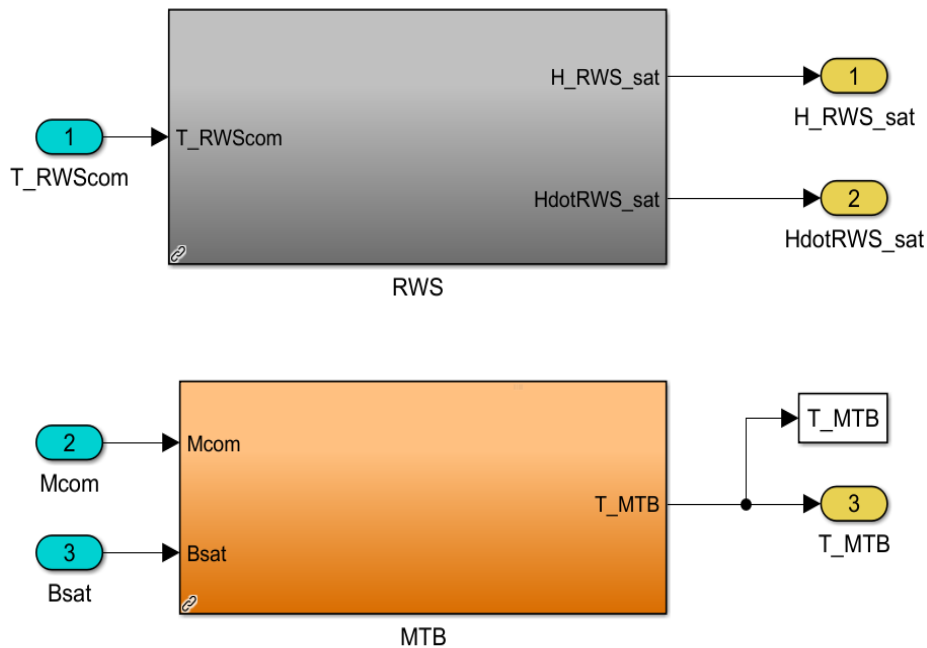


Figure 78 – Actuators

4.5.3.3.1. Reaction Wheels

These little wheels allow an attitude control without using fuel for rockets or other reaction devices. This is accomplished by equipping the spacecraft with an electric motor rotating a mass. When the rotation speed changes, the spacecraft begins to counter-rotate proportionately through conservation of the angular moment; the result is a constant rotation speed. Since the reaction wheel is a small fraction of the spacecraft's total mass, easily controlled, temporary changes in its speed result in small changes in angle. The wheels therefore permit very precise changes in a spacecraft's attitude.

As input we receive the torque command by the safe mode controller, then it is split in four vector elements, because we could have four reaction wheels instead of three; we do not consider having less than three wheels in our ATISE configuration. With the fourth wheel, it is possible to drastically reduce the gyroscopic derivation, but it depends on available space and attitude requirements.

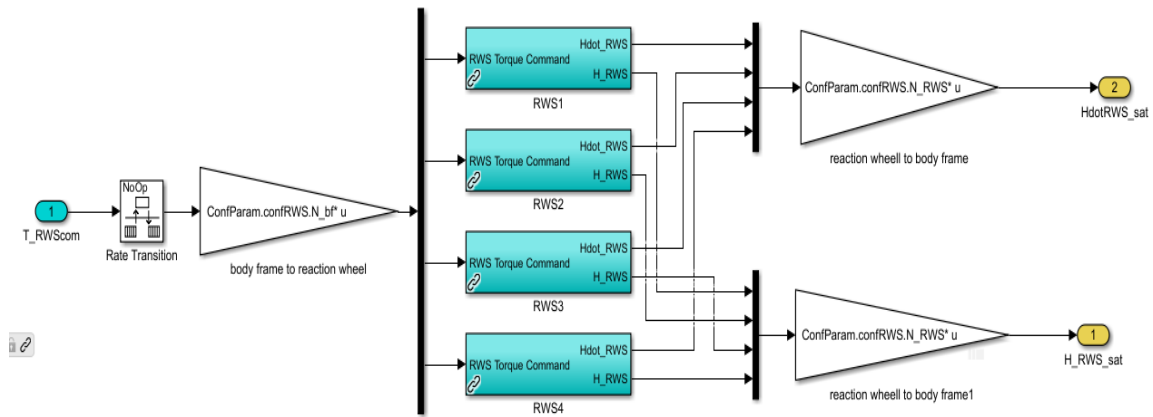


Figure 79 - Reaction Wheel Torque Command Vector Splitting

As outputs we need the inertial moment generated by the wheel in rotation, and its derivative to take into account the satellite dynamic.

4.5.3.3.2. Single Reaction Wheel

Keeping the modular path, we can use the single reaction wheel model, having the same input and outputs.

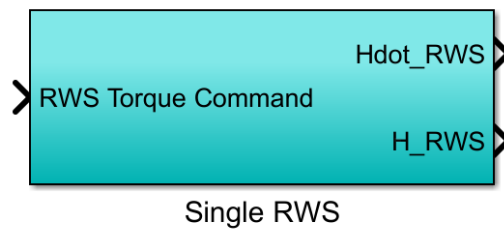


Figure 80 - Single Reaction Wheel Block

Inside each single reaction wheel models, we have a PI controller, that means a Proportional and Integrative controller. The command line is:

$$\omega_{RWS} = \frac{(T_{RWScom} + k_{noise})}{Js}$$

With J the reaction wheel inertia.

To this, we can add the white noise relative to our specific data sheet; moreover, it is necessary to put a couple of saturations, due to non-linear mechanical characteristics:

one for the torque, which can be generated by the reaction wheel, and another for the maximum rotation speed.

We set a speed control to keep a constant rotation speed until we receive a command torque not equal to zero.

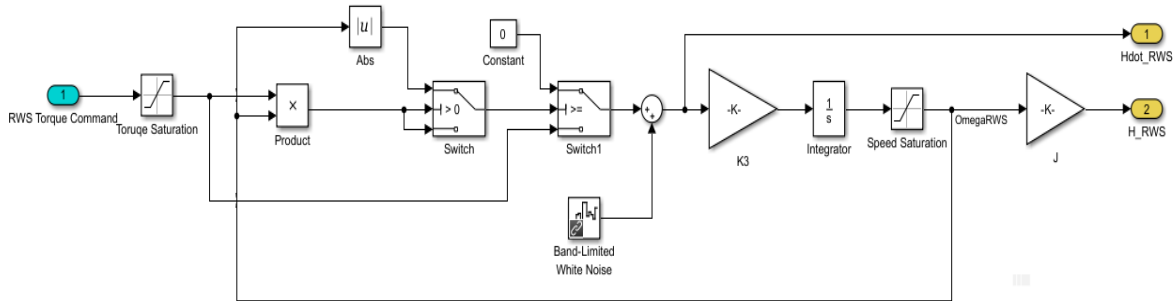


Figure 81 - Command Line Reaction Wheel Model

To obtain the inertial moment useful to complete the command ring we use:

$$H_{RWS} = \omega_{RWS} * J$$

RESULTS

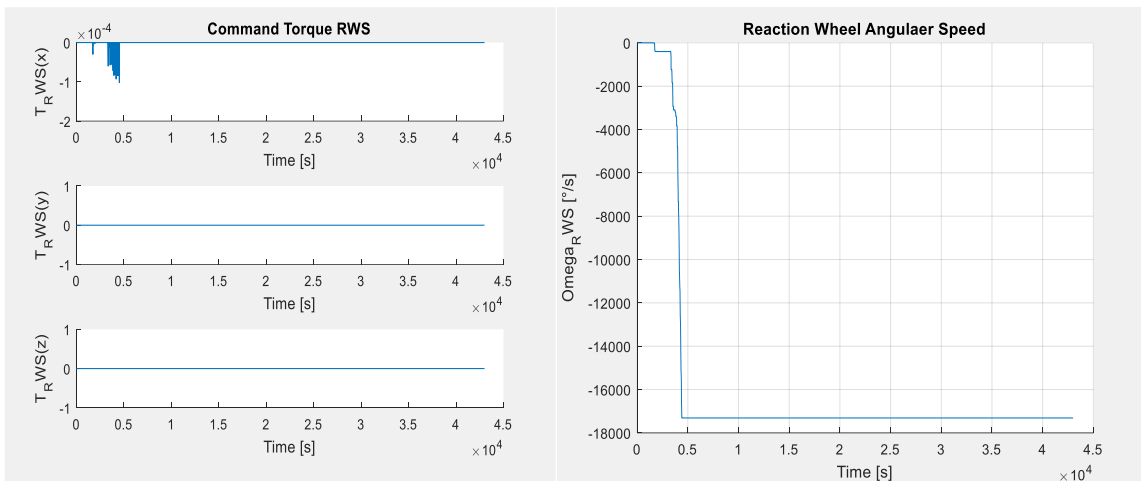


Figure 82 - Result in speed and torque for RWS

4.5.3.3.3. Magnetorquers

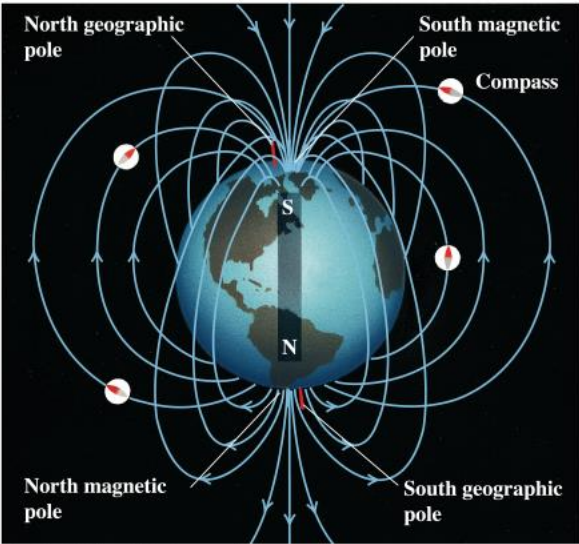
Three magnetic bars positioned orthogonally along the three satellite axes, $[x_{sat} \ y_{sat} \ z_{sat}]$, which can generate a magnetic field of arbitrary orientation (i.e. flip the North and South poles), up to the maximum vector sum of the dipole moment of each rod individually.

This artificial field interacts with the Earth's magnetic field to produce an external torque on the satellite that will tend to line up the fields. Mathematically, the torque is provided by:

$$\tau = \mu \times B$$

where τ is the torque on the satellite, B is the ambient magnetic field, and μ is the magnetic field of the satellite.

This torque only has two degrees of freedom, i.e. instantaneously the torque rods will tend to align the vehicle and Earth fields, with no control of the rotation of the vehicle around its magnetic poles. However, remember that the magnetic field lines around the Earth are themselves a dipole field, which has a toroidal shape.



Copyright © Addison Wesley Longman, Inc.

Figure 83 - Earth magnetic field

That said, the field is weak, so the actual torque produced by torque rods is very small. It's completely unsuitable for agile spacecraft, for which attitude control effectors like reaction wheels or control moment gyros are typically used. Torque rods are used to de-saturate these effectors which accumulate momentum due to disturbance torques like atmospheric drag, and to de-spin satellites.

According with that, our model should have as input earth magnetic field, that we get from the magnetometer, and the command moment from the safe mode controller; obviously in output we will obtain a magnetic torque.

As well, to realize a model more real, we have to add some adjustments like white noise, Residual Moment, Axes Misalignment, and saturation not to exceed the Magnetic Moment Maximum. Thus, the model should be:

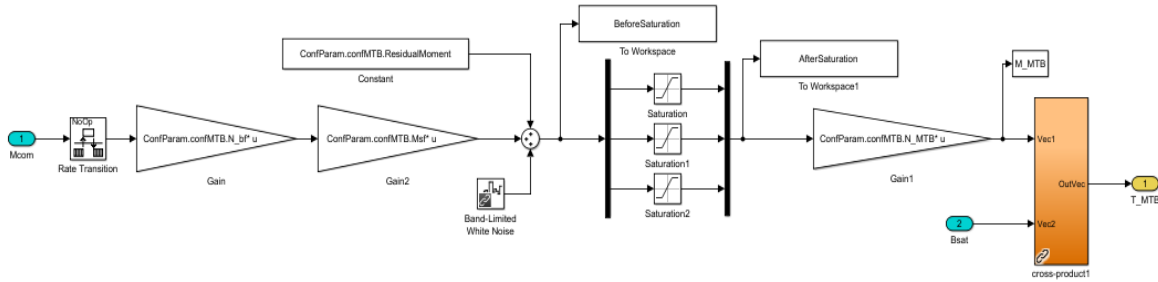


Figure 84 - Magnetorquers Model

RESULTS

As a result we can observe the difference before and after the saturation of the command moment which comes from the controller. We have a huge request at the beginning due to the high rotational speeds caused by the launcher; then, an irregular activity due to not constant perturbations and disturbances. We can see on the following graph the command torque in blue and the effect of the saturation in orange:

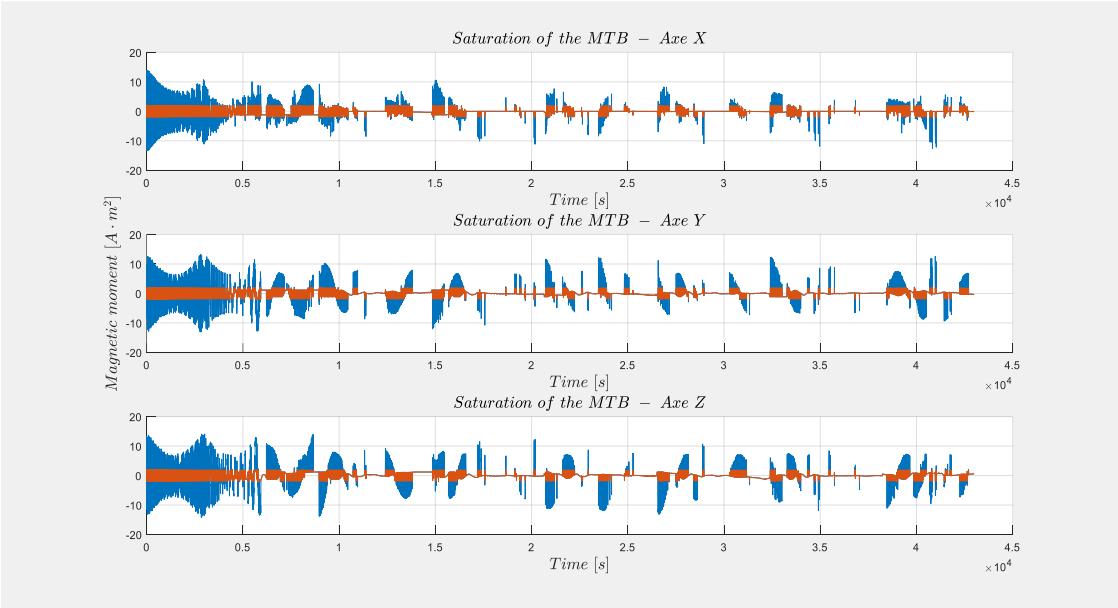


Figure 85 - Saturation of Magnetorquers

And here, the effective Magnetic Torques which move the satellite in correct position:

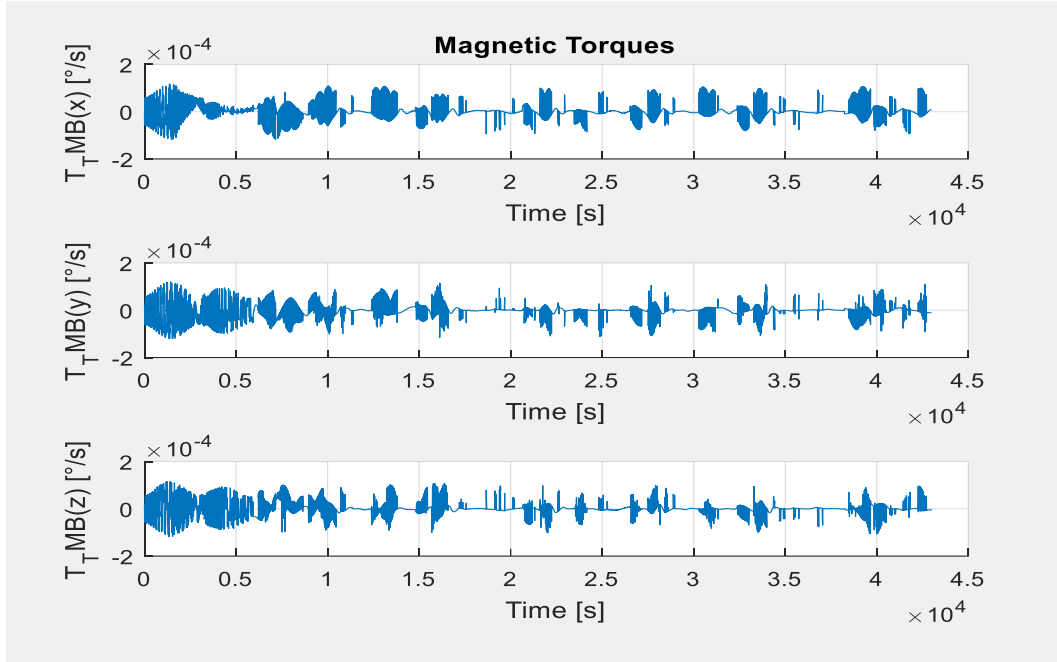


Figure 86 - Magnetic Torques requested

4.5.3.4. Satellite Dynamics

At that point, we just take all the forces, and define a double control in speed and position of satellite, without to forget that we have to transform the speed vector in a quaternion frame.

We write the dynamic equilibrium formula:

$$I_{Sat} \frac{d^2 \vec{\theta}}{dt^2} + \left(\vec{H}_{RWS} \times \frac{d\vec{\theta}}{dt} \right) + \vec{H}_{RWS} + \left(I_{Sat} \frac{d\vec{\theta}}{dt} \times \frac{d\vec{\theta}}{dt} \right) = \vec{T}_{ext} + \vec{T}_{MTB}$$

$$\frac{d^2 \vec{\theta}}{dt^2} = \left[- \left(\vec{H}_{RWS} \times \frac{d\vec{\theta}}{dt} \right) - \vec{H}_{RWS} - \left(I_{Sat} \frac{d\vec{\theta}}{dt} \times \frac{d\vec{\theta}}{dt} \right) + \vec{T}_{ext} + \vec{T}_{MTB} \right] * Inv(I_{Sat})$$

$$\frac{d\vec{\theta}}{dt} = \int \left\{ \left[-\left(\vec{H}_{RWS} \times \frac{d\vec{\theta}}{dt} \right) - \vec{H}_{RWS} - \left(I_{Sat} \frac{d\vec{\theta}}{dt} \times \frac{d\vec{\theta}}{dt} \right) + \vec{T}_{ext} + \vec{T}_{MTB} \right] * Inv(I_{Sat}) \right\} dt$$

$$\frac{d\vec{\theta}}{dt} = \vec{\omega}_{Sat} = \frac{1}{s} \left[-\left(\vec{H}_{RWS} \times \frac{d\vec{\theta}}{dt} \right) - \vec{H}_{RWS} - \left(I_{Sat} \frac{d\vec{\theta}}{dt} \times \frac{d\vec{\theta}}{dt} \right) + \vec{T}_{ext} + \vec{T}_{MTB} \right] * Inv(I_{Sat})$$

According with that, we obtain the satellite speed vector. Then about the position we pass to quaternion frame, that means to add an element to $\vec{\omega}_{Sat}$, which is a zero:

$$q' = (0, \vec{\omega}_{Sat})$$

And after that we do a quaternion product:

$$q' \cdot q = q''$$

Where q is the quaternion satellite position as feedback control, that is:

$$Q_{Sat} = q = \frac{1}{2} \int q'' dt = \frac{q''}{2s}$$

The model will receive in input all the torques and inertial moment, and return Q_{Sat} and ω_{Sat} :

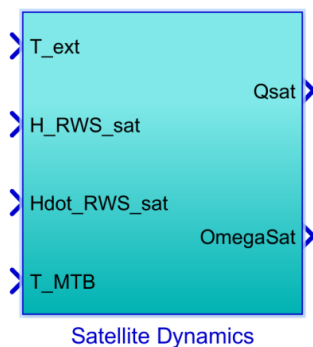


Figure 87 - Satellite Dynamics Block

Inside the block, there is a first model which computes the speed:

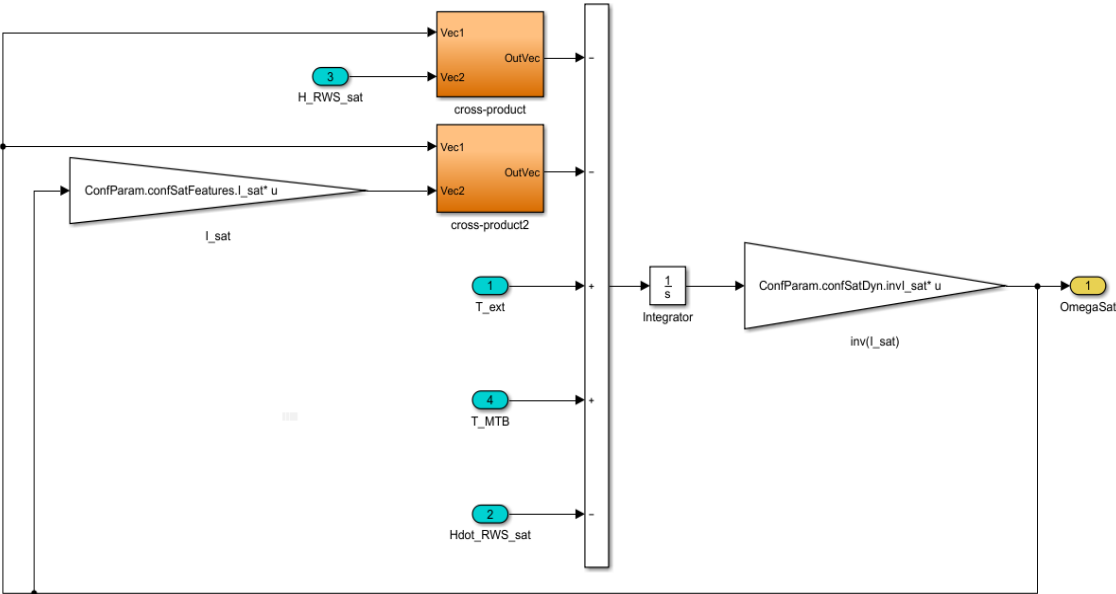


Figure 88 - Computing Satellite Speed Model

And following is a second part with the rotation in quaternion frame, and satellite position evaluation:

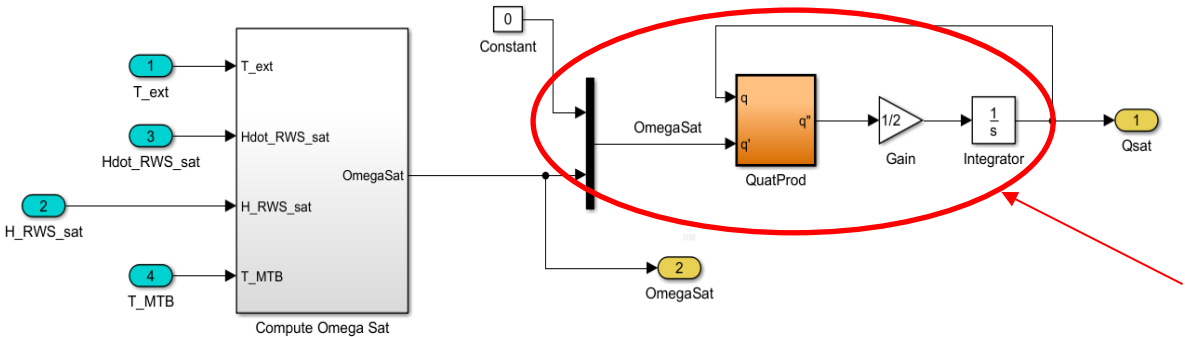


Figure 89 - Satellite Dynamics Model with a zoom on the Satellite Position Computation

4.5.4. Phases and Graph Analysis

As well, after it starts the sun pointing without coming back to instability, but just controlling the actuation. We can observe in the following graph this behaviour:

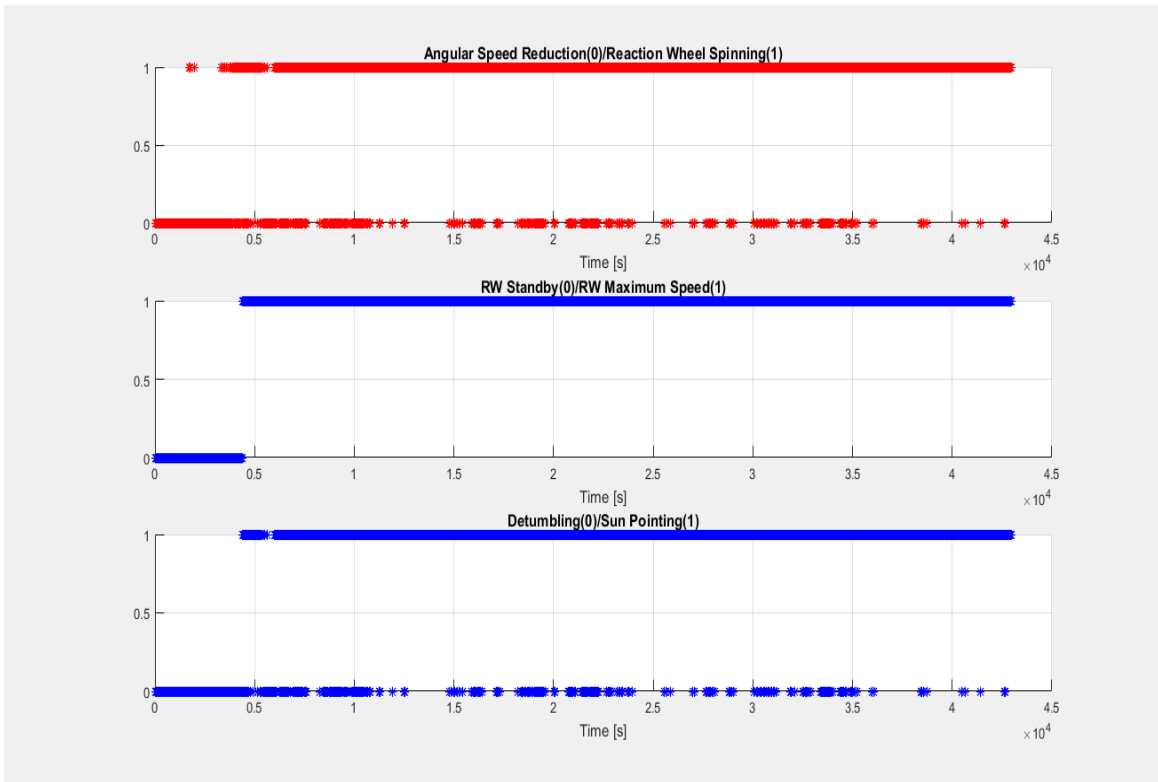


Figure 90 - Phases Analysis

According with this analysis, we can observe the de-tumbling, first with the strong speed reduction, and then a good control keeping, with low rotations, except for the ω_x influenced by the RW which have x as rotation axis:

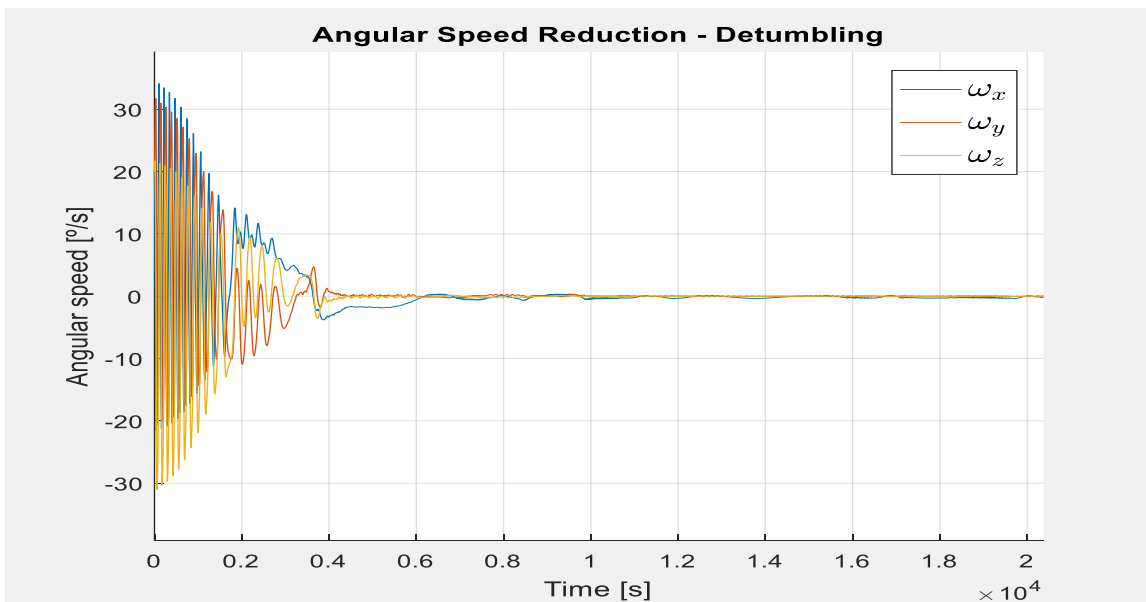


Figure 91 – De-tumbling

We can do a focus on the angular speed component ω_x , to verify the attitude requirement:

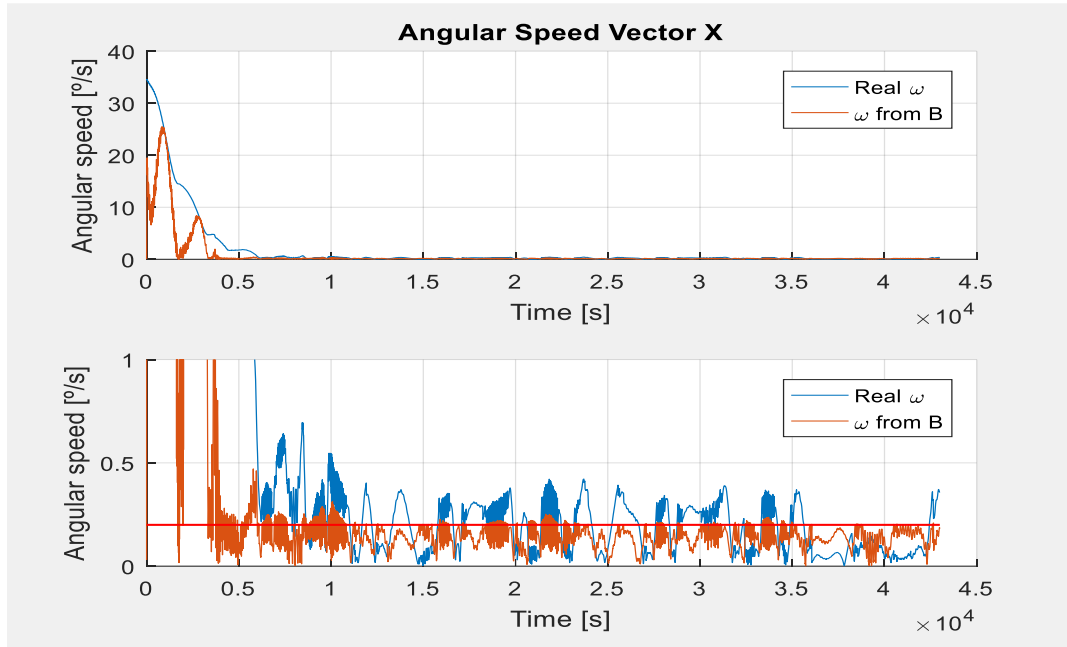


Figure 92 - Zoom on the Angular Speed in X axis

As well, the requirement about the rotation speed lower than 0.5 °/s, it's reached (4.1.2).

Another important parameter is the Convergence Time, useful to identify the performance of attitude controller, which in our case is:

$$T_{conv} = 6023.5 \text{ s}$$

ω_{Xmax}	ω_{Ymax}	ω_{Zmax}
-0.0087 °/s	-0.0021 °/s	0.0000364 °/s

For the third phase, we can measure the sun misalignment between the Sun Direction and Solar Panels Direction; for ATISE the requirement is to have a misalignment lower than 30°:

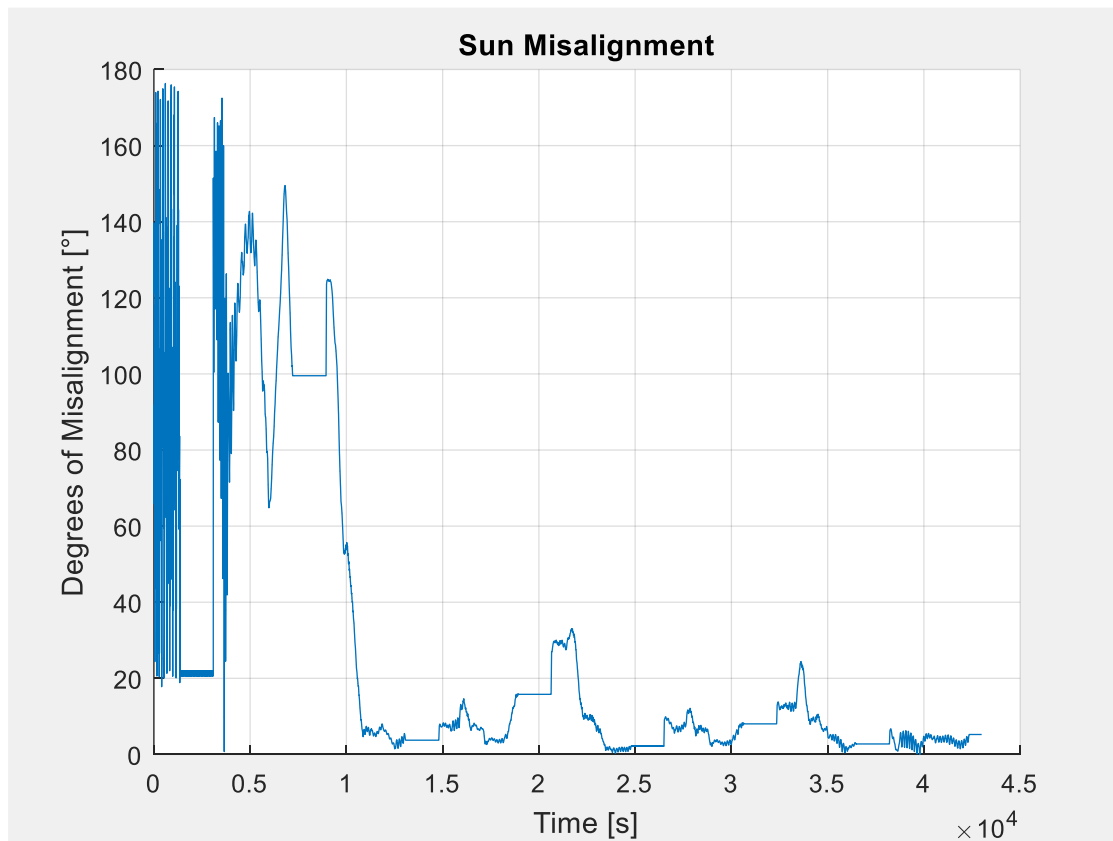


Figure 93 - Sun Misalignment

After the first phase, around 10000 s, we reach another requirement about the Sun Misalignment, which is lower than 20° almost all the time, with 30° required (4.1.1), and with partial oscillation due to the eclipse periods and maybe to the panel shadow. On the graph we can individuate also the eclipse periods as a short straight segment, during which the controller does not receive any information, thus does not command anything.

As far as we focus on the performances of the Safe Mode Model, it respects our requirements, in particular with a T_{conv} lower than maximum accepted of 12000 s, and angular speeds lower than $0.5^\circ/s$ (4.1.2); but it needs to admit that we used a determined initial condition, and during a simulation it is hard to take into account other error sources. However, we considered margins of security in order to avoid these errors. About the sun pointing, we reached the objective, with a discrete stability, considering the problem of the eclipse.

4.5.5. Mission Mode Simulator

More complex and powerful is the Mission Mode Model; from the left to the right it is possible to individuate, as always, the model of time, environment and perturbation torques, but then a sensor's block with one more output due to the presence of the Star Tracker, and following the estimator which calculate Sun Direction and satellite

rotation speeds; these are sent to the controller, which is managed by the Command Value. This output decides which control law is used inside the controller, that is, between sun pointing or target pointing; after that, the controller computes the necessary command input for the actuators, which act on the satellite dynamic. As well, the final dynamic results return as feedback for the control loop.

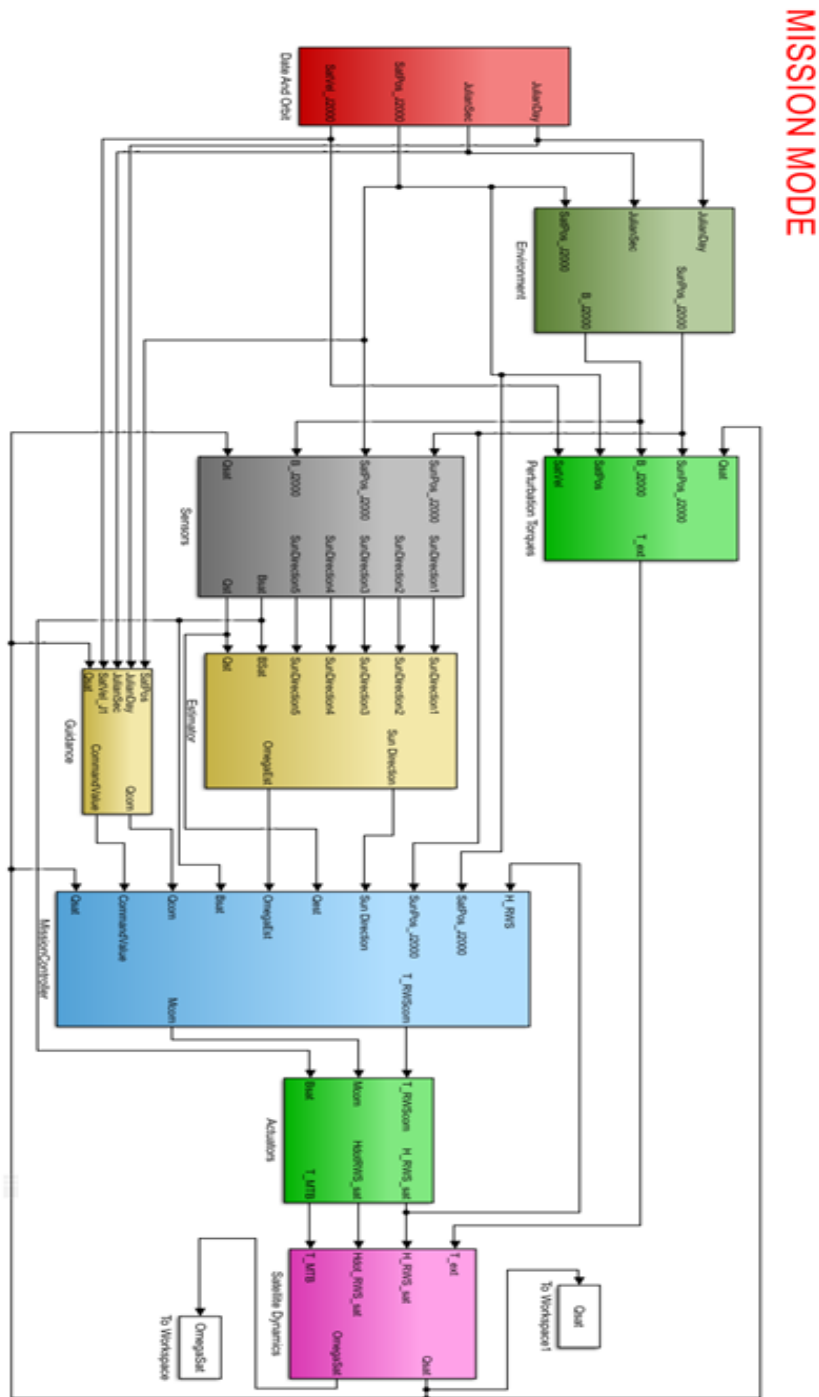


Figure 94 - Mission Mode Model

At this point, obviously some of the systems model is already built, like the actuators don't change, and as well sun sensors, or magnetometer; so, I will go through, and showing directly the conception of what else has been necessary to create and complete the mission model.

4.5.5.1. Star Tracker

Previously I shown how to compute the quaternion for the star tracker (section 4.4.5.1); now to build the model, we used the quaternion from the satellite dynamic, and we apply the mathematic solution already developed. In that way we obtain a quaternion delayed by the constant time, adding noise and bias.

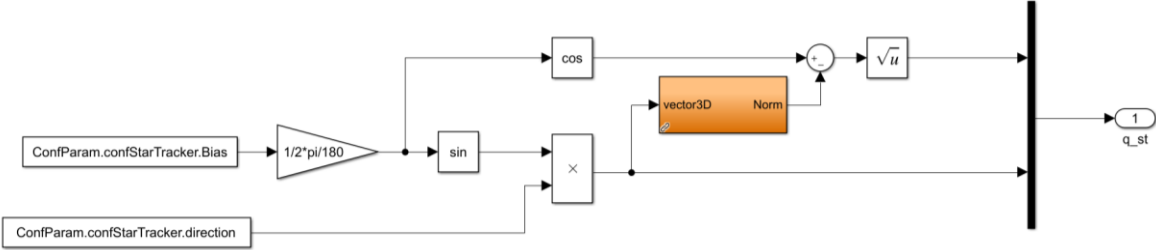


Figure 95 - Bias to the quaternion

Then, I considered the problem when the sun or Earth is inside the field of view of the sensor, each with an exact angle of exclusion given by the producers.

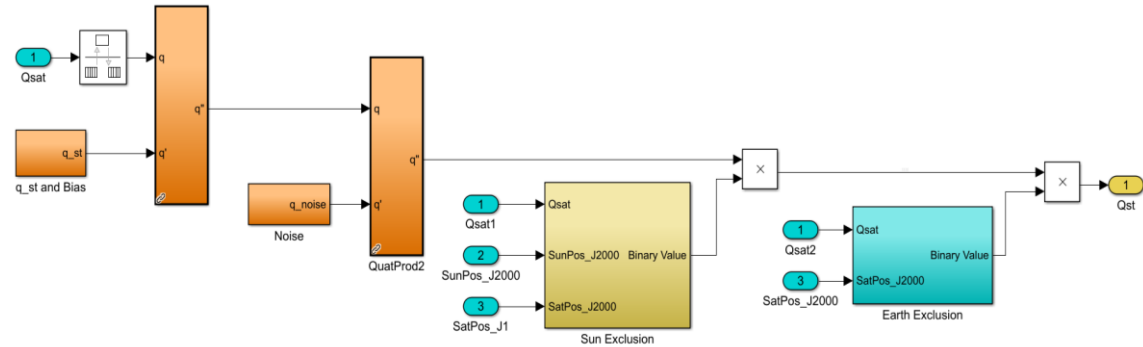


Figure 96 - Star Tracker Model

Easily to see, there is a first quaternion computation, starting with the real quaternion given by the dynamic equation of the satellite, and then the verification about Sun and Earth exclusion. This verification is computed with two separated angle evaluations, as already shown for the sun sensor case; so, for the first one I used the direction vector of the sensor and the direction of the Sun in the J2000 reference frame, then rotated in the satellite frame and calculating the angle between them, meanwhile for the second I used the negative satellite direction in J2000, which corresponds to the Earth direction, and then calculating in the same way the angle. In both case the output quaternion will be a zero vector.

4.5.5.2. Estimator

The goal of the Estimator is to use the data given by the sensors and compute a speed estimation of the satellite; as well, it gives an average of all the sun directions given by the sun sensors, in order to have just one direction for the controller, as well shown for the safe mode model.

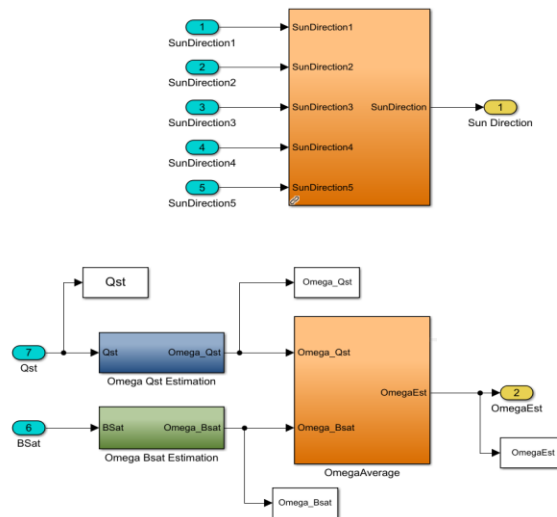


Figure 97 - Estimator in Mission Mode

I calculate with an iterative method the gain set for the average, between the speed computed with the magnetic field and quaternion estimated (section 4.4.5.2).

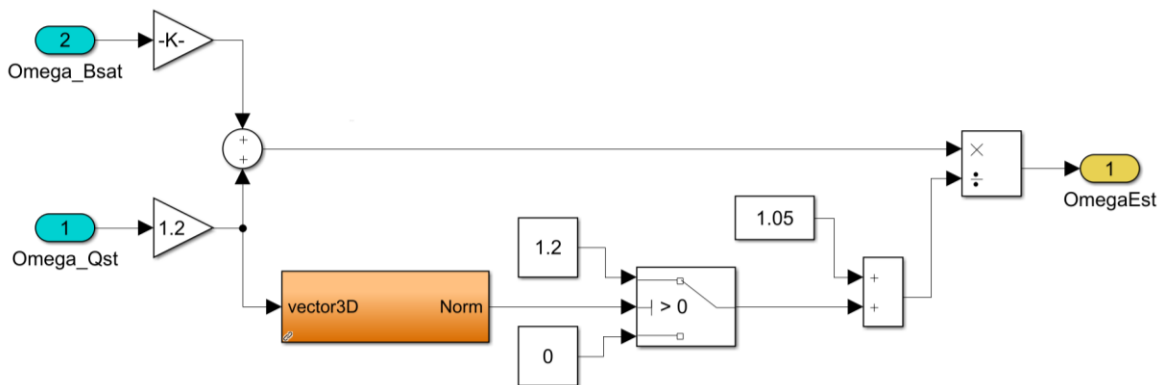


Figure 98 - Rotation speeds average

In the model there are two blocks able to evaluate the speed rotation using respectively the satellite magnetic field, and the satellite quaternion about its position. The first determines the magnetic variation, computing direction and modulus:

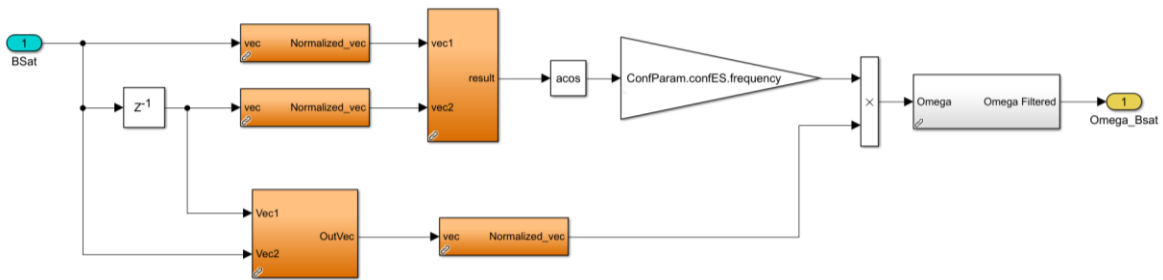


Figure 99 - Computation of magnetic field rotation

And the second using the mathematic approach developed previously (section 4.4.5.2).

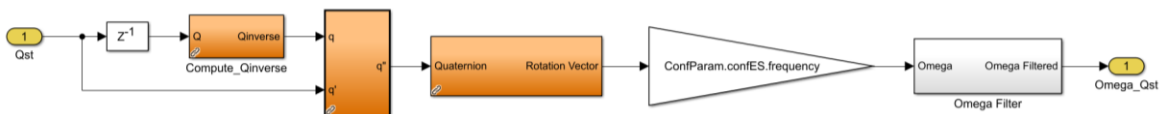


Figure 100 - Computation of quaternion speed rotation

It is implemented a filter, using the Discrete State-Space approach available in the Simulink library, for each direction.

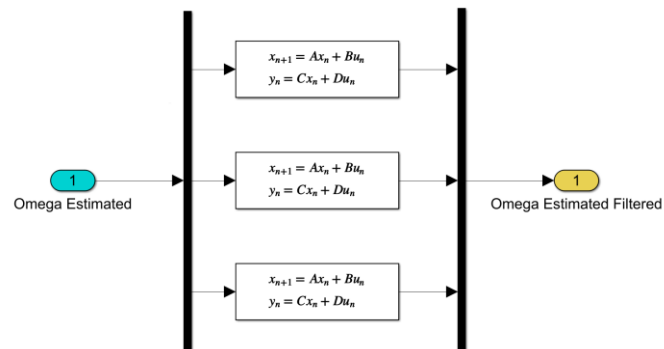


Figure 101 - Discrete State-Space Filter

4.5.5.3. Guidance

This block is useful to set a target that the satellite should point, when there are determinate conditions of angle of view and distance, for example of the ground station.

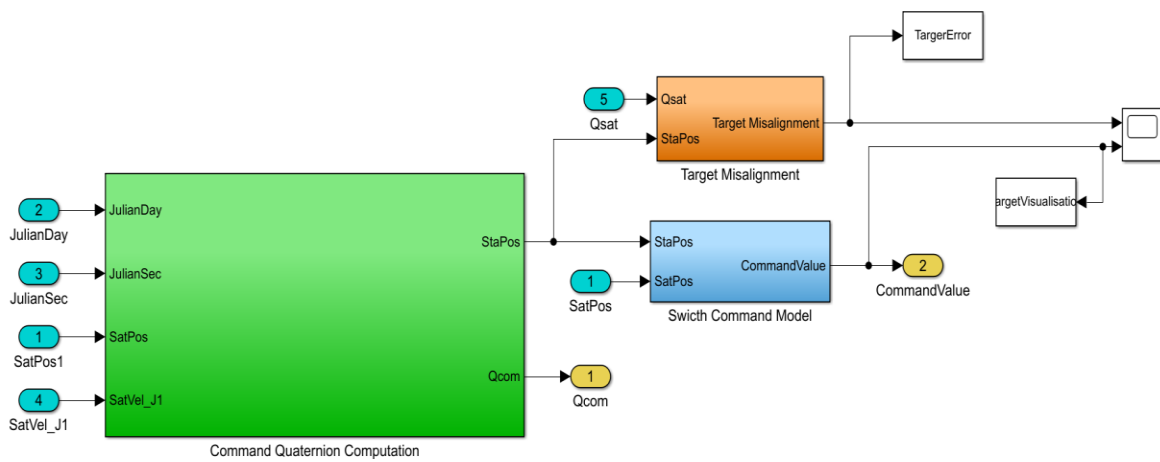


Figure 102 - Guidance Model

Thanks to this evaluation, I can control which law use in the controller, using an output called CommandValue, which leads the Boolean switch between the sun pointing and target pointing.

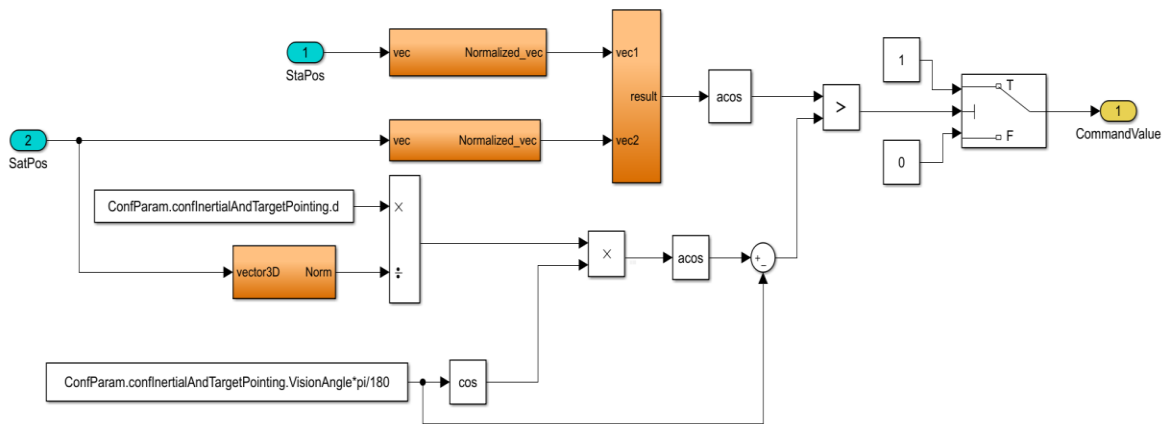


Figure 103 - Switch Command Model

The Command Quaternion Computation model is built in order to require just the coordinate of the target, in term of latitude, longitude, and altitude; in addition, it needs the vision angle, which depends on the satellite mission and instruments; then, it computes the command quaternion.

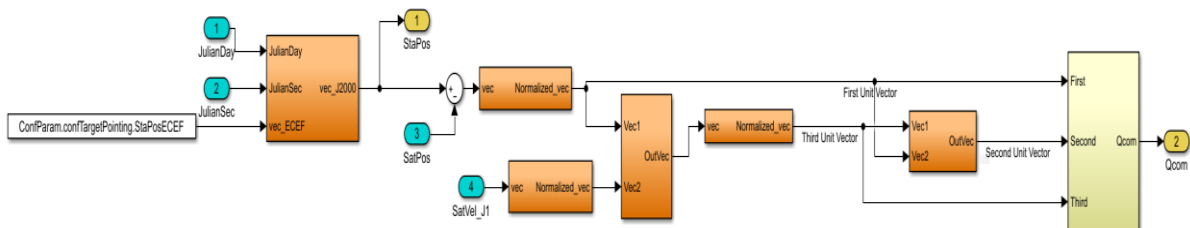


Figure 104 - Command Quaternion Computation Model

This function allows you to set the position (in the form latitude, longitude, altitude) of the ground station for example, that the satellite must point. You can then impose which axis of the satellite body frame must point the station and which other must be normal the satellite's velocity. Matlab structure contains the position of the ground station in the ECEF (Earth Centered Earth Fixed) frame and your choice of the axis for this kind of pointing.

4.5.5.4. Mission Mode Controller

At this point, I decided to divide into two phases the controller:

- Sun pointing;
- General target pointing, which could be the ground station, or the north pole etc...

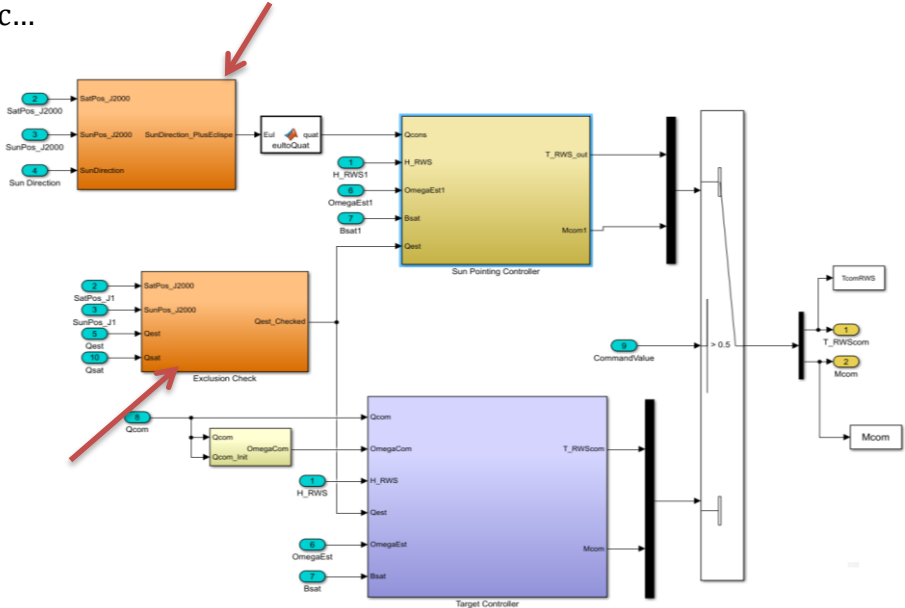


Figure 105 - Mission Mode Controller Model with Eclipse Check and Exclusion Check

It is possible to improve the accuracy of the pointing towards the sun; it means to have an error around 0.01°, and a higher stability. There is, as already implemented in the safe mode, an eclipse control before to the main control law; as well, I applied the same approach to the estimated quaternion in case like sun or earth exclusion.

The two laws are managed by the CommandValue from the Guidance model, and it determines which law use. And it is important to notice also the function used to turn the sun direction into a quaternion.

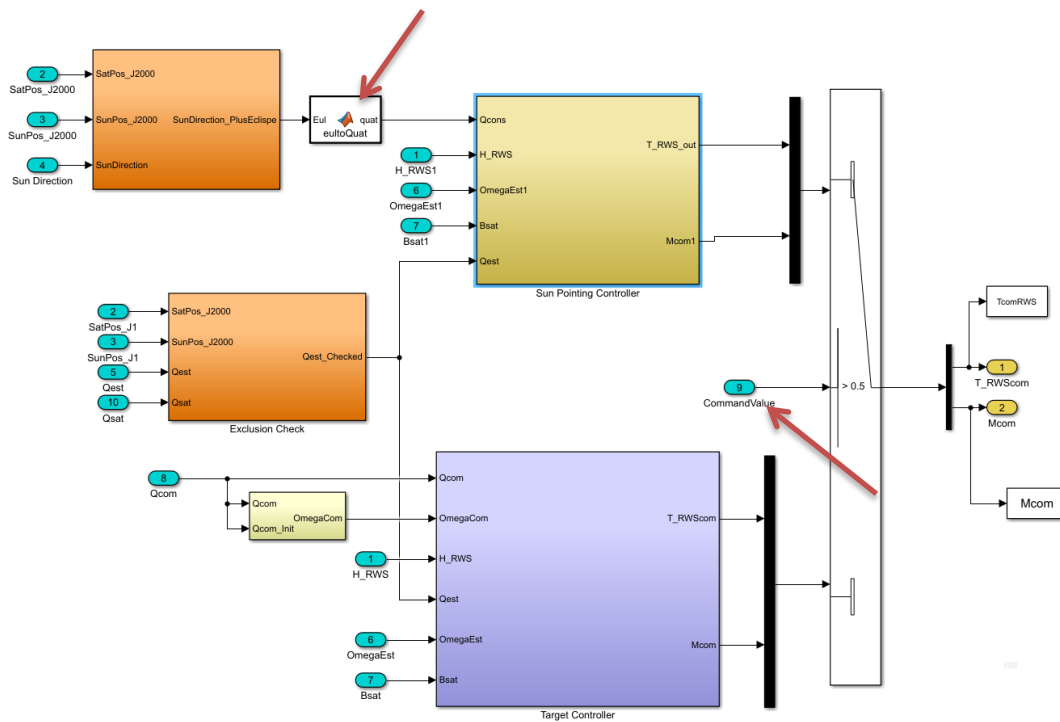


Figure 106 - Vector transformation into Quaternion and Command Value

4.5.5.4.1. Sun Pointing Controller

After transformed the sun direction vector into a quaternion, using the function previously explained (section 4.4.2.1), in order to get a command quaternion; I need a command quaternion, and consequently a command speed, because I have to compute two errors, respectively using the estimated quaternion, and the estimated rotation speed.

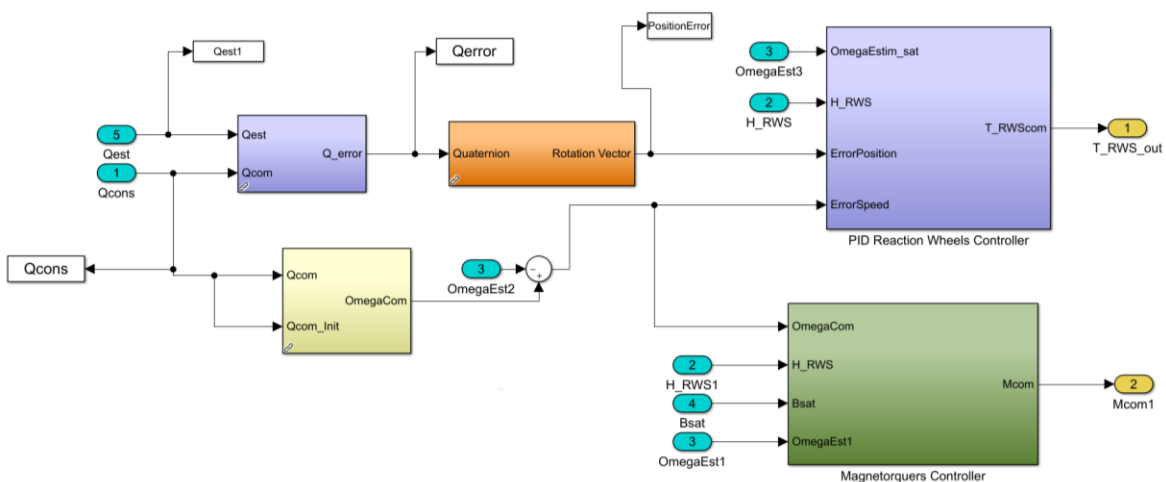


Figure 107 - Sun Pointing Controller Model

These errors are sent to the PID controller; inside that model, the error quaternion is turned into the rotation vector (section 4.4.2.2), and then applying on it the proportional and integration law, meanwhile the speed error is multiplied by the derivation gain.

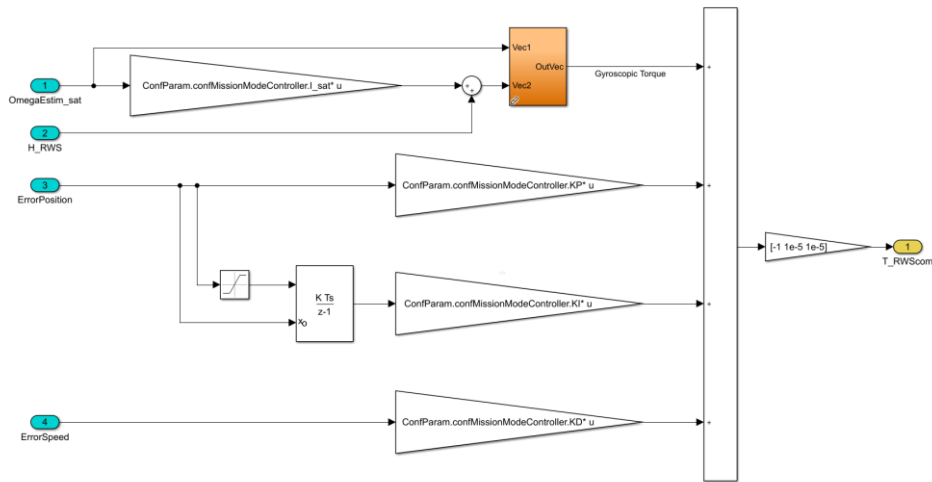


Figure 108 - Reaction Wheels PID Controller

In this phase, I set a gain differentiation on the wheels, based on the type of pointing; it means a higher concentration on the wheel in the solar panel direction, axis-x:

$$Gain_{Differentiation} = [-1 \quad 1 * 10^{-5} \quad 1 * 10^{-5}]$$

Over all that, it is not ignored the gyroscopic torque caused by the running wheels, and added to the law, computing with the estimated speed rotation and H_{RWS} .

After this precaution there is the sun pointing control law, with the PID controller for the reaction wheels, and the magnetorquers used for the desaturation, and damper with a B_{point} law in case of high speed rotation during the orbit.

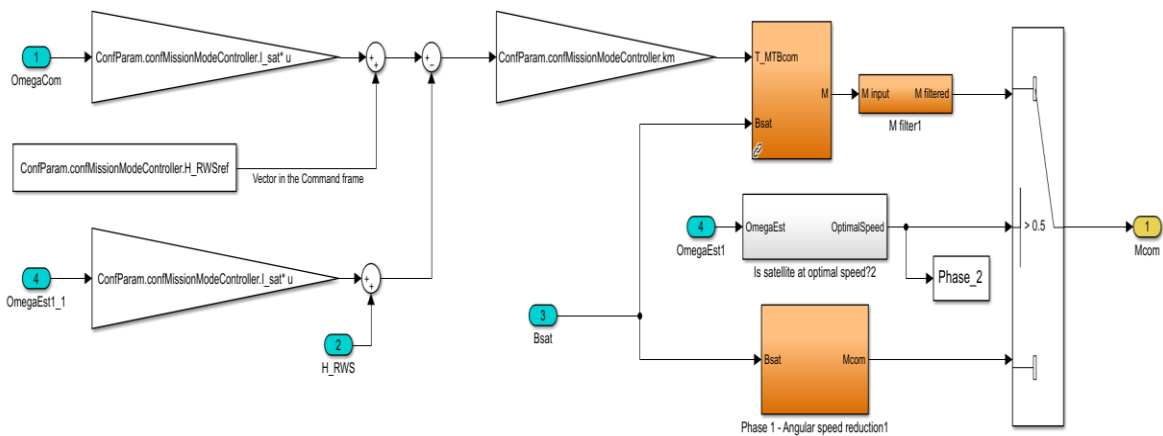


Figure 109 - Magnetorquers control law

4.5.5.4.2. Target Controller

On the other side, but mainly with the same approach is built the target controller, with as input command quaternion from the Guidance Model:

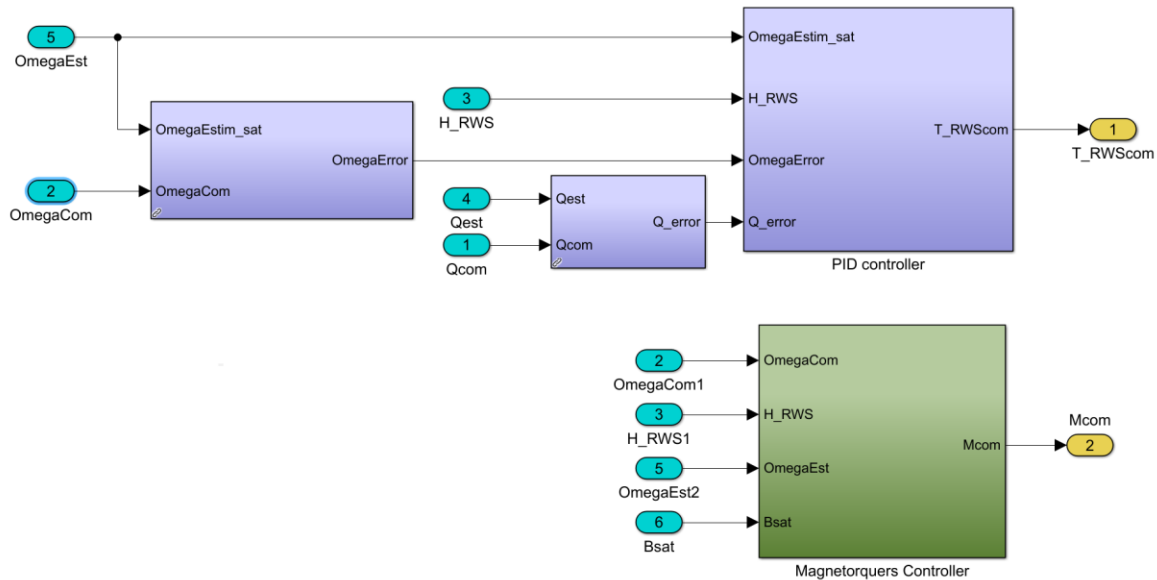


Figure 110 - Target Controller Model

Just few important differences are relevant to be explaining; In the PID controller there is a different gain differentiation due to the command of the wheel in the axis-y direction:

$$Gain_{Differentiation_{target}} = [-1 \quad -0.11 \quad 1 * 10^{-5}]$$

Because it is considered the direction axis-y to be directed towards the target, this involves generating a rotation around the y axis, always keeping the solar panels pointed towards the sun; in fact, the gain in the x direction remains the same, while the gain in the y direction is increased.

Another difference is inside the magnetorquers controller: it is not present a B_{point} law, because doesn't make sense to damp the fast rotation used to point towards the target; it is better to implement it in the sun pointing phase.

About the PID gains, the proportional gain changes, because to keep the position direct towards the sun, it better to set a gain lower, in order to not influence the stability; it involves the variation of the other two gains, following the Ziegler-Nichols method:

$$K_p = 21 * 10^{-4} \quad K_I = 1 * 10^{-7} \quad K_D = 0.0302$$

Anyway, it shouldn't be the best solution; indeed, below I will present the results with not the desired pointing accuracy.

4.5.5.5. Results

Starting with the sun pointing, the error obtained between panel direction and sun direction is lower confronting the result in the safe mode; we observe how the model keep a good stability, and pointing towards the sun direction, despite the fact that during orbit there is also a phase of pointing towards a target. That is possible thanks to the rigid rotation around the axis-x command by the target control law, which doesn't influence the rigidity for the axis-x. Otherwise the error doesn't go under the 2-3°, and the reasons are two:

- The normalized direction of the sun sent by the sensors is not precise enough. The zoom shows axis-x component never closes to 1;

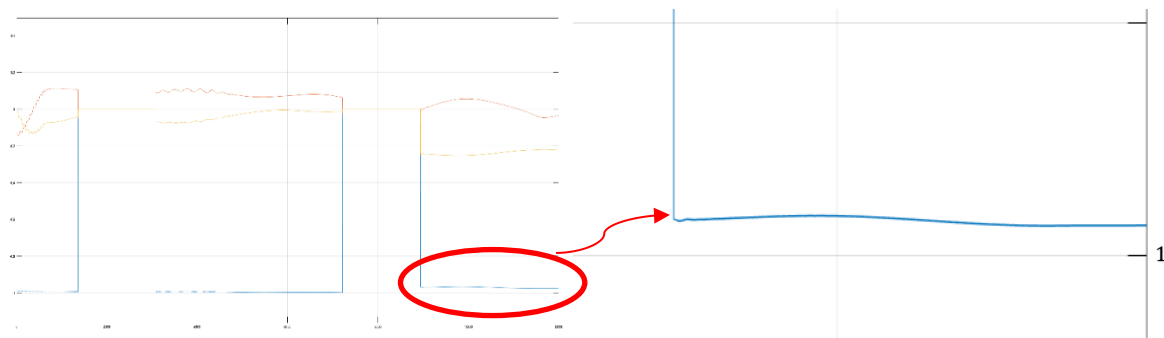


Figure 111 – Zoom on the sun direction normalized vector sent to the controller

- The parameters set up need to be improved.

Anyway, the result is:

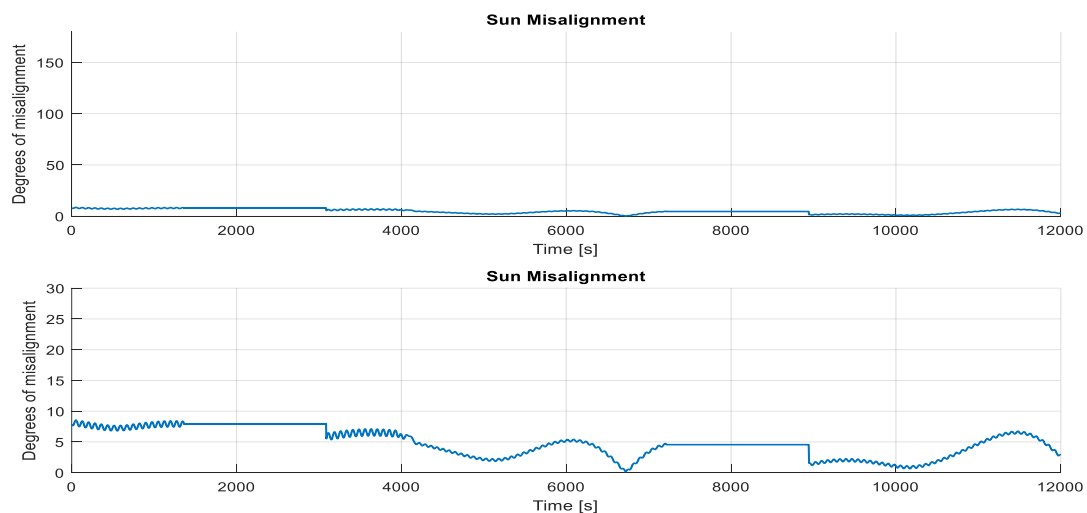


Figure 112 - Error between Panel Direction and Sun Direction for mission mode

The simulation is set on a period of 12000s, that means more than two orbits, and by the way, the accuracy is enough to charge properly the batteries; also, the oscillations are well controlled, considering the variation of 3° need more than 2000s (half an hour).

Now, looking at the axis-y direction, there are two moment in which the target is visible (the red line switch to 0), and in correspondence of these, we can observe a rapid rotation around the axis-y; it is the law of control that try to reach the position, cancelling the error between the axis-y and the direction of pointing chosen.

Unluckily, the result is not good, we observe that the satellite reaches the position just for few seconds, not enough for the mission requirement and to transmit or get any data (4.1.1-4.1.2). There is a delay of the control law response, and when the satellite is in position, the window to see the target is already closed.

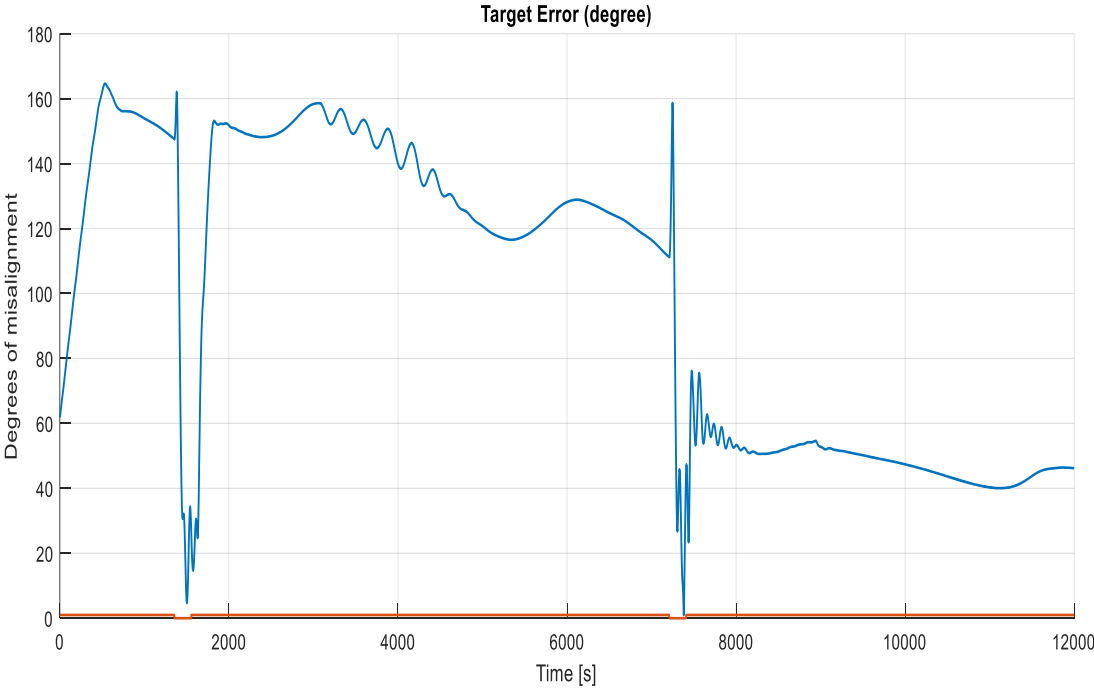


Figure 113 - Target Error in degree

The control law has to be improved, whereas the path taken is the right one; now the model needs a faster response, but without affecting its stability.

Another important parameter to check is the rotation speed, which allows to observe if the satellite is keeping stability, without rotating randomly; the result show, that the requirement is reached; indeed, all three rotation components are about 0°/s, except for the two moments when we change control law to point towards the target, but that

speed is justified. We can notice also a short instability around 4000s, but well damped by the controller, and in any case, we talk about very low speeds. The requirement asks a max shifting about $0.02^\circ/s$ (4.1.2), and that is accomplished.

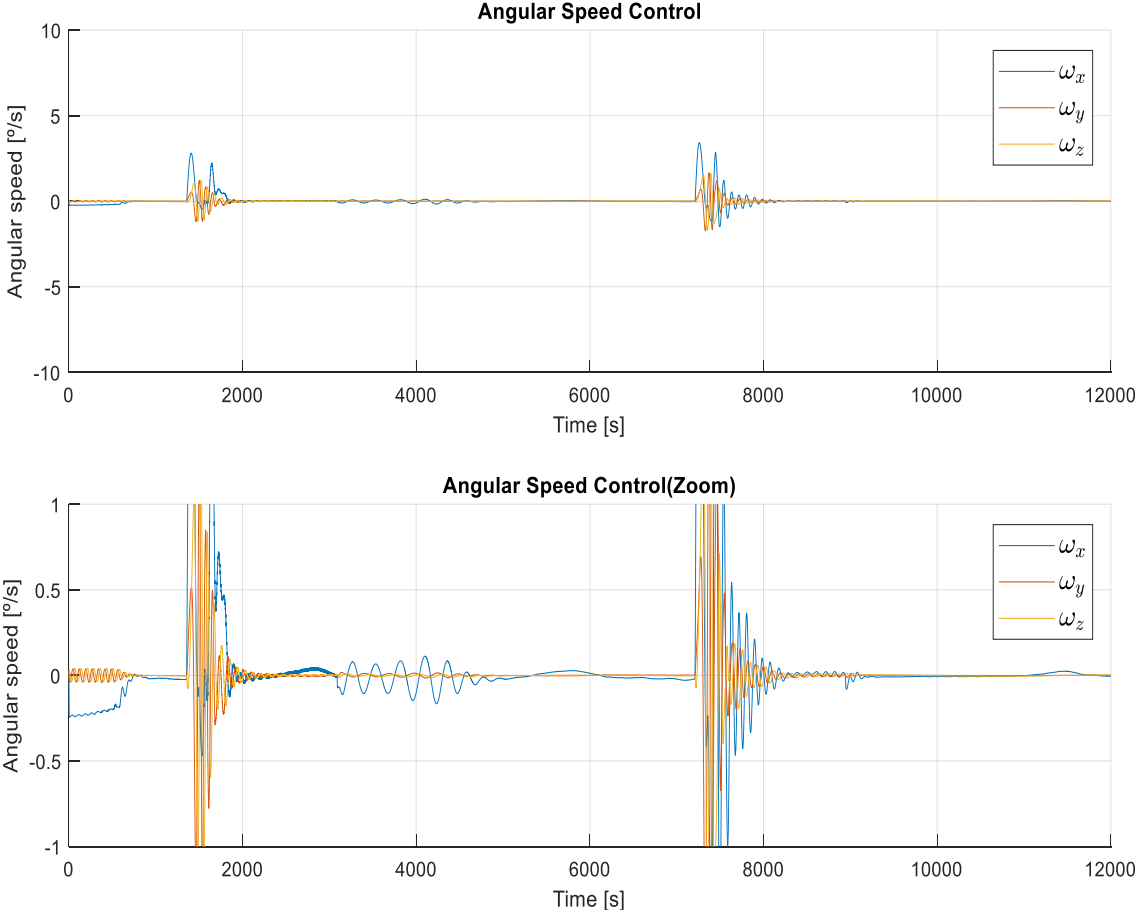


Figure 114 - Satellite angular speed for mission mode

Actually, it is not enough to consider exclusively the real rotation speed, because the controller bases its computation on the estimated rotation speed, which shows a relative difference from the real speed. Probably that happens due to the presence of the filter Discrete State-Space, which damps the oscillation, getting a higher stability.

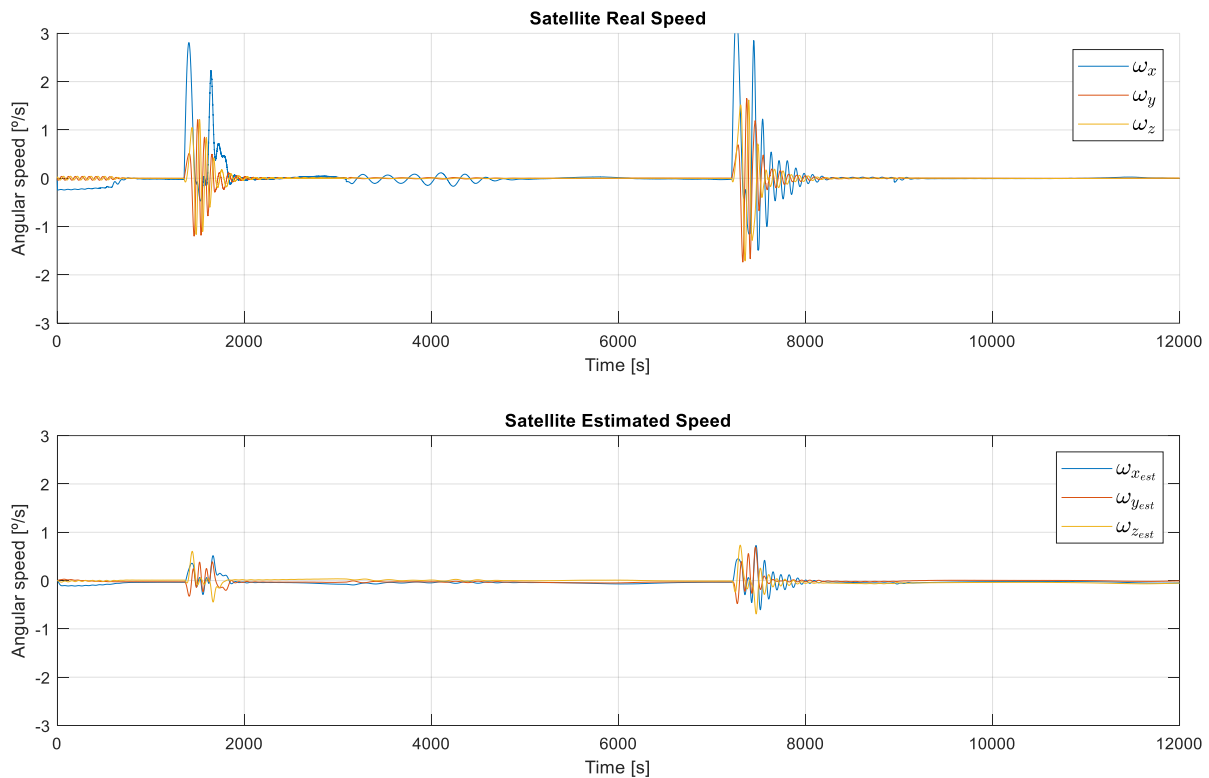


Figure 115 - Difference between real and estimated speed

About the magnetorquers, they are almost all the time in the desaturation mode; the torque requested is not high, so the intervention is not going to influence a lot the gyroscopic rigidity, but just acting as a brake on the wheels.

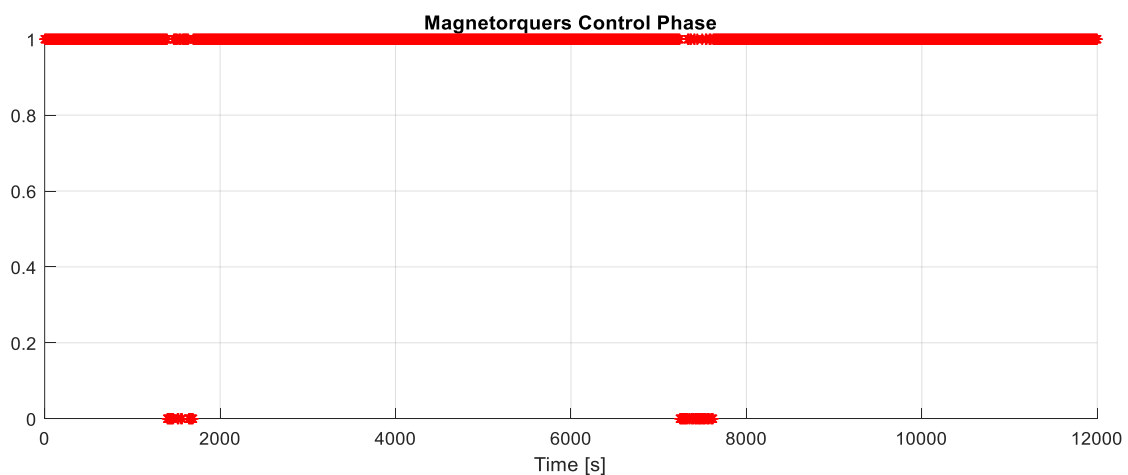


Figure 116 - Phase analysis between Desaturation and Bpoint law

As well, the B_{point} takes action in case of very high-speed rotation, that involves obviously two moments, after the intervention of the target controller, which

command a fast position change. In the following picture, there are plotted the three magnetic torque delivered, just during the desaturation phase, and it is just about 10^{-7} T.

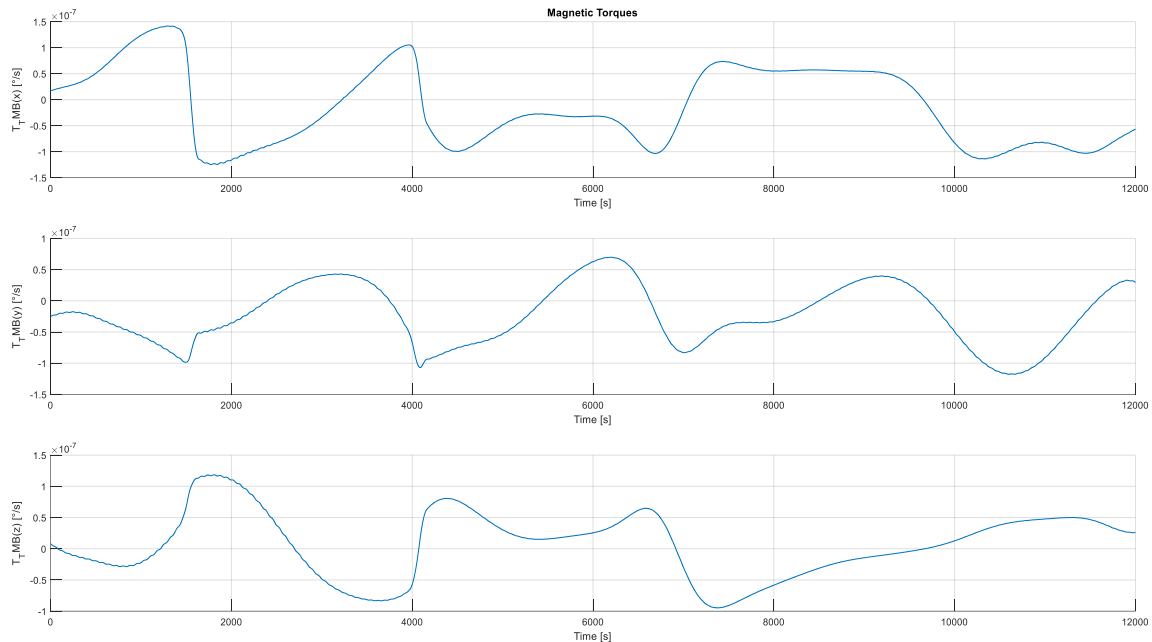


Figure 117 - Magnetic torque analysis

Another parameter always taken into account for the result analysis is the inertial momentum of the reaction wheels and the whole satellite. It is important to understand how it's varying and what value assumes; below there is the representation of the three components of H_{RWS} . The first value remarkable is H_{RWS_x} , which has a high value around 0.026-0.02 kg*m²/s most of the time, with a tiny oscillation cause by the magnetorquers; so, the controller keep the rigidity around the axis-x, as already explained, with a slow reduction due to the fact that the stability position is already reached, after the switch between the two laws.

About the switch between the two phases, there is a strong oscillation for the H_{RWS_x} , which should be related to the stability pointing already discussed. In contrast, the H_{RWS_y} has a variation in correspondence of the target pointing, but it keeps the inertial momentum rather than to be reduce by the magnetorquers; indeed, it changes again when the target controller acts. In any cases, it is not really remarkable, because the value got is around 0.002 kg*m²/s, that means 100 times less than H_{RWS_x} .

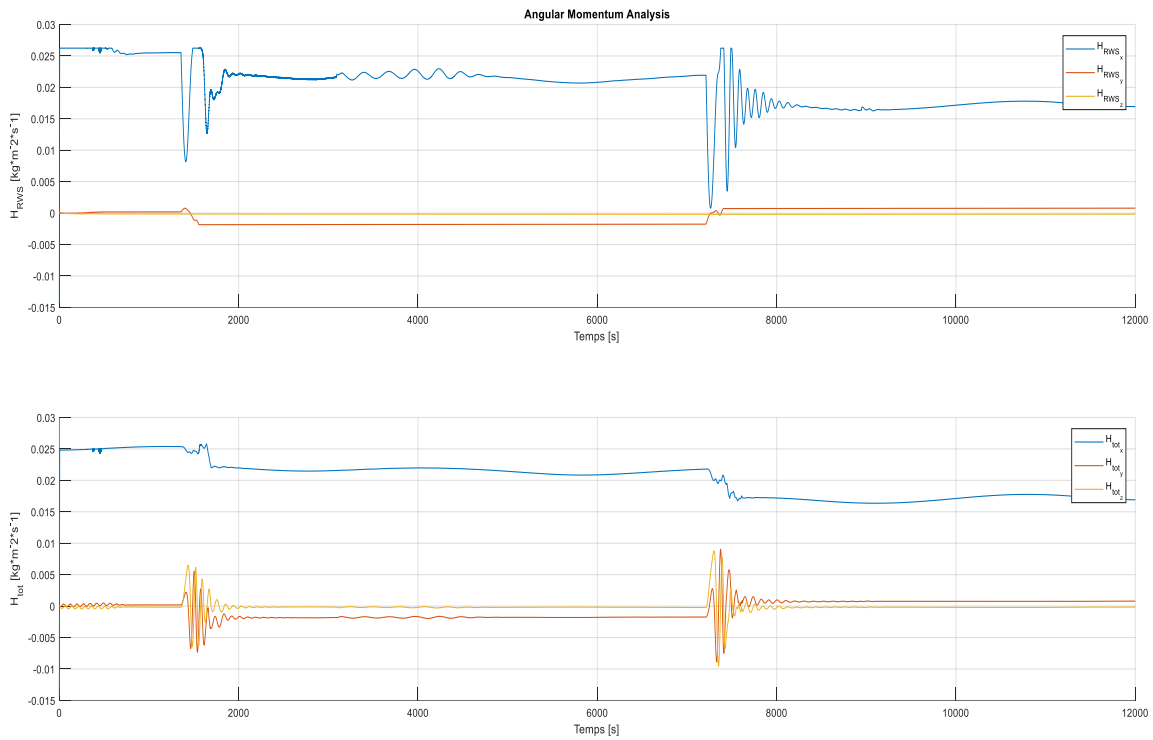


Figure 118 - Angular momentum analysis in mission mode

About the H_{tot} , the result is the opposite; for example, the H_{totx} doesn't change a lot, because the variation of inertial momentum in the y and z directions are not strong enough. On the other side, H_{toty} and H_{totz} present some important oscillation due to the oscillation of H_{RWSx} . This contrast is probably consequence of the target controller misfunction.

5. Conclusion

5.1. Technical Synthesis

As far as we focus on the performances of the Safe Mode Model, objectives have been reached; visualisations 3D with the tool VTS have been the final verification, showing the perfect control respectively for de-tumbling and sun pointing; also, during eclipse phases, the satellite stay mainly stable, and recovers in few minutes the right position. We should also consider the use of a single reaction wheel at constant speed and not high, allowing us not to consume too much batteries. Using only magnetorquers would not have been enough, both in terms of precision, both considering the size of the satellite, which having considerable size, can not be controlled are with magnetic fields. The importance of having a consistent safe mode simulation model is fundamental for the continuation of the project, because it is the first one that intervenes in the control of the satellite; if it were not such, even an excellent mission mode model, we could do nothing.

On the other side, the mission model doesn't match exactly with what the requirements ask; in fact, as already discussed, the problem related to the phase of pointing to a target remains open, because it remains rather far from the objective, both for not having had enough time, and for the complexity of the model. However, the complete model proves to be rather well directed towards solving the problem, not requiring major changes at the Simulink level, but probably at the mathematical level. The 3D visualisation proofs the perfect stability, with just really tiny movements, definitively irrelevant, .

It should be added that the development of simple and robust models, but equally real, is the real power of this project; the hard work to make scripts easy to interpret and modular blocks, is quantifiable perhaps as half of the time spent on the project. All the models implemented during this project will be useful and easy to understand for the next engineer, who will work on ATISE, or other satellites in CSUT company; also, being a modular model, i.e. adaptable to different missions and conditions, allows you to study and validate other CubeSat projects, not only for ATISE. A perfect example is the model of the sun sensor, which allows you to implement from 1 to 5 sensors, without changing the structure, but only by entering precise data in the script. Also, actuator models that allow you to control the components in a differential way or deciding how many wheels you want in the platform, from 1 to 4.

5.2. Recommendations

For the continuation of the project, it should be to:

- Solve the problem related to the pointing of a target; moreover, it would be to be considered the possibility to insert a Kalman filter in the estimator, it could also be of help in the calculation of the error sent to the controller.

- develop the data extraction logic that will then be inserted in the on-board computer.
- Insert, as my personal suggestion, a tetrahedron configuration of the reaction wheels, maybe it could solve the problem found; even if there is to consider the consequent problems of space, weight and consumption in the platform.

6. Glossary

- ADCS – Attitude Determination Control System
- CubeSat -Nano satellite with a size measured in U.
- 12U – size of the satellite, 1U is a standard unit for CubeSat, it means a cube 10x10x10 cm
- CSUT – Centre Spatial Universitaire de Toulouse
- CSUG – Centre Spatial Universitaire de Grenoble
- MONA – Platform 12U modular for CubeSat
- CNES – Centre National d'études Spatiales
- LM\EOF – Launch Mode \ End of Life
- CSS – Coarse Sun Sensor
- FSS – Fine Sun Sensor
- PILIA – library of Simulink models for CubeSat project
- PID – Control Proportional-Integrative-Derivative
- PI – Control Proportional-Integrative

7. Bibliography

- [1] COMAT, "COMAT_Products_for_Nanosatellites_2017," 2017.
- [2] New Space System, "000072-ICD-150276-1.0 NCTR-M012 Interface Control Document," 2017.
- [3] GOM Space, "gs-ds-nanosense-fss-2.0," 2017.
- [4] ZARM, Available: <https://www.zarm-technik.de/products/magnetometer/>.
- [5] S. ArianeGroup, "Datasheet_AURIGA_2017," 2017.
- [6] M. R. Greene, "The Attitude Determination and Control System of the Generic Nanosatellite Bus," University of Toronto Institute for Aerospace Studies, Toronto, 2009.
- [7] M. J. Amoruso, "Euler Angles and Quaternions in Six Degree Of Freedom Simulations of Projectiles," US Army Armament, Munitions and Chemicals Command, Picatinny Arsenal, New Jersey, March, 1996.
- [8] N. H. Hughes, "Quaternion to Euler Angle Conversion for Arbitrary Rotation Sequence Using Geometrics Methods," Braxton Technologies, Colorado Springs, Colorado.
- [9] D.-I. Z. Y. Ing. Karsten Groÿekatthöfer, "Introduction into quaternions for spacecraft attitude," Technical University of Berlin, Department of Astronautics and Aeronautics, Berlin, Germany, May 31, 2012.
- [10] D. M. Herderson, "Euler Angles, Quaternions, and Transformation Matrices," Mission Planning and Analysis Division, Houston, Texas, July, 1977.
- [11] F. Viaud, "Etude du systeme de controle d'attitude d'un cubesat," ISAE, 2014.
- [12] Y.-B. Jia, "Quaternions and Rotations," Sep 10, 2013.
- [13] J. a. N. Nichols, "Optimum Setting for Automatic Controller," New York, 1942.

